Chemical Functionalization and Modification of Au Clusters

A Thesis Submitted to the
College of Graduate and Postdoctoral Studies
In Partial Fulfillment of the Requirements
For the Degree of Master
Department of Chemistry
University of Saskatchewan
Saskatoon

By:

Maryam Alyari

Permission To Use

In presenting this thesis/dissertation in partial fulfillment of the requirements for a postgraduate degree from the University of Saskatchewan, I agree that the libraries of this university may make it freely available for inspection. I further agree that permission for copying of this thesis/dissertation in any manner, in whole or in part, for scholarly purposes may be granted by the professors who supervised my thesis/dissertation work or, in their absence, by the head of the department or the Dean of the College in which my thesis work was done. It is understood that any copying or publication or use of this thesis/dissertation or parts of thereof for financial gain shall not be allowed without my written permission. It is also understood that due recognition shall be given to me and to the University of Saskatchewan in any scholarly use which may be made of my material in my thesis/dissertation.

Requests for permission to copy or to make other uses of materials in this thesis/dissertation in whole or part should be addressed to:

- Dean
  College of Graduate and Postdoctoral Studies
  University of Saskatchewan
  116 Thorvaldson Building, 110 Science Place
  Saskatoon, Saskatchewan
  S7N 5C9, Canada

- Head of the Department of Chemistry
  University of Saskatchewan
  Thorvaldson Building, 110 Science Place
  Saskatoon, Saskatchewan
  S7N 5C9, Canada

Abstract

Atom-precise water-soluble amine-terminated Au nanoclusters (NCs) with various core sizes have been synthesized by a new single-phase synthetic method. The formed NCs are narrow-sized and the core size and size distribution can be controlled by the reducing agent concentration, with the formation of smaller NC core diameters at higher concentrations of the reducing agent. Furthermore, based on UV-Vis spectroscopy, three absorption peaks at around 690, 440, and 390 nm were observed at 0.30 M of the reducing agent, which are spectroscopic fingerprints of Au_{25} NCs and are strongly suggestive of the formation of fluorenylmethyloxycarbonyl (Fmoc)-glycine (Gly)-cystamine (CSA)-protected $Au_{25}(SR)_{18}$ NCs. The reactivity of surface amine functional groups of the resulting amine-terminated Au NCs was investigated by the Michael addition reaction of the primary amines with methyl acrylate. Based on the UV-Vis spectra and Transmission Electron Microscopy (TEM) images, the size of the NCs remained unchanged during the synthesis and after the functionalization reaction which suggests the high stability of these particles. The functionalization of the ligand was confirmed by Proton Nuclear Magnetic Resonance Spectroscopy (^{1}H NMR) and the NC size was characterized by TEM.

In the second part of this study, two synthetic methods, direct synthesis and post-functionalization (divergent synthesis) have been used to produce Au cluster-cored dendrimers. The ester-terminated Au cluster-cored dendrimers formed by direct synthesis are stable and resistant to aggregation in solution and in the presence of an excess of reducing agent. In contrast, amine-terminated cluster-cored dendrimers undergo aggregation in solution over time due to the high reactivity of the surface, which makes them unstable and limits their applications. The divergent method involves repeated two-reaction sequences on Gly-CSA Au NCs, consisting of

Michael addition and subsequent amidation by ethylenediamine, and produces stable amine-terminated Au cluster-cored dendrimers with no change in core size after the reaction based on TEM images. Therefore, various amine and ester-terminated Au cluster-cored dendrimers with various dendron generations and core sizes can be formed using the divergent strategy. Direct synthesis does not allow for control of cluster size, while the divergent method does not give fully uniform dendrons at higher generations. Finally, the catalytic activity of these Au cluster-cored dendrimers has been studied for the reduction of 4-nitrophenol.

Acknowledgements

I would like to thank all my friends and family for their continuous support and encouragement most importantly, my sister: Laura, along with my parents: Fatemeh and Abdulah. Also, I would like to thank all the past and present Scott group members, Dr. Yali Yao, Dr. Mahesh Gangishetty, Dr. Sudhessh Kumar Veeranmaril, Vy Phung, Brandon Chivers, William Barrett, Kazeem Sulaiman and Sara Aghakhaninejad. Thank you for all the help and happy times.

I would like to sincerely thank my supervisor Dr. Robert W. J. Scott for the knowledge, advice, patience, encouragement, and forgiveness throughout this research project. I also thank my advisory committee member, Dr. Timothy Kelly for his support and valuable suggestions.

I appreciate the opportunity to carry out my master's study at the University of Saskatchewan giving by Dr. Robert W. J. Scott and the Department of Chemistry. I thank the National Science and Engineering Research Council of Canada for providing financial support.

My thanks also go to the laboratory managers Dr. Alexandra Bartole-Scott and Marcelo Sales for their guidance in teaching CHEM 112 and CHEM 250. Finally, I would like to express my gratitude to many past and present staff in the department of chemistry, Leah Hildebrandt, Amber Bornhorst, Erin Wasylow, Bonita Wong, Linda Duxbury, and Pia Wennek, for their unconditional help.

Dedications

To my sister Laura, my parents, and friends

Thank you for all your love and support

Table of Contents

List of Figures

List of Schemes

List of Abbreviations

Boc	Tert-Butyloxycarbonyl
CSA	Cystamine
CTAB	Cetyltrimethylammonium Bromide
Cys	Cysteamine
DENs	Dendrimer-Encapsulated Nanoparticles
DMSO	Dimethylsulfoxide
DNA	Deoxyribonucleic Acid
Fmoc	Fluorenylmethyloxycarbonyl
FTIR	Transform Infrared Spectroscopy
Gn	Generation (Dendrimers)
Gly	Glycine
HBtU	*O*-Benzotriazole-*N*,*N*,*N*′,*N*′-Tetramethyl-Uronium Hexafluorophosphate
HOBT	*N*-Hydroxybenzotriazole
HOMO	Highest-Occupied Molecular Orbital
k_{app}	Apparent Reaction Rate Constant
L	Ligand
LUMO	Lowest-Unoccupied Molecular Orbital

MA	Methyl Acrylate
MPCs	Monolayer-Protected Clusters
NCs	Nanoclusters
NCDs	Nanoparticle-Cored Dendrimers
nm	nanometer
NMR	Nuclear Magnetic Resonance
4-NP	4-Nitrophenol
NPs	Nanoparticles
PAMAM	Poly(Amidoamine)
PPI	Poly(Propyleneimine)
ppm	Parts per million
RNA	Ribonucleic Acid
S_N2	Nucleophilic Substitution Reaction
SPR	Surface Plasmon Resonance
TEM	Transmission Electron Microscopy
THF	Tetrahydrofuran
TOAB	Tetraoctylammonium Bromide
UV-Vis	Ultra-violet and Visible

Chapter 1

1 Introduction

Recently, gold nanoclusters (Au NCs) have received a great deal of attention in nanoscience and nanotechnology because of their unique geometric and electronic structures and their key applications in catalysis[1,2], biomedicine[3,4], sensing[5,6] and biosensing[7]. The optical and chemical properties of thiolate-protected Au NCs directly depend on the Au core size, and due to the small size of the Au NCs, they behave as molecules rather than metallic nanoparticles. For example, thiolate-protected Au NCs of different sizes show unique molecular transitions in the UV-Vis region.[8,9] In addition, recent studies revealed that the catalytic activities of Au NCs are also size-dependent.[2,10] Therefore, designing new strategies to generate different atom-precise NCs is a key focus in recent NC research.

In the past few decades, a broad range of thiolate ligands with a variety of functional groups have been used to stabilize Au NCs.[11–14] The organic surface properties, such as type of ligand functionality, ligand bulkiness, as well as ligand coverage of Au NCs control properties such as the solubility, stability, and applications of Au NCs.[11] Direct synthesis of Au NCs with reactive functional groups, such as carboxylic acids and amines, is a big challenge due to the competitive binding of these functional groups to the Au surface. Furthermore, sometimes the same NC core size cannot be achieved using ligands with different functional groups under the same reaction conditions. To overcome these challenges, post-functionalization strategies can be used for surface

modification and tailoring desirable ligands and functionalities on the surface of NCs.

This thesis includes the design and synthesis of ligands, the preparation and modification of Au NCs of various core sizes, as well as the characterization and application of functional Au NCs in catalysis. In this thesis, I use a new single-phase synthetic method to produce narrow-sized and stable amine-terminated Au NCs with various core sizes. I show that the core size directly depends on the concentration of the reducing agent and higher concentrations of reducing agent result in smaller core sizes, including $Au_{25}L_{18}$ systems. The reactivity of surface amine and ester functional groups of Au NCs is investigated by the Michael addition reaction of primary amines with methyl acrylate and amide coupling reactions of ester groups with ethylenediamine; results show that the resulting NCs can be easily functionalized. Repeating the two-reaction sequences consisting of Michael addition and subsequent amidation produces Au cluster-core dendrimers.

1.1 Nanomaterials

Zero-dimensional colloidal nanomaterials can be classified based on the size of colloids into two main classes: nanoparticles (NPs) and NCs.[15] In this classification, NPs are objects with a structural diameter between 2 and 100 nm and NCs are below 2 nm in size. NPs and NCs are generally considered as intermediate species between bulk metals and metal atoms (Figure **1.1**). The main difference between NCs and NPs is their electronic properties which result in different physical properties.[16,17] Metallic NPs have electronic properties of the bulk material, while metallic clusters typically behave as molecules.

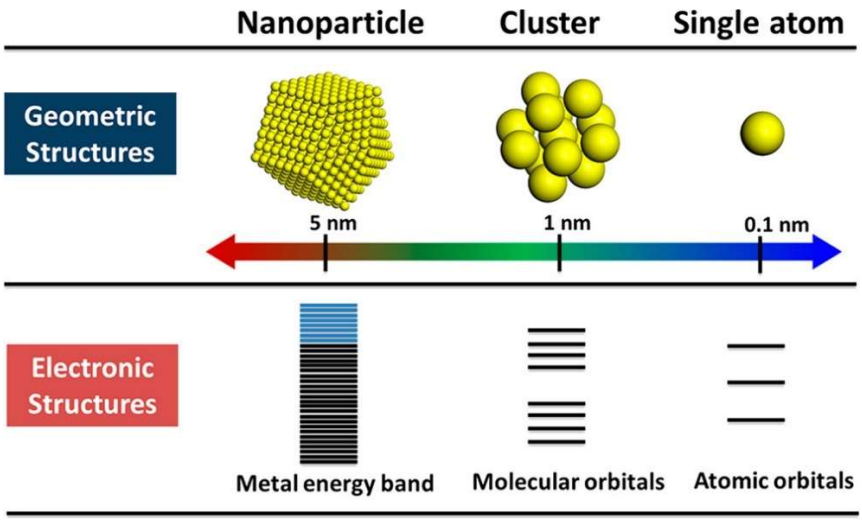

Figure 1.1. Energy levels of atoms, NCs, NPs, and bulk metals.[15] Reprinted with permission from ref 15. Copyright 2019 Chemistry-Sustainability-Energy-Materials.

1.1.1 Au NPs

Many efforts have been applied to the synthesis and understanding of the fundamental physical and chemical properties of monodisperse Au NPs and NCs. There are various synthetic methods and capping agents that can produce Au NPs with different core sizes. Ligand stabilized Au NPs (often also called Au monolayer-protected clusters) are often prepared by the reduction of Au salts in the presence of an appropriate stabilizing ligand, often thiolates or phosphines, which help prevent particle agglomeration. The ligand can change the electronic properties of those metal atoms which are linked with the ligand molecules.[18]

The unique optical properties of Au NPs give them a wide range of applications in both biology and technology.[19,20] These properties are often due to the interaction of the electrons of Au NPs with light. At a specific wavelength, Au NPs have a strong surface plasmon resonance (SPR) absorption in the visible region (Figure **1.2**) due to the resonance of incident photon frequency with the collective oscillation of electrons on the surface of the Au NPs which results

in strong absorption and scattering of light.[18,21,22] The resonance frequency of this phenomenon (SPR) depends on the size, shape, and dielectric constant of the NPs. Au NCs, as well as bulk Au, do not show such SPR bands.

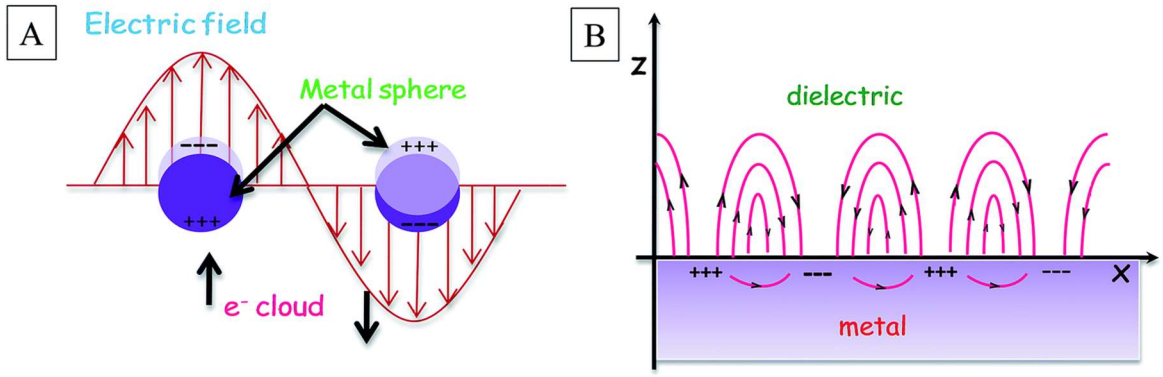

Figure 1.2. SPR absorption in NPs.[23] Reprinted with permission from ref 23. Copyright 2016 Royal Society of Chemistry.

1.1.2 Au NCs

The term "cluster" was applied by Cotton for the first time in the 1960s to compounds containing metal-metal bonds.[24] Au NCs generally contain countable numbers of atoms (from a dozen to a few hundred) and the diameters range from subnanometer to ~2.2 nm.[25] Among ligand-stabilized NCs, thiolate-functionalized Au NCs as functional materials have attracted attention for many years.[26] These NCs have very strong bonds between the metal core and thiolate ligands that provide them molecule-like stability. The properties of Au NCs are very sensitive to the number of atoms in the particle.[27] Therefore, atom-precise Au NCs are represented by their exact formula, $Au_n(SR)_m$, where, n and m represent the number of metal atoms and thiolate ligands (–SR), respectively.

1.1.2.1 The Importance of Small Au NCs

Au NCs show distinctive quantum confinement effects due to their ultra-small core size (<2 nm).[27,28] This property results in a discrete electronic structure and molecule-like properties, such as HOMO–LUMO electronic transitions and enhanced photoluminescence. Furthermore, Au NCs have a high surface-to-volume ratio, which makes them good candidates for catalysts and further surface modification and bioconjugation.[29] All the above properties make Au NCs suitable for a wide range of applications such as nanoelectronics, catalysis, chemical and biological sensing, biomedicine, and optical applications.[30–34] There is a class of stable and highly functional NCs which are called magic number NCs. Some of the NCs that are included in this class are $Au_{25}L_{18}$, $Au_{38}L_{24}$, and $Au_{144}L_{60}$ (where L is typically thiolate ligands). Their geometry makes them more stable as molecules compared to other NCs; furthermore, Au_{25} and Au_{35} are much more thermodynamically stable than other NC systems due to electronic effects.[35] $Au_{25}L_{18}$ NCs can be precipitated, redissolved, and even purified by chromatography without any change in properties.[36] Note that in many cases the NCs have a -1 charge state.

1.1.2.2 $Au_{25}L_{18}$ NCs

$Au_{25}L_{18}^-$ NCs are a ubiquitous system and have size-specific physical and chemical properties like photoluminescence, redox behavior, and catalytic activity that cannot be observed in metallic bulk Au.[37] $Au_{25}L_{18}$ NCs are stable in both solution and the solid state and can be considered a molecular species.[36,38]

1.1.2.2.1 Structure and Applications

Figure **1.3** shows the single-crystal structure of $[Oct_4N^+][Au_{25}(SCH_2CH_2Ph)_{18}^-]$.[39] The structure of $Au_{25}(RS)_{18}^-$ can be written $Au_{13}[(RS)_3Au_2]_6$ in which there is an icosahedral Au_{13} core surrounded by six RS-Au-RS-Au-RS protecting staple motifs. In this structure, each of the surface atoms of the core is connected to one sulfur atom. So, the actual protective ligands in the structure of $Au_{25}(RS)_{18}^-$ are the $Au_2(SR)_3$ staples. These motifs are attached to the metal core as a bidentate ligand which provides a close-packed structure with a shielded metal core. The reason for this unexpected structure is not due to geometric constraints but rather due to electronic interactions which lead to a highly stable structure.[30,31]

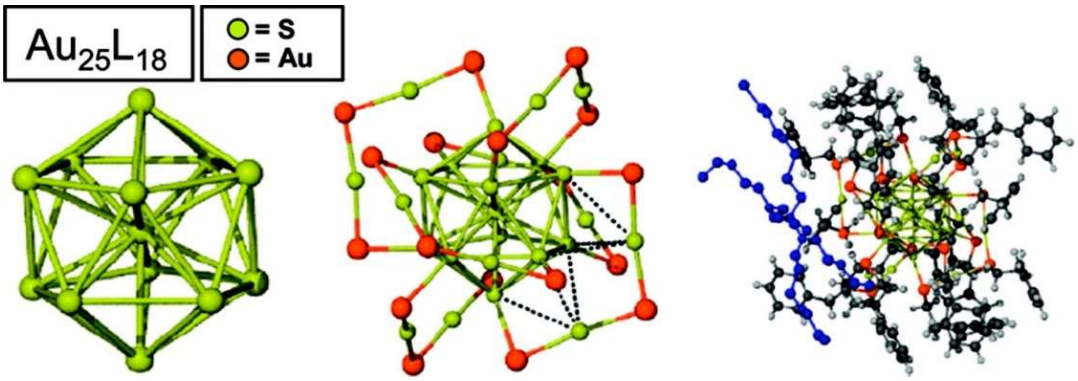

Figure 1.3. Crystal structure of $[Oct_4N^+][Au_{25}(SCH_2CH_2Ph)_{18}^-]$, the central Au_{13} cluster is on the left; in the middle figure, yellow atoms in the staples are S and Au atoms are red; the blue colour on the right is the charge balancing cation (Oct_4N^+).[39] Reprinted with permission from ref 39. Copyright 2010 American Chemical Society.

$Au_{25}L_{18}$ NCs show three absorption peaks in their UV-Vis spectra at 690, 450, and 400 nm. These peaks are a fingerprint for thiolate-functionalized $Au_{25}L_{18}$ NCs. The first band with the lowest energy at 690 nm (1.55 eV, peak **a** in Figure **1.4b**) belongs to the transition of electrons from the HOMO to the LUMO. The second band at 450 nm (2.63 eV, peak **b** in Figure **1.4b**) corresponds to the transition of an electron from the HOMO to the LUMO+1 and +2 and the

HOMO-2 to the LUMO orbitals. Finally, the third band at 400 nm (3.3 eV, peak **c** in Figure **1.4b**) shows the HOMO-5 to the LUMO electron transition.[31]

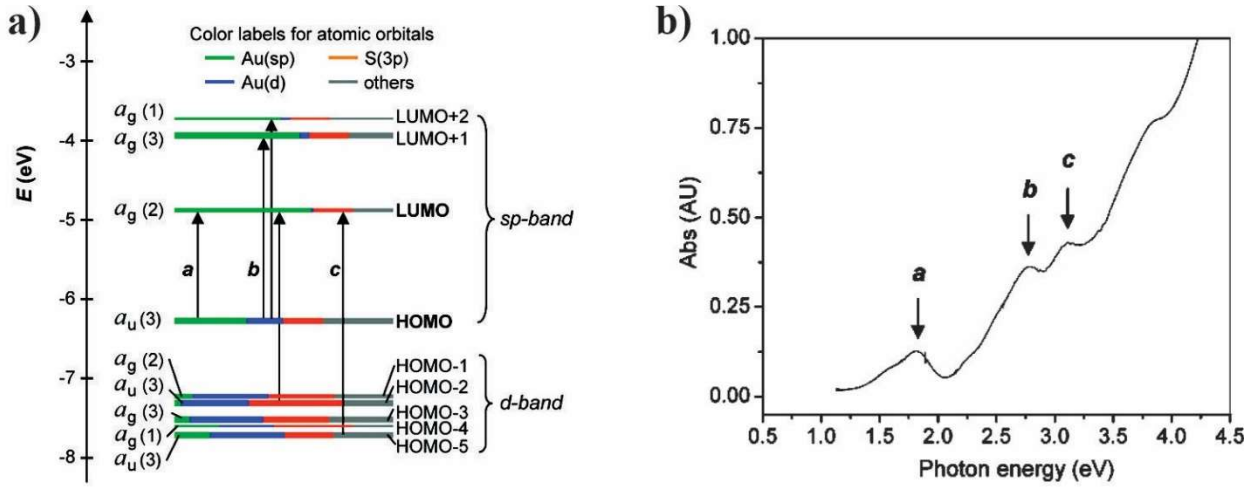

Figure 1.4. (a) Kohn-Sham orbital energy level diagram and (b) UV-Vis spectrum of Au_{25} NCs.[31] Reprinted with permission from ref 31. Copyright 2008 American Chemical Society.

Recently, $Au_{25}L_{18}$ NCs have received increased attention due to their unique optical and electronic properties which make them promising in various applications in catalysis[27,34] and electrocatalysis,[40,41] sensing,[5,6] and biomedicine.[42,43] For example, Au NCs, including $Au_{25}(SR)_{18}$, were shown to possess antimicrobial activity which is absent in bulk Au and Au NPs.[3,4] These properties can likely be further improved by modifying the surface chemistry of the NCs.

1.1.2.2.2 Synthetic Routes

There is significant interest in developing new synthetic methods to produce atom-precise NCs and at the same time have control over the surface functionality of these NCs. However, to date, there have been few reports published that allow one to synthesize particular atom-precise NCs in bulk quantities.[44] Therefore, due to the importance of this type of material, researchers have been trying to develop synthetic methods for the size-controlled synthesis of Au NCs. Despite

the large advances in the fabrication of atom-precise Au NCs, a vast majority of Au NCs are stabilized by ligands that cannot be used for further chemistry, such as alkanethiolates.[34,39,45]

Typically, four strategies have been used for the synthesis of atom-precise $Au_n(SR)_m$ NCs, including $Au_{25}L_{18}$ (Figure **1.5**).[46] High-resolution separation is the first strategy that can separate NCs of a specific size according to their number of constituent atoms from a mixture of NCs of various sizes (Figure **1.5a**). There are different methods for high-resolution separation of Au NCs such as polyacrylamide gel electrophoresis and solvent extraction.[47] Recently, reverse-phase HPLC has been used widely for high-resolution separation of Au NCs.[48,49] The second method involves exposing polydisperse NCs to severe oxidizing or reducing conditions (Figure **1.5b**). In this strategy, the most thermodynamically stable NCs survive the harsh conditions while less stable NCs are converted into stable NCs. For example, Jin and coworkers reported the synthesis of monodisperse $Au_{38}(SC_2H_4Ph)_{24}$ NCs by chemical etching of size-mixed $Au_m(SR)_n$ NCs using excess free ligand. [8] In this study, the $Au_m(SR)_n$ NCs were exposed to excess phenylethanethiol (PhC_2H_4SH) for 40 h at 80 °C. The $Au_{38}(SC_2H_4Ph)_{24}$ NCs show higher stability against etching than other NCs in the mixture. In the third strategy, atom-precise NCs are synthesized by controlling the growth rate of the NCs during the synthesis (Figure **1.5c**). This can happen by choosing an appropriate reducing agent under controlled reaction conditions. In the fourth strategy, ligand exchange of stable atom-precise NCs generates stable NCs with different chemical compositions, due to the dependency of the chemical composition on the ligand shell (Figure **1.5d**). In this method, the ligand of the NCs can typically be exchanged with bulkier ligands to get more stable atom-precise NCs and several functional ligands could be introduced with this method.

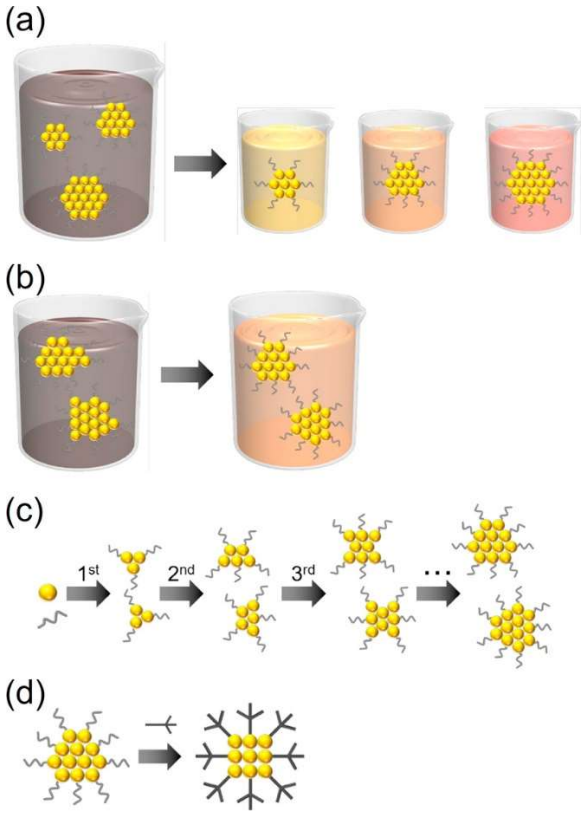

Figure 1.5. Typical methods for the precise synthesis of monodisperse atom-precise NCs: (a) high-resolution separation, (b) size focusing under severe conditions, (c) controlling the growth rate, and (d) ligand exchange.[46] Reprinted with permission from ref 46. Copyright 2016 Elsevier.

1.2 Functionalization of Au NPs and NCs

Functionalization is a useful tool to make metal NPs and NCs more attractive for different applications.[50,51] Various types of functionalization methods have been applied to create NPs and NCs with new and desired functions. One effective method involves the control of the functional group of the ligands which leads to more control over chemical and physical properties. Pradeep and coworkers have found that place-exchange reactions of $Au_{25}SG_{18}$ (SG-glutathione thiolate) by functionalized -SG or other ligands such as 3-mercapto-2-butanol change the photoluminescence properties of the NCs.[52] Heteroatom doping, which is another method, can result in new functional NPs and NCs. For example, it was observed that doping Au atoms in Pd NCs results in a high

activity catalyst for the glucose oxidation reaction due to negatively charged surface Au atoms.[53] Controlling bonding interactions between a metal and the ligand is another way to change the physical and chemical properties of these particles.[54] For example, changing the bond from Au-S to Au-Se results in a decrease in charge transfer from Au to the ligand in Au-Se bonds compared to Au-S bonds which results in bonds with less ionic character.[55]

Well-defined structures of NPs and NCs with specific properties can be tailored by controlling two parameters:[56] 1. Control of the size and composition of the core which can control the electronic and optical properties of NPs and NCs. For example, by choosing different reaction conditions during synthesis or by some modifications after synthesis such as size-selective purification,[57] one can have control over the size of the NP and NC core. 2. Judicious choice of ligands which can control chemical properties of the NPs and NCs such as solubility, reactivity, surface chemistry, and binding affinity.

Place-exchange reactions can produce functionalized Au NPs and NCs that preserve the core dimensions of precursor particles but exhibit unique physical and chemical properties like increased stability against heat-induced aggregation and decomposition.[56,58] Figure **1.6** shows the one-pot protocol developed by Schiffrin and coworkers to produce Au NCs, followed by a place-exchange reaction to form Au NCs with mixed ligands.[59,60] Reaction time strongly depends on the incoming ligand chain length and generally increases with increasing the chain length. This trend is due to steric effects that reduce the reactivity of the ligands.[50] Challenges for place-exchange reactions include incomplete exchange and a narrow choice of ligands. Other parameters that can be controlled (especially for Au NCs) are the precise nature of the atom-precise cluster and the identity of the new ligand. In place-exchange reactions, the size of the cluster core can also be

changed during the exchange.[58] The preservation of the small core dimensions and narrow size dispersity of the NCs are essential especially for electronic and optical applications which require functionalized NCs with controlled physical properties.[61]

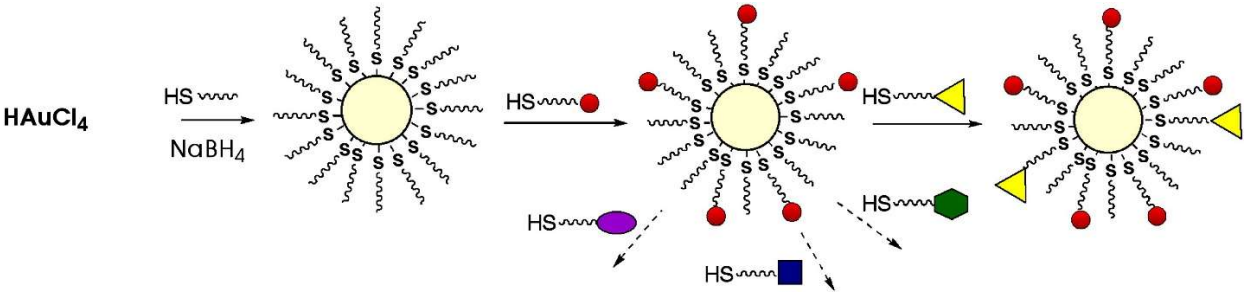

Figure 1.6. Formation of a wide variety of Au NPs and NCs with various ligands by using place-exchange reactions.[50] Reprinted with permission from ref 50. Copyright 1998 American Chemical Society.

Post-functionalization is the most convenient method to produce functionalized Au NCs (Figure **1.7**). Amide and ester coupling reactions are useful synthetic routes and powerful activating agents to produce a variety of functionalized NCs.[62] Ester coupling reactions (esterification) provide an efficient method of functionalizing and bioconjugating Au NCs.[63] Recently, Hökkin and coworkers reported the site-specific conjugation of functionalized Au NCs to viruses.[64] They used *N*-(6-hydroxyhexyl)maleimide as a linker molecule that binds to the NCs with an ester bond; the functionalized Au NCs can then conjugate with viruses via Michael addition reactions.

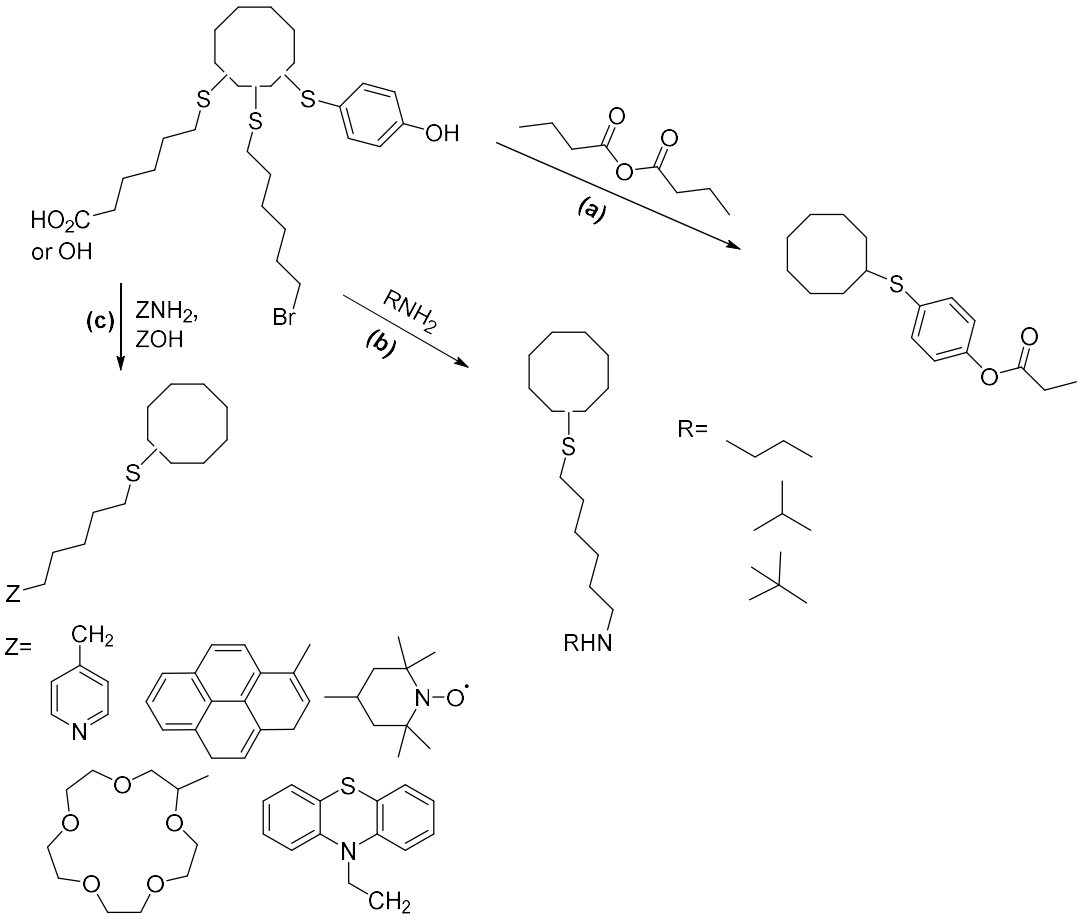

Figure 1.7. Functionalization of Au NCs using coupling (a,c) and S_N2 reactions (b). Adapted from ref 58.[58]

The other common coupling method to conjugate Au NCs to various functionalized head groups is the amide coupling reaction.[63] Carboxylic acid and active ester groups can be reacted with primary amines by a condensation reaction to yield amide bonds. Since amine functional groups are highly reactive, amide linkages are a common strategy for covalent coupling conjugations.[65,66] For example, Forbes and coworkers have constructed Au NCs with biological moieties attached by a synthetic route based on amide and ester coupling reactions to form $Au_{145}L_{50}$ NCs with various structural groups.[62] They used coupling reactions between alcohols or amines with NCs bearing carboxylic acid groups and also between carboxylic acids with NCs bearing alcohol groups.

One major challenge with post-functionalization is that further functionalization performed on the surface of particles can often result in some (undesirable) growth in the Au core size.[63] This is even more problematic with atom-precise Au NCs that are used for a specific application in which the core size is an important factor. Therefore, an effective approach is needed for the generation of desirable functional group surfaces on Au NCs using post-functionalization strategies, and at the same time retain control over the core size.

1.2.1 Synthetic Routes

Ligands with functional chemical groups provide a chance to use Au NPs in different areas such as catalysis, delivery applications, and biomolecule or chemical sensing.[51,54,67] For this approach there are three ways to achieve such functional ligands: (I) direct synthesis, (II) post-functionalization, and (III) place-exchange reactions. [58,61,67,68]

In direct synthesis, functionalized ligands are used to prepare the desired Au NPs with activated functional groups.[69] This method has a big drawback in that these functionalized ligands may not be stable in reaction conditions or may interfere with the synthesis of Au NPs (for example, by coordinating to the Au salt and/or the Au NP surface). Therefore, there is a demand to develop other alternative strategies.

Place-exchange reactions developed by Murray and coworkers are a powerful tool to change the functionality of the ligand shell of ligand stabilized NPs and NCs.[61,70,71] This approach is used to produce various organic and water-soluble NPs and NCs with a diverse range of core sizes and functional groups on ligand shells. For example, Briñas *et al.* used citrate- and dimethylaminopyridine Au NPs in place-exchange reaction to produce water-soluble NPs using water-soluble ligands such as amino acids, peptides, and carbohydrates.[61] Place-exchange

reactions are limited by several challenges. The first challenge is that incorporating functional ligands into the ligand shell is not easy due to synthetic incompatibilities.[72] Secondly, complete replacement of the original ligand with a new ligand is a big challenge that is hard to control, and the use of different ligands can lead to incomplete or even no exchange.

Another approach to prepare functionalized Au NPs is using ligands that have terminal reactive functional groups that can undergo secondary synthetic reactions like nucleophile substitution reactions (e.g. S_N2 reactions) and coupling reactions.[58] The most important reactions that can produce a variety of structural groups on Au NPs are amide and ester coupling reactions. These reactions can be made by diverse amine, carboxylic acid, or alcohol molecules (Figure **1.7**). For example, Murray and coworkers studied the S_N2 reactivity of ω-bromoalkanethiolate-functionalized monolayer-protected Au clusters (MPCs) with primary amines.[50] They studied the effect of the bulkiness of the incoming nucleophiles as well as the chain length of the ω-bromoalkanethiolates on the S_N2 reactivity of Au MPCs. Also, they published a series of amide and ester coupling reactions on hydroxyl and carboxylate MPCs with a variety of reagents and produced various polyfunctionalized Au MPCs.[62]

1.2.2 Applications of Functionalized Au NPs and NCs

One important strategy that allows one to tailor Au NPs for desired applications is to functionalize them and modify their physicochemical properties. The initial interaction of NPs with cells is a fundamental factor controlling the efficiency of such NPs in biomedical applications and strongly depends on the surface moieties that exist on both NPs and cells.[67] It is believed that type, charge, and length of the surface ligand of NPs play an important role in their antimicrobial efficiency.[4] Recently, Au NPs have been received huge attention as an attractive vehicle for the

delivery of small drug molecules and large biomolecules (like DNA, RNA, and proteins) due to their unique chemical and physical properties[73] (Figure **1.8**). The first advantage that makes Au NPs a good candidate for drug delivery purposes is their inert and non-toxic core.[74] Au NPs can be synthesized easily with a wide range of core sizes (2-150 nm). In addition, the ease of functionalization through thiol linkages allows one to control the surface chemistry.[75]

Au NPs and NCs are amongst the most investigated nanomaterials in sensing applications due to their unique optical properties. Sensing can either involve plasmonic interactions and/or luminescence from NPs or NCs. Various functionalized Au NPs have been generated to be used as sensors for biological specimens, such as DNA, RNA, cells, metal ions, small organic compounds, and proteins.[76] For example, Au NPs modified by synthetic biopolymers can be used as potential bio-sensors for labelling, imaging, and assaying.[77] The role of the biopolymers is to decrease the high surface energy of the Au NPs and as a result, prevent the aggregation of NPs.

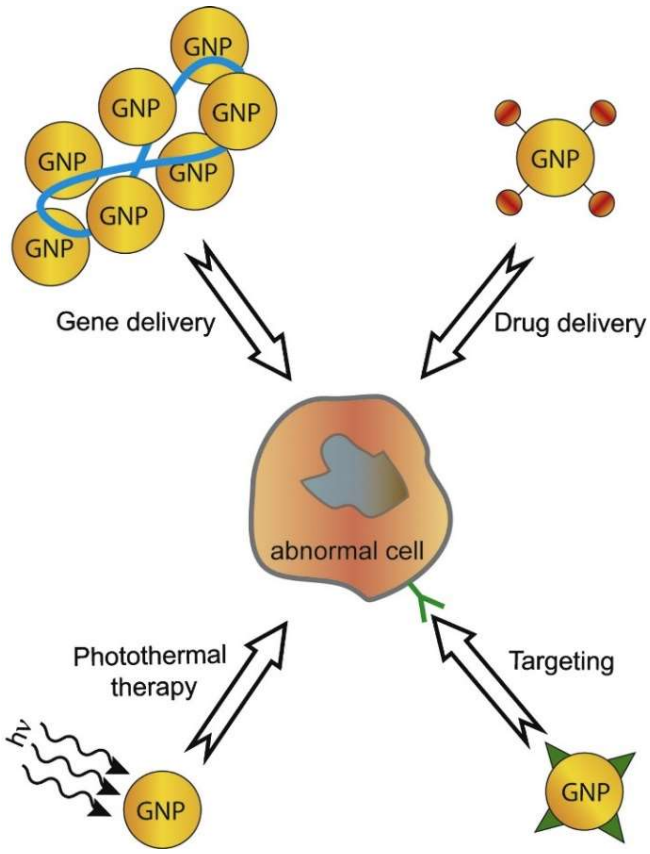

Figure 1.8. Biological applications of Au NPs.[67] Reprinted with permission from ref 67. Copyright 2008 Elsevier.

Finally, Au NPs and NCs have been shown to exhibit catalytic activity for the formation of C-C, C-N, C-S, and C-O bonds, and can also be catalysts for oxidation and reduction reactions.[78,79] For example, it has been recently observed that Au NPs are capable of catalyzing the regioselective hydroamination of alkynes.[80] For this purpose, the Au NPs are supported on a natural polysaccharide biopolymer (chitosan). Also, it has been reported that Au/CeO_2 catalyzes the Sonogashira cross-coupling of aryl halides and terminal alkyls to form C-C bonds.[81] Even though the catalytic reactions take place on the surface of Au particles, functional groups and length of ligands/capping agents can control the activity and selectivity of the catalyst. Recently, our group reported the reduction of 4-nitrophenol using $Au_{25}L_{18}$ NCs with a variety of alkanethiolate ligands, such as phenylethanethiol, hexanethiol and dodecanethiol.[34] The effect of

ligand chain length and composition on the reduction of 4-nitrophenol was studied, and it was observed that there was a decrease in reaction rate by increasing the chain length of ligands due to greater availability of the Au surface when using short-chain thiol ligands.

1.3 Amine-Functionalized Au NCs

The most common functional groups on the surface of Au NCs are hydroxyl groups and carboxylic acids, along with a limited number of amine systems.[11,29,82] Generation of amine-terminated Au NCs and subsequent post-functionalization can give access to a diverse selection of organic surface functional groups on Au NCs.[58] Attractive features of incorporating surface amine groups are the following: 1) high reactivity of these functional groups makes them highly attractive to be used for coupling reactions, 2) a wide variety of target molecules with carboxylic acid and alcohol substituents are available for post-synthetic reactions, 3) the place-exchange pathway which is often required to form functionalized Au NCs is avoided. However, the formation of amine-terminated Au NCs by direct synthesis is a large challenge due to the strong affinity of both amine and thiol groups towards Au. In addition, the stability of amine-terminated Au NCs in water can be problematic due to the aggregation of the NCs via hydrogen bonding.

So far, very few examples of atom-precise Au NCs with amine terminal groups have been reported.[83–89] In 2002, Hicks *et al.* synthesized 4-mercaptophenylamine Au MPCs and used them for the preparation of polymer/MPC multilayers by post-functionalization strategies.[86] Later in 2012, $Au_{25}(Cys)_{18}$ Au NCs (Cys = cysteine) were synthesized by a protection-deprotection method using cetyltrimethylammonium bromide (CTAB) as a protecting layer.[88] Steric protection of organic ligands controls the reduction process during the synthesis and leads to the formation of atom-precise Au NCs (Figure **1.9**).[11,88] The protecting groups are attached to the ligands by

electrostatic interactions. Therefore, the presence of negatively charged organic ligands is crucial in this method which limits the scope.

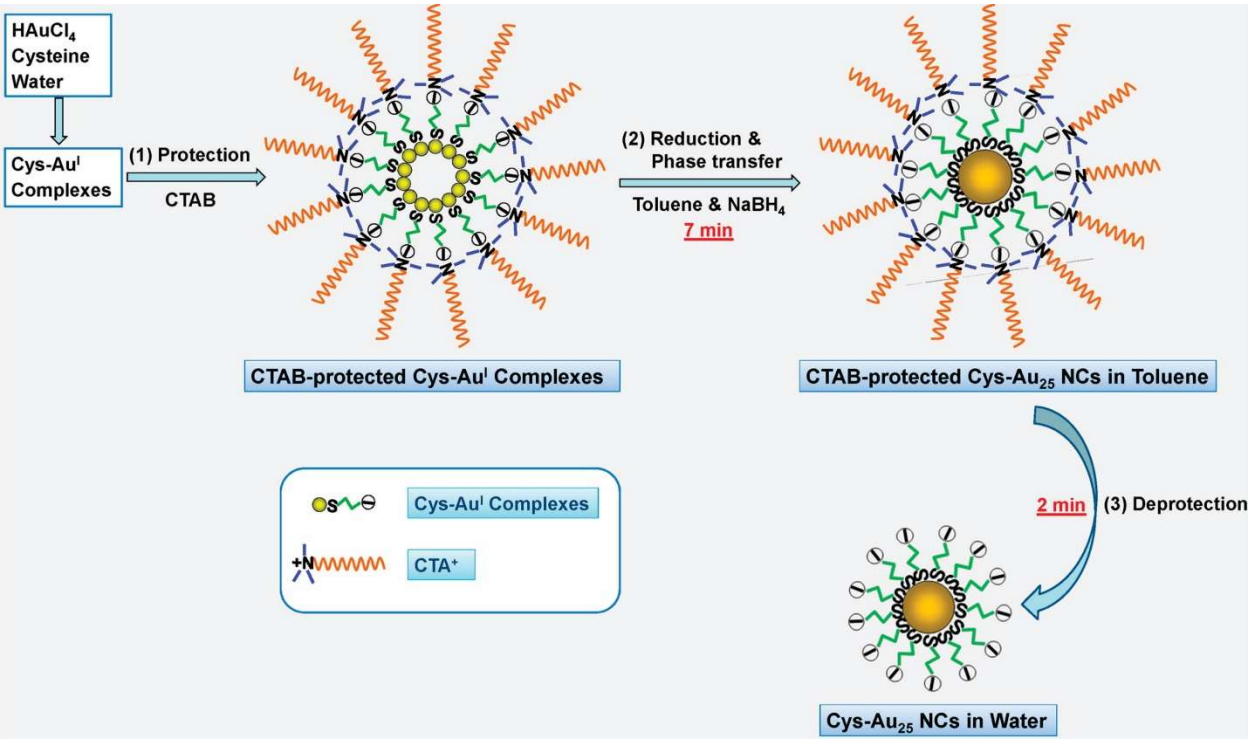

Figure 1.9. Synthesis of cysteine-Au_{25} NCs by the protection-deprotection method.[88] Reprinted with permission from ref 88. Copyright 2012 American Chemical Society.

In 2012, CO-directed synthesis of atom-precise $Au_{25}(Cys)_{18}$ NCs was shown by Xie and coworkers.[84] Recently, Gavriilidis and coworkers have also reported the synthesis of $Au_{25}(Cys)_{18}$ NCs by employing CO as a reducing agent in a tube-in-tube membrane reactor under 80 ℃.[90] Using CO as a mild reducing agent causes slow growth and controls the size-focusing process. However, the reduction capability of CO is pH-dependent and pH-induced aggregation could take place during the process.[91]

In another study, Lavenn *et al.* developed a new synthetic strategy for the synthesis of $Au_{25}L_{17}$ NCs with 4-aminothiophenolate ligands ($HSPhNH_2$) and found the clusters to be partly

stabilized by amino-Au interactions.[87] Xie and coworkers reported the synthesis of various mono-, bi-, tri-functionalized thiolate protected Au_{25} NCs including $Au_{25}(Cys)_x(MPA)_{18-x}$ NCs (MPA = 3-mercaptopropanoic acid) using a NaOH-mediated $NaBH_4$ reduction method.[89] This bi-functionalized ligand Au NC was the first report of direct synthesis of Au NCs bearing amino groups.

Previously our group studied the synthesis, characterization and post functionalization of Au NPs protected with glycine-cystamine (Gly-CSA) groups.[65,66,92] Peptide-stabilized Au MPCs were synthesized via the Brust-Schiffrin method by using tert-butyloxycarbonyl(Boc)-Gly-CSA or fluorenylmethyloxycarbonyl(Fmoc)-Gly-CSA capping agents, followed by deprotection. In both systems, atom-precise NCs were not formed. Deprotection of Boc in acidic solution gave Gly-CSA protected Au NPs which were 4 nm in size according to a weak plasmon shoulder around 540 nm at UV-Vis spectra. A small shift in the UV-Vis spectra from 530 nm to 540 nm and a slight increase in the intensity of the surface plasmon resonance band after deprotection suggests that there was growth and aggregation between particles. No such growth was seen in the Fmoc system after deprotection with piperidine. Further studies were carried out towards understanding the surface properties and reactivity of the Au NPs and found that these amine-terminated Au NPs could be functionalized by amide coupling reaction with activated esters.[65,92]

1.4 Dendrimers

Dendrimers are highly branched, star-shaped synthetic macromolecules with well-defined compositions and structures which consist of three parts: a central core, branches, and functional surface groups.[93–95] They have attracted growing interest among researchers because of their unique properties, such as size, reactivity and diversity of end groups, easy preparation, and

biocompatibility which make them suitable for biological, catalysis, and sensing applications.[96–100] High density of reactive functional groups of dendrimers makes them a suitable carrier in drug delivery and gene therapy. Their branched molecular structure significantly improves some physical and chemical properties of dendrimers compared to linear chain polymers. Branch end groups are responsible for some properties, such as solubility and reactivity of dendrimers. As a result, dendrimers with different chemical structures have different solubility and can have host-guest interactions with guest molecules. A variety of dendrimers with a wide range of structure and end groups have been discovered, such as poly(amidoamine) (PAMAM) dendrimers, poly(propyleneimine) (PPI) dendrimers, PEGylated dendrimers, and many others.[101]

1.4.1 Structure and synthesis

Dendrimers consist of three parts: a central core, branching layer, and end groups.[102,103] The generation of a dendrimer is defined as the number of repeat units in the branches from the core towards the end groups. Various generations of dendrimers can be formed by stepwise organic reactions. Dendrimers can be generated with a variety of sizes, end groups, and the number of branches. There are two strategies for dendrimer synthesis: divergent and convergent approaches. In divergent strategies, the synthesis is initiated with a multifunctional core, such as ethylenediamine. Different generations of dendrimers can be formed by a sequential series of reactions from the core outward. In convergent approaches, dendrons are synthesized first from the small molecules and are eventually attached to the core; thus, the reaction proceeds inward in this strategy.

1.4.2 Dendrimer-Encapsulated NPs (DENs)

Dendrimer-Encapsulated NPs (DENs) are of scientific and technological interest due to the uniform structure and composition of dendrimers which make them suitable to host metal NPs.[104] The metal NPs are entrapped within dendrimers and do not agglomerate. The dendrimer controls the availability of the surface of a metal NP and can be a selective gate for small molecules. Also, the terminal functional groups of dendrimers can be used to control some properties of the metal-encapsulated NPs such as solubility and facilitate the linking of these materials with other surfaces and molecules. For example, recently Fujita and coworkers have used poly(amidoamine)-dendrimer-encapsulated Au NPs as a catalyst for carboxylative cyclization of various propargylic amines.[105]

Recent studies suggest that Au DENs are interesting materials for applications in biology and medicine.[106] Au DENs prepared using amine-terminated dendrimers as a template have been used in cancer cell targeting and imaging by covalently linking the DENs to ligands such as folic acid and imaging molecules such as fluorescein isothiocyanate molecules. To decrease the toxicity and keep a neutral charge on the particle surface, a final acetylation step was done to convert the remaining amine-terminal groups to acetamides.[107]

Recently, Shi *et al.*[108] have reported the synthesis of AuAg alloy DENs using generation-5 poly(amidoamine) dendrimers as templates. The formed NPs had variable and controllable sizes, optical properties, X-ray attenuation characteristics, and high cytocompatibility after acetylation and showed great potential for CT imaging and other biomedical applications. Similarly, poly(amidoamine) (PAMAM) dendrimers modified with Gd(III) chelators and polyethylene

glycol have been used as templates to synthesize Au DENs for dual-mode computed tomography (CT)/ magnetic resonance (MR) imaging applications.[109]

1.4.3 Nanoparticle-Cored Dendrimers (NCDs)

Nanoparticle-cored dendrimers (NCDs) are a class of materials that possess a metal NP core stabilized by dendrons of different generations.[110] The huge advantage of these materials over DENs is their high stability. Furthermore, the stabilization of nanometer-sized particles with dendrons provides a small core with a thin organic layer with a precisely defined structure and composition, and tunable surface chemistry which makes them promising materials for many biomedical applications such as drug delivery, gene therapy, and biosensing.[106,109–111] Synthetic methodologies for NCDs are classified into three categories, as shown in Figure **1.10**.[112] Direct synthesis is one of the strategies in which the thiol-containing dendrons and/or dendrimers are used as stabilizers during the synthesis of the NP. NCDs formed by this method have a large void space close to the metal core and a large fraction of the surface area of the metallic core is unpassivated.[112] These features can increase the catalytic activity of the NP without sacrificing colloidal stability. The second method involves place-exchange reactions of the thiolate protecting groups by suitably capped dendrons. However, as mentioned earlier, using place exchange strategies causes some disadvantages such as 1) complete exchange can be hard to achieve, 2) functional ligands cannot be used in this method, and 3) it can result in NCDs with different core sizes. Post-functionalization is the third strategy that involves sequential reactions on the organic surface of MPCs (divergent approach) or reaction of the end groups of MPCs with suitable dendrons (convergent approach) to make NCDs of different generations.[112] This method provides

a wide variety of NCDs with various end groups and dendron generations as well as a uniform core size.

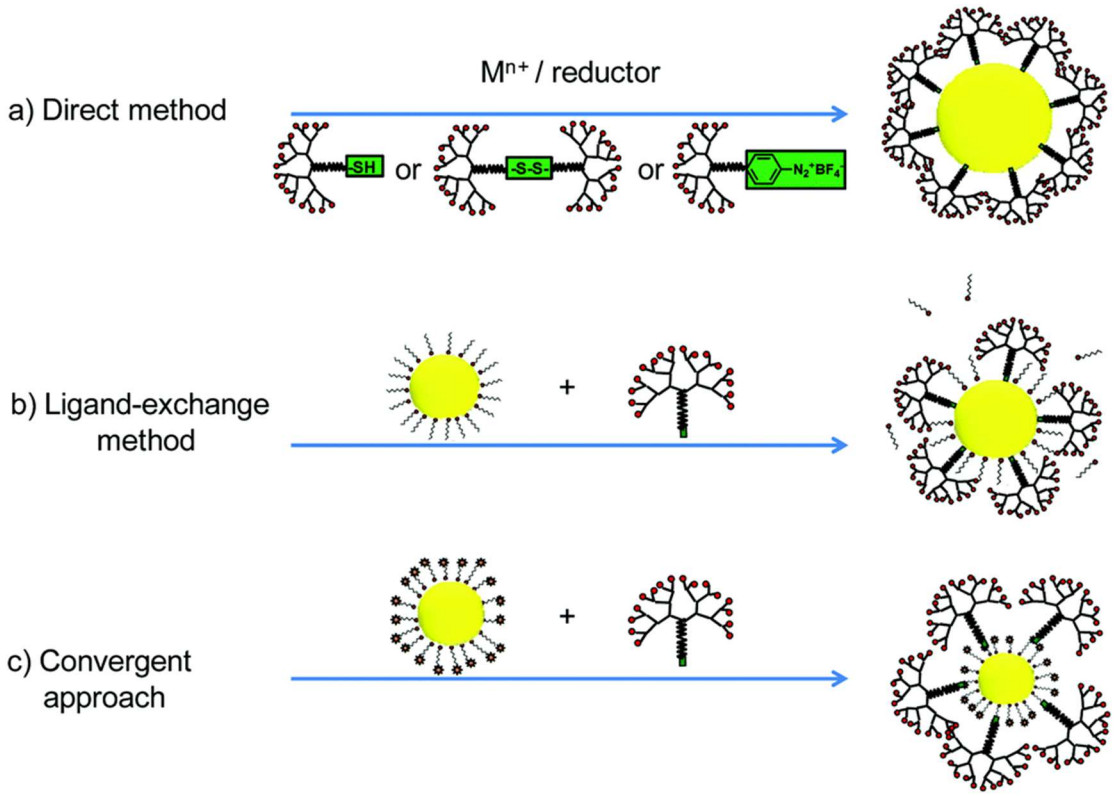

Figure 1.10. Three general synthetic strategies of NCDs.[110] Reprinted with permission from ref 110. Copyright 2015 The Royal Society of Chemistry.

1.4.4 DENs and NCDs in Catalysis

Recently, stabilization of NPs such as Pd, Pt, and Au by dendrimers and their application in catalysis have been increasingly reported.[113] For example, Pd-NCDs are an effective catalyst for Heck and Suzuki reactions,[114] and Pt-NCDs have been produced and used as a catalyst for the reduction of nitrobenzenes.[115] In particular, research attention has been focused on Au-NCDs due to their stability and unique features. Many chemical reactions such as carbon monoxide oxidation, selective hydrogenation of alkenes, and selective epoxidation of alkenes are catalyzed by Au catalysts.[116] In all these reactions, the size of the NPs, as well as the surface chemistry and density

of the dendrons/dendrimers, reportedly affected the catalytic activity and selectivity of Au catalysts, such that they could vary with chain length and composition. Chen and coworkers have modified generation-5 polyamidoamine by maleic anhydride and cysteamine,[117] followed by using the modified dendrimers to generate dendrimer-encapsulated Au NPs. The resulting NPs were reported to have higher stability, compatibility, and catalytic activity due to the ligand composition. Consequently, many methods have been developed to prepare Au NPs with specific size and surface properties.[34] In addition, it has been shown that catalysts consist of sterically bulky surfaces, such as dendrimer-templated catalysts, are effective for enabling chemical separations based on the size, shape, and charge of the organic surface of catalysts or the species being separated.[118,119] Crooks and coworkers studied the catalytic activity of three different generations of hydroxyl-terminated poly(amidoamine)-encapsulated Pd NPs.[120] They reported lower turnover frequencies for higher generations of dendrimer-encapsulated NPs and larger substrates. By controlling the steric hindrance of the ligand, it is possible to selectively control the access of substrates to the Au clusters. Generally, a higher density of the organic layer and organic ligands with sterically-bulky structures have preference for linear or small substrates.[34]

1.5 Thesis Objectives

Designing new strategies to generate atom-precise Au NCs is becoming more prominent due to their unique geometric and electronic structures and key applications as catalysts and biomarkers.[1-7] Since direct synthesis of atom-precise Au NCs with functionalized ligands is a big challenge, it is highly desirable to synthesize atom-precise Au NCs bearing reactive functional groups such as primary amines and generate a variety of functionalities on the surface of these NCs by using a post-functionalization strategy. The second chapter of this thesis provides a

synthetic method to produce monodisperse water-soluble amine-terminated Au NCs. This method is also a suitable strategy to produce stable atom-precise amine-terminated Au_{25} NCs. Also, it describes the subsequent functionalization of Au NCs by methyl acrylate via a Michael addition reaction with no change in core size.

Au cluster-cored dendrimers have received intense attention due to their molecular-like stability. There are various synthetic methods available for the preparation of amine-terminated Au cluster-cored dendrimers using thiolate-functionalized PAMAM-dendrons. However, due to the existence of amine functional groups, control of the size and agglomeration of these particles is a big challenge.[121] As a result, a surface modification approach is needed to make desirable functional groups on the organic surface and avoid any agglomeration after preparation. Furthermore, while cluster-cored dendrimers have been made via direct synthetic routes starting with branched ligands, divergent approaches that build functional groups on a cluster have not been attempted. The third chapter of this thesis looks to address whether making such clusters using such a divergent approach (post-functionalization) is viable, and what the advantages/disadvantages of such an approach are compared to convergent (direct synthesis) approaches in which the dendrons are made first, followed by cluster formation. Post functionalization should allow for greater control of the core size of the cluster, but may also result in a great degree of defects in the ligands due to incomplete reactions. In this chapter, a synthetic strategy has been developed to generate amine-terminated cluster-cored dendrimers with various core sizes and dendron generations. Finally, the catalytic activity of these Au cluster-cored dendrimers covered by different ligands has been studied for 4-nitrophenol reduction reactions, and structure/activity relationships are examined.

1.6 References

(1) Zhu, Y.; Qian, H.; Drake, B. A.; Jin, R. Atomically Precise $Au_{25}(SR)_{18}$ Nanoparticles as Catalysts for the Selective Hydrogenation of α,β-Unsaturated Ketones and Aldehydes. *Angew. Chem., Int. Ed.* **2010**, *122*, 1317–1320.

(2) Zhu, Y.; Qian, H.; Zhu, M.; Jin, R. Thiolate-Protected Au_n Nanoclusters as Catalysts for Selective Oxidation and Hydrogenation Processes. *Adv. Mater.* **2010**, *22*, 1915–1920.

(3) Zheng, K.; Setyawati, M. I.; Leong, D. T.; Xie, J. Surface Ligand Chemistry of Gold Nanoclusters Determines Their Antimicrobial Ability. *Chem. Mater.* **2018**, *30*, 2800–2808.

(4) Zheng, K.; Setyawati, M. I.; Leong, D. T.; Xie, J. Antimicrobial Gold Nanoclusters. *ACS Nano* **2017**, *11*, 6904–6910.

(5) Ani, B.; Brun, E.; Wang, Y.; Salassa, G.; Lacour, J.; Bürgi, T. Combined Spectroscopic Studies on Post-Functionalized Au_{25} Cluster as an ATR-FTIR Sensor for Cations. *Chem. Sci.* **2021**, *12*, 7419–7427.

(6) Zhang, L.; Wang, E. Metal Nanoclusters: New Fluorescent Probes for Sensors and Bioimaging. *Nano Today* **2014**, *9*, 132–157.

(7) Zhang, Y.; Zhang, C.; Xu, C.; Wang, X.; Liu, C.; Waterhouse, G. I. N.; Wang, Y.; Yin, H. Ultrasmall Au Nanoclusters for Biomedical and Biosensing Applications: A Mini-Review. *Talanta* **2019**, *200*, 432–442.

(8) Qian, H.; Zhu, Y.; Jin, R. Size-Focusing Synthesis, Optical and Electrochemical Properties of Monodisperse $Au_{38}(SC_2H_4Ph)_{24}$ Nanoclusters. *ACS Nano* **2009**, *3*, 3795–3803.

(9) Qian, H.; Jin, R. Ambient Synthesis of $Au_{144}(SR)_{60}$ Nanoclusters in Methanol. *Chem. Mater.* **2011**, *23*, 2209–2217.

(10) Chen, W.; Chen, S. Oxygen Electroreduction Catalyzed by Gold Nanoclusters: Strong Core Size Effects. *Angew., Chem. Int. Ed.* **2009**, *48*, 4386–4389.

(11) Nasaruddin, R. R.; Chen, T.; Yan, N.; Xie, J. Roles of Thiolate Ligands in the Synthesis,

Properties and Catalytic Application of Gold Nanoclusters. *Coord. Chem. Rev.* **2018**, *368*, 60–79.

(12) Kurashige, W.; Yamaguchi, M.; Nobusada, K.; Negishi, Y. Ligand-Induced Stability of Gold Nanoclusters: Thiolate versus Selenolate. *J. Phys. Chem. Lett.* **2012**, *3*, 2649–2652.

(13) Wan, X.-K.; Wang, J.-Q.; Nan, Z.-A.; Wang, Q.-M. Ligand Effects in Catalysis by Atomically Precise Gold Nanoclusters. *Sci. Adv.* **2017**, *34*, e1701823.

(14) Li, X.; Zhang, C.; Cai, S.; Lei, X.; Altoe, V.; Hong, F.; Urban, J. J.; Ciston, J.; Chan, E. M.; Liu, Y. Facile Transformation of Imine Covalent Organic Frameworks into Ultrastable Crystalline Porous Aromatic Frameworks. *Nat. Commun.* **2018**, *9*, 1–8.

(15) Munir, A.; Joya, K. S.; Ul Haq, T.; Babar, N. U. A.; Hussain, S. Z.; Qurashi, A.; Ullah, N.; Hussain, I. Metal Nanoclusters: New Paradigm in Catalysis for Water Splitting, Solar and Chemical Energy Conversion. *ChemSusChem* **2019**, *12*, 1517–1548.

(16) Sattler, K. The Energy Gap of Clusters, Nanoparticles, and Quantum Dots. Chapter 2 in Handbook of Thin Film Materials; Nalwa, H.S., Ed.; Nanomaterials and Magnetic Thin Films, Vol. 5; Academic Press: New York, 2002.

(17) Roduner, E. Size Matters: Why Nanomaterials Are Different. *Chem. Soc. Rev.* **2006**, *35*, 583–592.

(18) Daniel, M.-C.; Astruc, D. Gold Nanoparticles: Assembly, Supramolecular Chemistry, Quantum-Size-Related Properties, and Applications toward Biology, Catalysis, and Nanotechnology. *Chem. Rev.* **2004**, *104*, 293–346.

(19) Sýkora, D.; Kašička, V.; Mikšík, I.; Řezanka, P.; Záruba, K.; Matějka, P.; Král, V. Application of Gold Nanoparticles in Separation Sciences. *J. Sep. Sci.* **2010**, *33*, 372–387.

(20) Daraee, H.; Eatemadi, A.; Abbasi, E.; Aval, S. F.; Kouhi, M.; Akbarzadeh, A. Application of Gold Nanoparticles in Biomedical and Drug Delivery. *Artif. Cell. Nanomed. B.* **2016**, *44*, 410–422.

(21) Eustis, S.; El-Sayed, M. A. Why Gold Nanoparticles Are More Precious than Pretty Gold:

Noble Metal Surface Plasmon Resonance and Its Enhancement of the Radiative and Nonradiative Properties of Nanocrystals of Different Shapes. *Chem. Soc. Rev.* **2006**, *35*, 209–217.

(22) Amendola, V.; Pilot, R.; Frasconi, M.; Maragò, O. M.; Iatì, M. A. Surface Plasmon Resonance in Gold Nanoparticles: A Review. *J. Phys. Condens. Mat.* **2017**, *29*, 203002-203050.

(23) Jana, J.; Ganguly, M.; Pal, T. Enlightening Surface Plasmon Resonance Effect of Metal Nanoparticles for Practical Spectroscopic Application. *RSC adv*. **2016**, *6*, 86174-86211.

(24) Ye, R.; Zhukhovitskiy, A. V.; Deraedt, C. V.; Toste, F. D.; Somorjai, G. A. Supported Dendrimer-Encapsulated Metal Clusters: Toward Heterogenizing Homogeneous Catalysts. *Acc. Chem. Res.* **2017**, *50*, 1894–1901.

(25) Jin, R.; Zeng, C.; Zhou, M.; Chen, Y. Atomically Precise Colloidal Metal Nanoclusters and Nanoparticles: Fundamentals and Opportunities. *Chem. Rev.* **2016**, *116*, 10346–10413.

(26) Akola, J.; Kacprzak, K. A.; Lopez-Acevedo, O.; Walter, M.; Grönbeck, H.; Häkkinen, H. Thiolate-Protected Au_{25} Superatoms as Building Blocks: Dimers and Crystals. *J. Phys. Chem. C* **2010**, *114*, 15986–15994.

(27) Zhu, Y.; Jin, R.; Sun, Y. Atomically Monodisperse Gold Nanoclusters Catalysts with Precise Core-Shell Structure. *Catalysts* **2011**, *1*, 3–17.

(28) Jin, R. Quantum Sized, Thiolate-Protected Gold Nanoclusters. *Nanoscale* **2010**, *2*, 343–362.

(29) Chen, L. Y.; Wang, C. W.; Yuan, Z.; Chang, H. T. Fluorescent Gold Nanoclusters: Recent Advances in Sensing and Imaging. *Anal. Chem.* **2015**, *87*, 216–229.

(30) Akola, J.; Walter, M.; Whetten, R. L.; Ha¨kkinen, H.; Gro¨nbeck, H. On the Structure of Thiolate-Protected Au_{25}. *J. Am. Chem. Soc.* **2008**, *130*, 3756–3757.

(31) Zhu, M.; Aikens, C. M.; Hollander, F. J.; Schatz, G. C.; Jin, R. Correlating the Crystal Structure of A Thiol-Protected Au_{25} Cluster and Optical Properties. *J. Am. Chem. Soc.* **2008**, *130*, 5883–5885.

(32) Yau, S. H.; Varnavski, O.; Gilbertson, J. D.; Chandler, B.; Ramakrishna, G.; Goodson, T. Ultrafast Optical Study of Small Gold Monolayer Protected Clusters: A Closer Look at Emission. *J. Phys. Chem. C* **2010**, *114*, 15979–15985.

(33) Dasog, M.; Hou, W.; Scott, R. W. J. Controlled Growth and Catalytic Activity of Gold Monolayer Protected Clusters in Presence of Borohydride Salts. *Chem. Commun.* **2011**, *47*, 8569–8571.

(34) Shivhare, A.; Ambrose, S. J.; Zhang, H.; Purves, R. W.; Scott, R. W. J. Stable and Recyclable Au_{25} Clusters for the Reduction of 4-Nitrophenol. *Chem. Commun.* **2013**, *49*, 276–278.

(35) Negishi, Y.; Chaki, N. K.; Shichibu, Y.; Whetten, R. L.; Tsukuda, T. Origin of Magic Stability of Thiolated Gold Clusters: A Case Study on $Au_{25}(SC_6H_{13})_{18}$. *J. Am. Chem. Soc.* **2007**, *129*, 11322–11323.

(36) Zhu, M.; Lanni, E.; Garg, N.; Bier, M. E.; Jin, R. Kinetically Controlled, High-Yield Synthesis of Au_{25} Clusters. *J. Am. Chem. Soc.* **2008**, *130*, 1138–1139.

(37) Venzo, A.; Antonello, S.; Gascon, J. A.; Guryanov, I.; Leapman, R. D.; Perera, N. V.; Sousa, A.; Zamuner, M.; Zanella, A.; Maran, F. Effect of the Charge State (z = -1, 0, +1) on the Nuclear Magnetic Resonance of Monodisperse $Au_{25}[S(CH_2)_2Ph]_{18}$ z Clusters. *Anal. Chem.* **2011**, *83*, 6355–6362.

(38) Luo, Z.; Nachammai, V.; Zhang, B.; Yan, N.; Leong, D. T.; Jiang, D. E.; Xie, J. Toward Understanding the Growth Mechanism: Tracing All Stable Intermediate Species from Reduction of Au(I)-Thiolate Complexes to Evolution of Au_{25} Nanoclusters. *J. Am. Chem. Soc.* **2014**, *136*, 10577–10580.

(39) Parker, J. F.; Fields-Zinna, C. A.; Murray, R. W. The Story of a Monodisperse Gold Nanoparticle: $Au_{25}L_{18}$. *Acc. Chem. Res.* **2010**, *43*, 1289–1296.

(40) Antonello, S.; Hesari, M.; Polo, F.; Maran, F. Electron Transfer Catalysis with Monolayer Protected Au_{25} Clusters. *Nanoscale* **2012**, *4* (17), 5333–5342.

(41) Kawawaki, T.; Negishi, Y. Gold Nanoclusters as Electrocatalysts for Energy Conversion. *Nanomaterials* **2020**, *10*, 238-259.

(42) Luo, Z.; Zheng, K.; Xie, J. Engineering Ultrasmall Water-Soluble Gold and Silver Nanoclusters for Biomedical Applications. *Chem. Commun.* **2014**, *50*, 5143–5155.

(43) Katla, S. K.; Zhang, J.; Castro, E.; Bernal, R. A.; Li, X. Atomically Precise $Au_{25}(SG)_{18}$ Nanoclusters: Rapid Single-Step Synthesis and Application in Photothermal Therapy. *ACS Appl. Mater. Interfaces* **2018**, *10*, 75–82.

(44) Wu, Z.; Suhan, J.; Jin, R. One-Pot Synthesis of Atomically Monodisperse, Thiol-Functionalized Au_{25} Nanoclusters. *J. Mater. Chem.* **2009**, *19*, 622–626.

(45) Qian, H.; Zhu, M.; Andersen, U. N.; Jin, R. Facile, Large-Scale Synthesis of Dodecanethiol-Stabilized Au_{38} Clusters. *J. Phys. Chem. A* **2009**, *113*, 4281–4284.

(46) Kurashige, W.; Niihori, Y.; Sharma, S.; Negishi, Y. Precise Synthesis, Functionalization and Application of Thiolate-Protected Gold Clusters. *Coord. Chem. Rev.* **2016**, *320–321*, 238–250.

(47) Negishi, Y. Toward the Creation of Functionalized Metal Nanoclusters and Highly Active Photocatalytic Materials Using Thiolate-Protected Magic Gold Clusters. *Bull. Chem. Soc. Jpn.* **2014**, *87*, 375–389.

(48) Jimenez, V. L.; Georganopoulou, D. G.; White, R. J.; Harper, A. S.; Mills, A. J.; Lee, D.; Murray, R. W. Hexanethiolate Monolayer Protected 38 Gold Atom Cluster. *Langmuir* **2004**, *20*, 6864–6870.

(49) Chaudhari, V. S.; Borkar, R. M.; Murty, U. S.; Banerjee, S. Analytical Method Development and Validation of Reverse-Phase High-Performance Liquid Chromatography (RP-HPLC) Method for Simultaneous Quantifications of Quercetin and Piperine in Dual-Drug Loaded Nanostructured Lipid Carriers. *J. Pharm. Biomed. Anal.* **2020**, *186*, 113325–113336.

(50) Templeton, A. C.; Hostetler, M. J.; Kraft, C. T.; Murray, R. W. Reactivity of Monolayer-

Protected Gold Cluster Molecules: Steric Effects. *J. Am. Chem. Soc.* **1998**, *120*, 1906–1911.

(51) Liu, S.; Lämmerhofer, M. Functionalized Gold Nanoparticles for Sample Preparation: A Review. *Electrophoresis* **2019**, *40*, 2438–2461.

(52) Shibu, E. S.; Muhammed, M. A. H.; Tsukuda, T.; Pradeep, T. Ligand Exchange of $Au_{25}SG_{18}$ Leading to Functionalized Gold Clusters: Spectroscopy, Kinetics, and Luminescence. *J. Phys. Chem. C* **2008**, *112*, 12168–12176.

(53) Zhang, H.; Watanabe, T.; Okumura, M.; Haruta, M.; Toshima, N. Catalytically Highly Active Top Gold Atom on Palladium Nanocluster. *Nat. Mater.* **2012**, *11*, 49–52.

(54) Kurashige, W.; Niihori, Y.; Sharma, S.; Negishi, Y. Recent Progress in the Functionalization Methods of Thiolate-Protected Gold Clusters. *J. Phys. Chem. Lett.* **2014**, *5*, 4134–4142.

(55) De La Llave, E.; Scherlis, D. A. Selenium-Based Self-Assembled Monolayers: The Nature of Adsorbate - Surface Interactions. *Langmuir* **2010**, *26*, 173–178.

(56) Woehrle, G. H.; Brown, L. O.; Hutchison, J. E. Thiol-Functionalized, 1.5-nm Gold Nanoparticles through Ligand Exchange Reactions: Scope and Mechanism of Ligand Exchange. *J. Am. Chem. Soc.* **2005**, *127*, 2172–2183.

(57) Chen, X.; Addicoat, M.; Jin, E.; Zhai, L.; Xu, H.; Huang, N.; Guo, Z.; Liu, L.; Irle, S.; Jiang, D. Locking Covalent Organic Frameworks with Hydrogen Bonds: General and Remarkable Effects on Crystalline Structure, Physical Properties, and Photochemical Activity. *J. Am. Chem. Soc.* **2015**, *137*, 3241–3247.

(58) Templeton, A. C.; Wuelfing, W. P.; Murray, R. W. Monolayer-Protected Cluster Molecules. *Acc. Chem. Res.* **2000**, *33*, 27–36.

(59) Brust, M.; Walker, M.; Bethell, D.; Schiffrin, D. J.; Whyman, R. Synthesis of Thiol-Derivatised Gold Nanoparticles in a Two-Phase Liquid-Liquid System. *J. Chem. Soc. Chem. Commun.* **1994**, *7*, 801–802.

(60) Goulet, P. J. G.; Lennox, R. B. New Insights into Brust-Schiffrin Metal Nanoparticle

Synthesis. *J. Am. Chem. Soc.* **2010**, *132*, 9582–9584.

(61) Briñas, R. P.; Maetani, M.; Barchi, J. J. A Survey of Place-Exchange Reaction for the Preparation of Water-Soluble Gold Nanoparticles. *J. Colloid Interface Sci.* **2013**, *392*, 415–421.

(62) Templeton, A. C.; Hostetler, M. J.; Warmoth, E. K.; Chen, S.; Hartshorn, C. M.; Krishnamurthy, V. M.; Forbes, M. D. E.; Murray, R. W. Gateway Reactions to Diverse, Polyfunctional Monolayer-Protected Gold Clusters. *J. Am. Chem. Soc.* **1998**, *120*, 4845–4849.

(63) Jazayeri, M. H.; Amani, H.; Pourfatollah, A. A.; Pazoki-Toroudi, H.; Sedighimoghaddam, B. Various Methods of Gold Nanoparticles (GNPs) Conjugation to Antibodies. *Sens. Bio-Sensing Res.* **2016**, *9*, 17–22.

(64) Marjomäki, V.; Lahtinen, T.; Martikainen, M.; Koivisto, J.; Malola, S.; Salorinne, K.; Pettersson, M.; Häkkinen, H. Site-Specific Targeting of Enterovirus Capsid by Functionalized Monodisperse Gold Nanoclusters. *Proc. Natl. Acad. Sci.* **2014**, *111*, 1277–1281.

(65) Dasog, M.; Kavianpour, A.; Paige, M. F.; Kraatz, H. B.; Scott, R. W. J. Chemical Functionalization and Modification of Surface-Bound Cystamine-Giycine Monolayers on Gold Nanoparticles. *Can. J. Chem.* **2008**, *86*, 368–375.

(66) Lu, Y.; Dasog, M.; Leontowich, A. F. G.; Scott, R. W. J.; Paige, M. F. Fluorescently Labeled Gold Nanoparticles with Minimal Fluorescence Quenching. *J. Phys. Chem. C* **2010**, *114*, 17446–17454.

(67) Ghosh, P.; Han, G.; De, M.; Kim, C. K.; Rotello, V. M. Gold Nanoparticles in Delivery Applications. *Adv. Drug Deliv. Rev.* **2008**, *60*, 1307–1315.

(68) Yan, L.; Marzolin, C.; Terfort, A.; Whitesides, G. M. Formation and Reaction of Interchain Carboxylic Anhydride Groups on Self-Assembled Monolayers on Gold. *Langmuir* **1997**, *13*, 6704–6712.

(69) Sardar, R.; Funston, A. M.; Mulvaney, P.; Murray, R. W. Gold Nanoparticles: Past, Present, and Future. *Langmuir* **2009**, *25*, 13840–13851.

(70) Ingram, R. S.; Hostetler, M. J.; Murray, R. W. Poly-Hetero-ω-Functionalized Alkanethiolate-Stabilized Gold Cluster Compounds. *J. Am. Chem. Soc.* **1997**, *119*, 9175–9178.

(71) Hostetler, M. J.; Templeton, A. C.; Murray, R. W. Dynamics of Place-Exchange Reactions on Monolayer-Protected Gold Cluster Molecules. *Langmuir* **1999**, *15*, 3782–3789.

(72) Gunawardene, P. N.; Corrigan, J. F.; Workentin, M. S. Golden Opportunity: A Clickable Azide-Functionalized $[Au_{25}(SR)_{18}]^-$ Nanocluster Platform for Interfacial Surface Modifications. *J. Am. Chem. Soc.* **2019**, *141*, 11781–11785.

(73) Tiwari, P.; Vig, K.; Dennis, V.; Singh, S. Functionalized Gold Nanoparticles and Their Biomedical Applications. *Nanomaterials* **2011**, *1*, 31–63.

(74) Goodman, C. M.; McCusker, C. D.; Yilmaz, T.; Rotello, V. M. Toxicity of Gold Nanoparticles Functionalized with Cationic and Anionic Side Chains. *Bioconjug. Chem.* **2004**, *15*, 897–900.

(75) Qu, X.; Li, Y.; Li, L.; Wang, Y.; Liang, J.; Liang, J. Fluorescent Gold Nanoclusters: Synthesis and Recent Biological Application. *J. Nanomater.* **2015**, *2015*, 784097.

(76) Zeng, S.; Yong, K. T.; Roy, I.; Dinh, X. Q.; Yu, X.; Luan, F. A Review on Functionalized Gold Nanoparticles for Biosensing Applications. *Plasmonics* **2011**, *6*, 491–506.

(77) Uehara, N. Polymer-Functionalized Gold Nanoparticles as Versatile Sensing Materials. *Anal. Sci.* **2010**, *26*, 1219–1228.

(78) Roy, S.; Pericàs, M. A. Functionalized Nanoparticles as Catalysts for Enantioselective Processes. *Org. Biomol. Chem.* **2009**, *7*, 2669–2677.

(79) Corma, A.; Garci, H. Supported Gold Nanoparticles as Catalysts for Organic Reactions. *Chem. Soc. Rev.* **2008**, *37*, 2096–2126.

(80) Corma, A.; Concepción, P.; Domínguez, I.; Forné, V.; Sabater, M. J. Gold Supported on a Biopolymer (Chitosan) Catalyzes the Regioselective Hydroamination of Alkynes. *J. Catal.* **2007**, *251*, 39–47.

(81) González-Arellano, C.; Abad, A.; Corma, A.; García, H.; Iglesias, M.; Sánchez, F. Catalysis by Gold(I) and Gold(III): A Parallelism between Homo- and Heterogeneous Catalysts for Copper-Free Sonogashira Cross-Coupling Reactions. *Angew. Chem., Int. Ed.* **2007**, *46*, 1536–1538.

(82) Kaur, N.; Aditya, R. N.; Singh, A.; Kuo, T. R. Biomedical Applications for Gold Nanoclusters: Recent Developments and Future Perspectives. *Nanoscale Res. Lett.* **2018**, *13*, 1–12.

(83) Li, J.; Nasaruddin, R. R.; Feng, Y.; Yang, J.; Yan, N.; Xie, J. Tuning the Accessibility and Activity of $Au_{25}(SR)_{18}$ Nanocluster Catalysts through Ligand Engineering. *Chem. - Eur. J.* **2016**, *22*, 14816–14820.

(84) Yu, Y.; Luo, Z.; Yu, Y.; Lee, J. Y.; Xie, J. Observation of Cluster Size Growth in CO-Directed Synthesis of $Au_{25}(SR)_{18}$ Nanoclusters. *ACS Nano* **2012**, *6*, 7920–7927.

(85) Choi, M. M. F.; Douglas, A. D.; Murray, R. W. Ion-Pair Chromatographic Separation of Water-Soluble Gold Monolayer-Protected Clusters. *Anal. Chem.* **2006**, *78*, 2779–2785.

(86) Hicks, J. F.; Seok-Shon, Y.; Murray, R. W. Layer-by-Layer Growth of Polymer/Nanoparticle Films Containing Monolayer-Protected Gold Clusters. *Langmuir* **2002**, *18*, 2288–2294.

(87) Lavenn, C.; Albrieux, F.; Bergeret, G.; Chiriac, R.; Delichère, P.; Tuel, A.; Demessence, A. Functionalized Gold Magic Clusters: $Au_{25}(SPhNH_2)_{17}$. *Nanoscale* **2012**, *4*, 7334–7337.

(88) Yuan, X.; Yu, Y.; Yao, Q.; Zhang, Q.; Xie, J. Fast Synthesis of Thiolated Au_{25} Nanoclusters via Protection-Deprotection Method. *J. Phys. Chem. Lett.* **2012**, *3*, 2310–2314.

(89) Yuan, X.; Zhang, B.; Luo, Z.; Yao, Q.; Leong, D. T.; Yan, N.; Xie, J. Balancing the Rate of Cluster Growth and Etching for Gram-Scale Synthesis of Thiolate-Protected Au_{25}

Nanoclusters with Atomic Precision. *Angew. Chem., Int. Ed.* **2014**, *53*, 4623–4627.

(90) Gavriilidis, A.; Parkin, I. P.; Hwang, G. B.; Wu, G.; Shin, J.; Panariello, L.; Sebastian, V.; Karu, K.; Allan, E. Continuous Single-Phase Synthesis of [$Au_{25}(Cys)_{18}$] Nanoclusters and Their Photobactericidal Enhancement. *ACS Appl. Mater. Interfaces* **2020**, *12*, 49021–49029.

(91) Chen, T.; Xie, J. Carbon Monoxide: A Mild and Efficient Reducing Agent towards Atomically Precise Gold Nanoclusters. *Chem. Rec.* **2016**, *16*, 1761–1771.

(92) Leontowich, A. F. G.; Calver, C. F.; Dasog, M.; Scott, R. W. J. Surface Properties of Water-Soluble Glycine-Cysteamine-Protected Gold Clusters. *Langmuir* **2010**, *26*, 1285–1290.

(93) Tomalia, D. A. Birth of a New Macromolecular Architecture: Dendrimers as Quantized Building Blocks for Nanoscale Synthetic Polymer Chemistry. *Prog. Polym. Sci.* **2005**, *30*, 294–324.

(94) Yemul, O.; Imae, T. Synthesis and Characterization of Poly(Ethyleneimine) Dendrimers. *Colloid Polym. Sci.* **2008**, *286*, 747–752.

(95) Abbasi, E.; Aval, S. F.; Akbarzadeh, A.; Milani, M.; Nasrabadi, H. T.; Joo, S. W.; Hanifehpour, Y.; Nejati-Koshki, K.; Pashaei-Asl, R. Dendrimers: Synthesis, Applications, and Properties. *Nanoscale Res. Lett.* **2014**, *9*, 1–10.

(96) Cloninger, M. J. Biological Applications of Dendrimers. *Curr. Opin. Chem. Biol.* **2002**, *6*, 742–748.

(97) Lee, C. C.; MacKay, J. A.; Fréchet, J. M. J.; Szoka, F. C. Designing Dendrimers for Biological Applications. *Nat. Biotechnol.* **2005**, *23*, 1517–1526.

(98) Jang, W.-D.; Kamruzzaman Selim, K. M.; Lee, C.-H.; Kang, I.-K. Bioinspired Application of Dendrimers: From Bio-Mimicry to Biomedical Applications. *Prog. Polym. Sci.* **2009**, *34*, 1–23.

(99) Klajnert, B.; Bryszewska, M. Dendrimers: Properties and Applications. *Acta Biochim. Pol.* **2001**, *48*, 199–208.

(100) Mhlwatika, Z.; Aderibigbe, B. A. Application of Dendrimers for the Treatment of Infectious Diseases. *Molecules* **2018**, *23*, 2205–2237.

(101) Sowinska, M.; Urbanczyk-Lipkowska, Z. Advances in the Chemistry of Dendrimers. *New J. Chem.* **2014**, *38*, 2168–2203.

(102) Gupta, V.; Nayak, S. K. Dendrimers: A Review on Synthetic Approaches. *J. Appl. Pharm. Sci.* **2015**, *5*, 117–122.

(103) Augustus, E. N.; Allen, E. T.; Nimibofa, A.; Donbebe, W. A Review of Synthesis, Characterization and Applications of Functionalized Dendrimers. *Am. J. Polym. Sci.* **2017**, *7*, 8–14.

(104) Crooks, R. M.; Zhao, M.; Sun, L.; Chechik, V.; Yeung, L. K. Dendrimer-Encapsulated Metal Nanoparticles: Synthesis, Characterization, and Applications to Catalysis. *Acc. Chem. Res.* **2001**, *34*, 181–190.

(105) Matsuo, H.; Fujii, A.; Choi, J. C.; Fujitani, T.; Fujita, K. I. Carboxylative Cyclization of Propargylic Amines with Carbon Dioxide Catalyzed by Poly(Amidoamine)-Dendrimer-Encapsulated Gold Nanoparticles. *Synlett* **2019**, *30*, 1914–1918.

(106) Pietsch, T.; Appelhans, D.; Gindy, N.; Voit, B.; Fahmi, A. Oligosaccharide-Modified Dendrimers for Templating Gold Nanoparticles: Tailoring the Particle Size as a Function of Dendrimer Generation and Molecular Structure. *Colloid Surf., A* **2009**, *341*, 93–102.

(107) Shi, X.; Wang, S.; Meshinchi, S.; Van Antwerp, M. E.; Bi, X.; Lee, I.; Baker, J. R. Dendrimer-Entrapped Gold Nanoparticles as a Platform for Cancer-Cell Targeting and Imaging. *Small* **2007**, *3*, 1245–1252.

(108) Liu, H.; Shen, M.; Zhao, J.; Guo, R.; Cao, X.; Zhang, G.; Shi, X. Tunable Synthesis and Acetylation of Dendrimer-Entrapped or Dendrimer-Stabilized Gold-Silver Alloy Nanoparticles. *Colloid Surf. B-Biointerfaces* **2012**, *94*, 58–67.

(109) Wen, S.; Li, K.; Cai, H.; Chen, Q.; Shen, M.; Huang, Y.; Peng, C.; Hou, W.; Zhu, M.; Zhang, G.; Shi, X. Multifunctional Dendrimer-Entrapped Gold Nanoparticles for Dual-

Mode CT/MR Imaging Applications. *Biomaterials* **2013**, *34*, 1570–1580.

(110) Brunetti, V.; Bouchet, L. M.; Strumia, M. C. Nanoparticle-Cored Dendrimers: Functional Hybrid Nanocomposites as a New Platform for Drug Delivery Systems. *Nanoscale* **2015**, *7*, 3808–3816.

(111) Gopidas, K. R.; Whitesell, J. K.; Fox, M. A. Nanoparticle-Cored Dendrimers: Synthesis and Characterization. *J. Am. Chem. Soc.* **2003**, *125*, 6491–6502.

(112) Kumar, V. K. R.; Gopidas, K. R. Synthesis and Characterization of Gold-Nanoparticle-Cored Dendrimers Stabilized by Metal-Carbon Bonds. *Chem. -Asian J.* **2010**, *5*, 887–896.

(113) Li, N.; Echeverría, M.; Moya, S.; Ruiz, J.; Astruc, D. "Click" Synthesis of Nona-PEG-Branched Triazole Dendrimers and Stabilization of Gold Nanoparticles That Efficiently Catalyze p-Nitrophenol Reduction. *Inorg. Chem.* **2014**, *53*, 6954–6961.

(114) Gopidas, K. R.; Whitesell, J. K.; Fox, M. A.; Carolina, N. Synthesis, Characterization, and Catalytic Applications of a Palladium-Nanoparticle-Cored Dendrimer. *Nano Lett.* **2003**, *3*, 1757–1760.

(115) Yang, P.; Zhang, W.; Du, Y.; Wang, X. Hydrogenation of Nitrobenzenes Catalyzed by Platinum Nanoparticle Core-Polyaryl Ether Trisacetic Acid Ammonium Chloride Dendrimer Shell Nanocomposite. *J. Mol. Catal. A* **2006**, *260*, 4–10.

(116) Villa, A.; Dimitratos, N.; Chan-Thaw, C. E.; Hammond, C.; Veith, G. M.; Wang, D.; Manzoli, M.; Prati, L.; Hutchings, G. J. Characterisation of Gold Catalysts. *Chem. Soc. Rev.* **2016**, *45*, 4953–4994.

(117) Wang, L.; Yang, Q.; Cui, Y.; Gao, D.; Kang, J.; Sun, H.; Zhu, L.; Chen, S. Highly Stable and Biocompatible Dendrimer-Encapsulated Gold Nanoparticle Catalysts for the Reduction of 4-Nitrophenol. *New J. Chem.* **2017**, *41*, 8399–8406.

(118) Gray, A. L.; Hsu, J. T. Novel Sulfonic Acid-Modified Starburst Dendrimer Used as a Pseudostationary Phase in Electrokinetic Chromatography. *J. Chromatogr., A* **1998**, *824*, 119–124.

(119) Gao, H.; Carlson, J.; Stalcup, A. M.; Heineman, W. R. Separation of Aromatic Acids, DOPA, and Methyl-DOPA by Capillary Electrophoresis with Dendrimers as Buffer Additives. *J. Chromatogr. Sci.* **1998**, *36*, 146–154.

(120) Niu, Y.; Yeung, L. K.; Crooks, R. M. Size-Selective Hydrogenation of Olefins by Dendrimer-Encapsulated Palladium Nanoparticles. *J. Am. Chem. Soc.* **2001**, *123*, 6840–6846.

(121) Wang, R.; Yang, J.; Zheng, Z.; Carducci, M. D.; Jiao, J.; Seraphin, S. Dendron-Controlled Nucleation and Growth of Gold Nanoparticles. *Angew. Chem., Int. Ed.* **2001**, *7965*, 549–552.

Chapter 2

2 Size-Controlled Synthesis of Modifiable Glycine-Terminated Au Nanoclusters as a Platform for Further Functionalization

2.1 Abstract

An improved and simple synthetic method for producing stable narrow-sized glycine-cystamine (Gly-CSA)-protected Au nanoclusters (NCs) from protected Fmoc-glycine-cystamine-(Fmoc-Gly-CSA-) protected Au NCs is demonstrated in this study. The NC size and size distribution can be controlled directly as a function of reducing agent concentration with the formation of smaller NC core diameters at higher concentrations of $NaBH_4$. Furthermore, when using 0.30 M $NaBH_4$, three UV-Vis absorption peaks at 690, 440, and 390 nm were seen, which are consistent with the formation of Fmoc-Gly-CSA-protected $Au_{25}L_{18}$ NCs. After deprotection of the Gly-CSA functionalized Au NCs, the reactivity of the primary amine groups was investigated. Methyl acrylate-glycine-cystamine (MA-Gly-CSA)-protected Au NCs with terminal acetyl groups were formed via a Michael addition reaction of terminal amine groups with methyl acrylate. This reaction resulted in the formation of ester-terminated Au NCs including atom-precise MA-Gly-CSA $Au_{25}(SR)_{18}$ NCs. The functionalization was confirmed by ^1H NMR and UV-Vis spectra and TEM images of MA-Gly-CSA- and Gly-CSA-protected Au NCs showed the size of the NCs remained unchanged after the reaction. With controllable NC size and facile functionalization of

the Gly-CSA-protected Au NCs, these clusters have promising potential as scaffolds for biomedical applications.

2.2 Introduction

It is well-recognized that modifying the organic surface of nanoclusters (NCs) is a useful strategy to form new functional groups on metal NCs which makes them attractive for different applications.[1,2] One effective functionalization method involves terminal functional groups on the ligands which can be further derivatized to allow more control over chemical and physical properties.[3,4] Despite the large advances in the fabrication of atom-precise Au NCs, a vast majority of fundamental studies have been done on Au NCs stabilized by ligands that cannot be used for further chemistry, such as alkanethiolates.[5-8] Up to now, the most common functional groups on the surface of Au NCs are hydroxyl, carboxylate, ester, and amine groups.[9] Several studies have shown the preparation of carboxylic acid-terminated Au NCs with potential applications in many fields such as catalysts, sensors, and biological probes.[10-12] For example, Li *et al.* reported on the preparation of different ligands terminated with carboxylic acids for the functionalization of Au NCs ($Au_{25}L_{18}$) and studied the catalytic activity of the NCs for 4-nitrophenol hydrogenation.[13] More recently, Lu *et al*. have prepared 11-mercaptoundecanoic acid-functionalized Au NCs and showed they can be used for selective fluorometric hydrogen sulfide determination via a solvent-mediated aggregation-enhanced emission mechanism.[14] Furthermore, post-functionalization studies of Au NCs and particularly, atom-precise Au NCs, are quite rare.[1,15-18] Murray and coworkers studied the S_N2 reactivity of ω-bromoalkanethiolate-functionalized monolayer-protected gold clusters (MPCs) with primary amines.[1] Also, they published a series of amide and ester coupling reactions on hydroxyl and carboxylate MPCs and produced various

polyfunctionalized Au MPCs.[15] Mathew *et al.* demonstrated surface functionalization of $Au_{25}L_{18}$ NCs by the formation of host/guest inclusion complexes between the (*t*-butyl)benzyl groups of the Au surface and *β*-cyclodextrin.[17] Also, Gunawardene *et al.* reported the surface modification of $[Au_{25}L_{18}]^-$ NCs with azide moieties using azide-amide cycloaddition chemistry.[18] Such methods open up the possibility of functionalization and surface modification of very prominent Au_{25} NCs.

It is highly desirable to directly synthesize Au NCs with terminal amine surfaces due to their high reactivity which makes it a very useful functional group for further chemical functionalization. However, the formation of thiol-protected Au NCs with amine terminal groups by direct synthesis is a significant challenge due to the strong affinity of both nitrogen and sulfur groups towards Au and the aggregation of amine-terminated Au NCs via hydrogen bonding.[19] While a number of carboxylic acid and hydroxyl-terminated Au NCs have been synthesized,[20,21] very few examples of amine-terminated gold NCs have been reported.[13,19,22-26] In early work, Murray and coworkers reported ion-pair chromatography for size separation of polydisperse Au MPCs using N-acetyl-L-cysteine and tiopronin ligands.[22] Xie and coworkers introduced a CO-directed synthesis to produce atom-precise Au NCs ($Au_{25}(Cys)_{18}$) with cysteine ligands.[19] The Xie research group has also shown that steric protection using cetyltrimethylammonium bromide (CTAB) can control the reduction process during the synthesis and lead to the formation of $Au(Cys)_{25}$ NCs.[10,25] The same group developed a NaOH-mediated $NaBH_4$ reduction method to prepare various mono-, bi-, tri-functionalized thiolate protected Au_{25} NCs including $Au_{25}(Cys)_x(MPA)_{18-x}$ NCs (MPA = 3-mercaptopropanoic acid).[13,26] Lavenn *et al.* developed a new synthesis strategy for the synthesis of $Au_{25}L_{17}$ NCs with 4-aminothiophenolate ligands ($HSPhNH_2$) and found the clusters to be partly stable due to amino-Au interactions.[24] Place exchange pathways using thiolate ligands have also been used to functionalize NCs to add desired functional groups

such as carboxylic acids and amines.[23] However, this method is not facile, gives poor control over exact ligand exchange, and complete exchange is challenging. There are no effective synthetic protocols for atomically precise Au NCs bearing reactive primary amines. Therefore, a new and effective approach is essential for the generation of such atom-precise amine-terminated Au NCs.

Previously we studied the synthesis of glycine-cystamine stabilized MPCs which the surface chemistry can be modified by amide coupling reactions.[27-29] This work presents a new synthetic strategy that effectively overcomes some of the problems like the poor long-term stability of previously reported peptide-stabilized MPCs, and shows that atom-precise systems can be obtained. In this work we used a new single-phase synthetic method to produce narrow-sized and stable amine-terminated Au NCs with various core sizes in high yield using Fmoc-protected glycine-cystamine ligands; the use of the Fmoc protecting group prevents unwanted interactions between Au surfaces and amines during the Au NC synthesis. We show that the core size directly depends on the concentration of the reducing agent, and higher concentrations of reducing agent resulted in smaller core sizes, including $Au_{25}(SR)_{18}$ systems. Following Fmoc deprotection, stable Au NCs with primary amine functional groups on the surface were generated with little to no change of NC size. The reactivity of surface amine functional groups of Gly-CSA-protected Au NCs was investigated by the Michael addition reaction of these primary amines with methyl acrylate, and we show that the resulting NCs can be functionalized to give branched dendritic surfaces. Such amine-terminated Au NCs are appealing because they offer possibilities of post-functionalization of various molecules and biomolecules by coupling with amine groups.

2.3 Experimental Section

2.3.1 Materials

All solvents and chemicals were purchased commercially and used as received without any further purification. *N*-hydroxybenzotriazole (HOBT) and *O*-benzotriazole-*N*,*N*,*N*′,*N*′-tetramethyl-uronium hexafluorophosphate (HBtU) were purchased from AK Scientific. Cystamine dihydrochloride (98%), triethylamine (Et_3N, 99.5%), sodium cyanide (97%), sodium borohydride ($NaBH_4$), tetrahydrofuran (THF), dichloromethane (CH_2Cl_2), methanol (MeOH), and acetonitrile (CH_3CN) were purchased from Fisher Scientific. Fmoc-glycine (Fmoc-Gly-OH) was purchased from Millipore Sigma. Hydrogen tetrachloroaurate(III) trihydrate ($HAuCl_4 \cdot 3H_2O$, 99.9% on metal basis), tetraoctylammonium bromide (TOAB, 98%), piperidine (99%), and methyl acrylate (99%) were purchased from Sigma Aldrich. Deionized water (resistivity 18.2 MΩ.cm) was used for all experiments. Deuterated chloroform ($CDCl_3$, 99.8 atom % D), deuterium oxide (D_2O, 99.9 atom % D), and deuterated dimethylsulfoxide (d_6-DMSO, 99.9 atom % D) were purchased from Cambridge Isotope Laboratories.

2.3.2 Synthesis of Fmoc-Gly-CSA

Fmoc-Gly-CSA was synthesized by established literature protocols previously reported.[30] Briefly, Fmoc-Gly-OH (20 mmol, 5.94 g), cystamine dihydrochloride (10 mmol, 2.25 g), HOBT hydrate (30 mmol, 4.59 g), and HBTU (30 mmol, 1138 g) were added to 300 mL CH_2Cl_2 in a round-bottomed flask. Then 10 mL of triethylamine was added to the solution. The mixture was milky white in colour before the addition of triethylamine, and after adding the solution became clear. The mixture was left for 24 h and became milky white in colour again. Then the white solid was collected by filtration and washed several times by chloroform and methanol. The organic

layer was washed with saturated $NaHCO_3$ following by several washings with methanol and water. The solvent was removed by rotary evaporation under vacuum and the remaining product was washed several times by chloroform and methanol to remove impurities and excess triethylamine. Yield: (6.15 g, 87%); ^{1}H NMR (500 MHZ, *d*$_6$-DMSO, ppm): δ 8.06 (t, 1H, J= 5.2 Hz, cystamine NH), 7.89 (d, 2H, J= 7.5 Hz, Fmoc Ar), 7.72 (d, 2H, J= 7.5 Hz, Fmoc Ar), 7.54 (t, 1H, H= 6.0 Hz, Gly NH), 7.42 (t, 2H, J= 7.5 Hz, Fmoc), 7.33 (t, 2H, J= 7.2 Hz, Fmoc), 4.29 (d, 2H, J= 7 Hz, Fmoc CH_2), 4.22 (t, 1H, J= 6.7 Hz, Fmoc CH), 3.60 (d, 2H, J= 6 Hz, Gly CH_2), 3.34-3.37 (m, 2H, cystamine CH_2-N), 2.78 (t, 2H, J=6.7 Hz, CH_2S); ^{13}C NMR (125 MHz, *d*$_6$-DMSO, ppm): δ 37.5 (CH_2-S), 38.5 (CH_2-NH cystamine), 43.9 (CH_2 of Gly), 47.1 (CH of Fmoc), 66.2 (CH_2 of Fmoc), 120.6, 125.7, 127.5, 128.1, 141.2, 144.3, 156.9 (C=O of Fmoc), 169.7 (C=O of Fmoc).

2.3.3 Synthesis of Fmoc-Gly-CSA- and Gly-CSA-Protected Au NCs

$HAuCl_4 \cdot 3H_2O$ (0.147 mmol, 50 mg) was added to 10 mL THF followed by the addition of TOAB (0.177 mmol, 0.10 g). The colour changed from yellow to red. After 10 min, Fmoc-Gly-CSA (0.294 mmol, 0.21 g) was added to the solution. After stirring for 5 min, freshly prepared $NaBH_4$ (using variable concentrations) in 2.0 mL water was added to the solution all at once. In total, four concentrations of $NaBH_4$ (0.15, 0.23, 0.30, and 0.32 M) were used in this synthesis. After 48 h, the solution was centrifuged (8000 rpm, 5 min) to remove larger particles. The resulting supernatant is pale brown and contains Fmoc-Gly-CSA-protected Au NCs.

Fmoc-protected Au NCs were either precipitated out by methanol for characterization or were directly reacted to remove Fmoc protecting groups from the surface by piperidine and form Gly-CSA-protected Au NCs. To obtain purified Fmoc-Gly-CSA Au NCs, 10 mL methanol was added to the supernatant and the precipitate was collected by centrifugation at 8000 rpm for 10

min. The resulting brown powder was washed several times with methanol for further purification. To remove the protecting Fmoc group from the Au NCs, 5 mL piperidine was added to the supernatant immediately following the synthesis of Fmoc-Gly-CSA Au NCs. After stirring for 30 min, the solution was centrifuged (8000 rpm, 5 min), and the Gly-CSA-protected Au NCs were washed several times by $CHCl_3$ for further purification. Fmoc-Gly-CSA Au NC yields (mg): for 0.15 M $NaBH_4$: 4.5 mg; for 0.23 M $NaBH_4$: 4.3 mg; for 0.30 M $NaBH_4$: 4.0 mg.

2.3.4 Synthesis of MA-Gly-CSA-Protected Au NCs

Au NCs synthesized using 0.23 M and 0.30 M $NaBH_4$ were used to study the reactivity of amine groups on Gly-CSA-protected Au NCs. Gly-CSA-protected Au NCs (5.0 mg) were dissolved in a 6 mL mixture of water:acetonitrile (1:1 volume ratio) followed by the addition of methyl acrylate (33.1 mmol, 3.0 mL). The reaction mixture was kept under N_2 for 24 h. Then 10 mL CH_2Cl_2 was added to the solution and the organic phase was separated and dried over sodium sulfate. CH_2Cl_2 and excess methyl acrylate were removed under vacuum. The yield of the resulting MA-Gly-CSA Au NCs and Au_{25}(CSA-Gly-MA)$_{18}$ NCs was 4.6 mg and 4.5 mg, respectively.

2.3.5 Cyanide Etching of MA-Gly-CSA-Protected Au NCs

A solution of MA-Gly-CSA-protected Au NCs in chloroform (5.0 mg/ml) was mixed with an aqueous solution of sodium cyanide (1.0 M) in a 1:1 volume ratio. The mixture was stirred at room temperature under air until the organic layer turned colourless. The organic layer was separated and washed with water several times and characterized by ^{1}H NMR.

2.3.6 Characterization

UV-Vis analyses were done using a Varian Cary 50 UV-Visible spectrophotometer with an optical path length of 1 cm. Au NCs were analyzed by transmission electron microscopy (TEM) using a Hitachi HT 7700 TEM operating at 100 kV. TEM samples were prepared by drop-casting NC solutions onto a carbon-coated 400 mesh Cu TEM grid (Electron Microscopy Sciences, Hatfield, PA) and dried under ambient conditions prior to TEM analysis. Average NC diameters were determined by manually measuring about 100 NCs from images obtained for each sample using the ImageJ program.[31] All NMR spectra (1D and 2D-COSY) were recorded on a Bruker AMX-500 spectrometer operating at 500 and 125 MHz for ^{1}H and ^{13}C, respectively. Chemical shifts were referenced to the residual proton and carbon signals of deuterated solvents. Fourier-Transform Infrared Spectroscopy (FTIR) measurements were made on a Bruker Tension 27 ATR FTIR spectrometer.

2.4 Results and Discussion

Previously, we reported the synthesis and characterization of peptide-stabilized Au MPCs via the Brust-Schiffrin method by using Boc-Gly-CSA and Fmoc-Gly-CSA capping agents, followed by deprotection of the Boc or Fmoc groups.[27-30] We observed that smaller, more monodisperse Au MPCs were formed by using a much bulkier protecting group (Fmoc). However, the synthesized Gly-CSA-protected Au MPCs were not atom-precise and pH-dependent aggregation between particles after deprotection was seen.[27,30] In this study we proposed a new single-phase synthetic approach to address these challenges (Scheme **2. 1**).

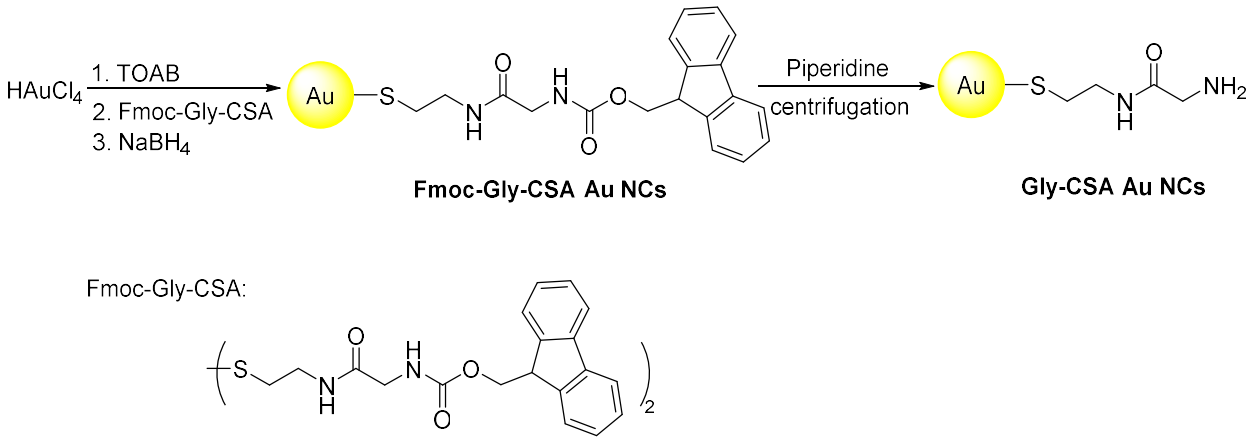

Scheme 2.1. Synthesis of Gly-CSA-protected Au NCs (note, only one thiolate is shown for clarity).

To investigate the influence of the amount of reducing agent on the size of Fmoc-Gly-CSA-protected Au NCs and to examine if atom-precise clusters could be obtained, Au NCs were prepared by using various concentrations of sodium borohydride ($NaBH_4$). Recently, we found that atom-precise Au MPCs could be synthesized using a novel BH_4^- purification strategy.[32] We utilized this approach in the present study and found that by tuning the amount of $NaBH_4$, fairly monodisperse atom-precise Gly-CSA-protected Au NCs could be formed. According to UV-Vis measurements, increasing the concentration of the reducing agent in the reaction mixture in the range from 0.15 M up to 0.32 M results in the formation of Au Fmoc-Gly-CSA-protected NCs with decreasing core diameter (Figure **2.1a**), albeit with a small sacrifice in yields. As seen in Figure **2.1a**, a weak and broad surface plasmon band at 520-530 nm in the UV-Vis was observed using 0.15 M $NaBH_4$, whereas at 0.23 M $NaBH_4$ the plasmon band disappeared, which indicates a decreasing core size. As seen in Figure **2.1b**, at 0.30 M $NaBH_4$, three absorption peaks were observed at around 690, 440, and 390 nm which are spectroscopic fingerprints of Au_{25} NCs and are strongly suggestive of the formation of Fmoc-Gly-CSA-protected $Au_{25}(SR)_{18}$ NCs.[29] We were not able to obtain mass spectrometric verification of this structure using 1,8,9-

trihydroxyanthracene as the matrix in THF; however, TEM analysis (below) confirms that the resulting clusters have a core size that is consistent with Au_{25} clusters. With a further increase in the concentration of the reducing agent concentration (0.32 M $NaBH_4$ and above), rapid precipitation takes place, and the solution turns clear immediately (i.e., no clusters remain in solution).

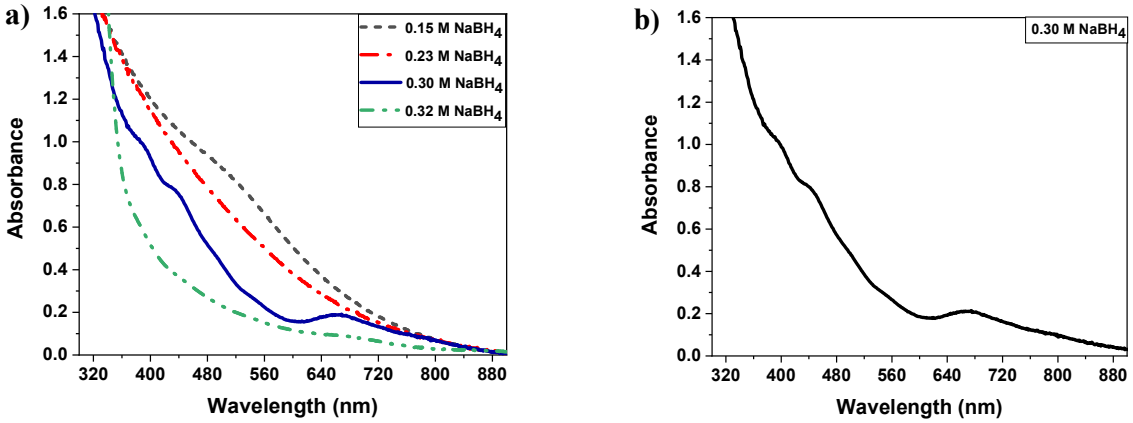

Figure 2.1. UV-Vis spectra of Fmoc-Gly-CSA-protected Au NCs synthesized using (a) various concentrations of $NaBH_4$ and (b) 0.30 M $NaBH_4$.

Figure **2.2** shows TEM images of the NCs which show that the diameter of the Au cores decreases with increased $NaBH_4$ concentration. The formed Fmoc-Gly-CSA-protected Au NCs shown are almost monodisperse with average sizes of 2.2 ± 0.3 nm (0.15 M $NaBH_4$, Figure **2.2a**), 1.7 ± 0.3 nm (0.23 M $NaBH_4$, Figure **2.2c**), and 1.1 ± 0.2 nm (0.30 M $NaBH_4$, Figure **2.2e**). Particle size histograms can be found in Figure **2.3**. In order to obtain amine-terminated Au NCs, the Fmoc group was removed by using piperidine. Subsequent centrifugation results in water-soluble amine-terminated Au NCs as shown in Scheme **2.1**. UV-Vis and TEM analysis were conducted before and after deprotection. Little to no change in the UV-Vis spectra of Au NCs after deprotection (Figure **2.4**) was seen, which suggests that there was no change in NC size upon deprotection by

piperidine, demonstrating the stability of the particles. Figure **2.2b, d, f** show TEM images of the final Gly-CSA-protected Au NCs after deprotection. The TEM results clearly show that after deprotection the Au NC sizes remained fairly consistent in both systems, with average NC sizes of 2.0 ± 0.4 nm (0.15 M $NaBH_4$, Figure **2.2b**), 1.8 ± 0.3 nm (0.23 M $NaBH_4$, Figure **2.2d**) and 1.2 ± 0.3 nm (0.30 M $NaBH_4$, Figure **2.2f**). For the latter, the average TEM NC size is a good agreement with literature values reported for $Au_{25}L_{18}$ NC core sizes.[33]

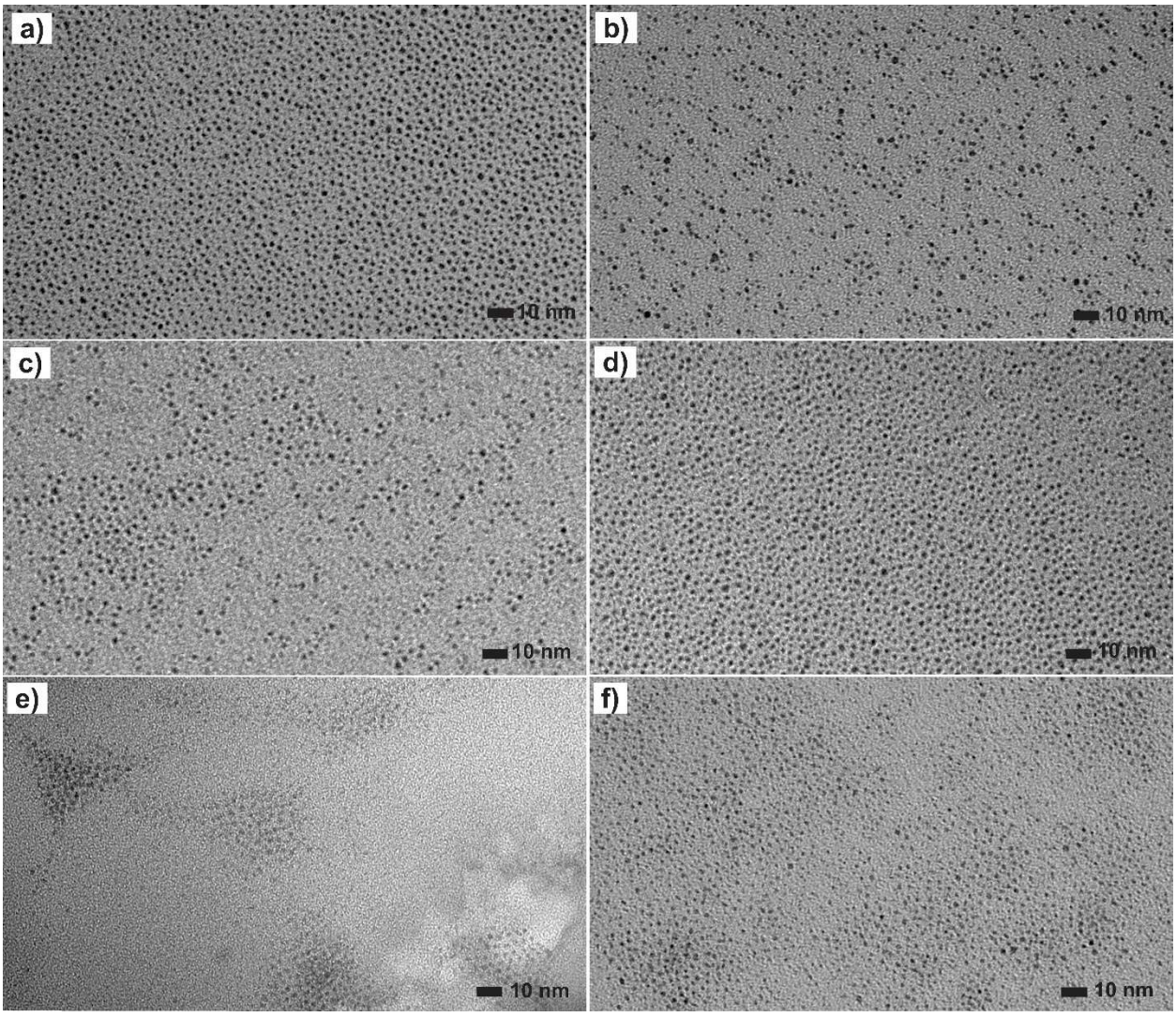

Figure 2.2. TEM images of Au NCs (a) before and (b) after deprotection using 0.15 M $NaBH_4$ for synthesis, (c) before and (d) after deprotection using 0.23 M $NaBH_4$ for synthesis, and (e) before (f) after deprotection using 0.30 M $NaBH_4$ for synthesis.

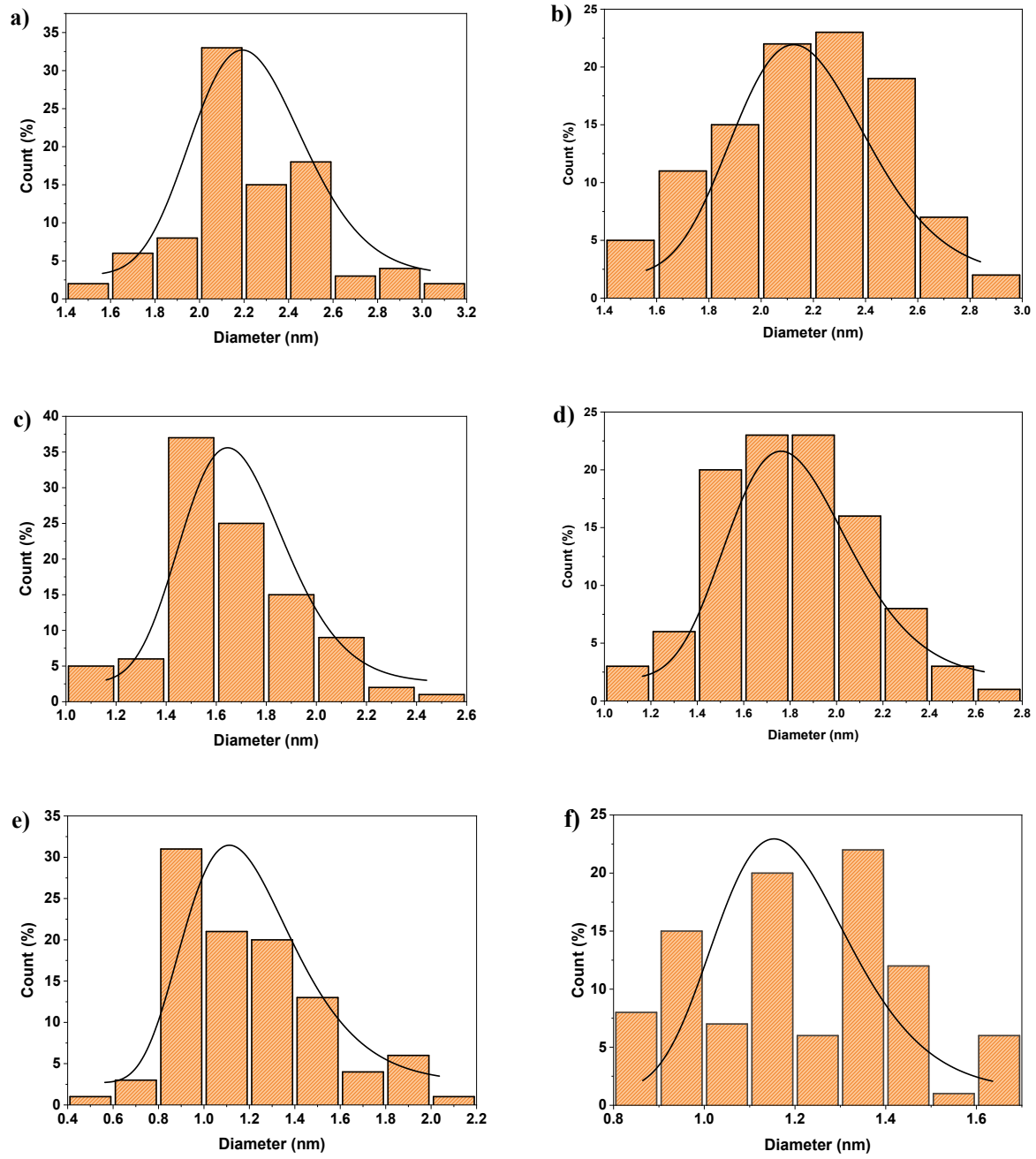

Figure 2.3. Size distribution histograms and normal distribution fit (solid line) of Au NCs (a) before and (b) after deprotection using 0.15 M $NaBH_4$ for synthesis, (c) before and (d) after deprotection using 0.23 M $NaBH_4$ for synthesis, and (e) before (f) after deprotection using 0.30 M $NaBH_4$ for synthesis.

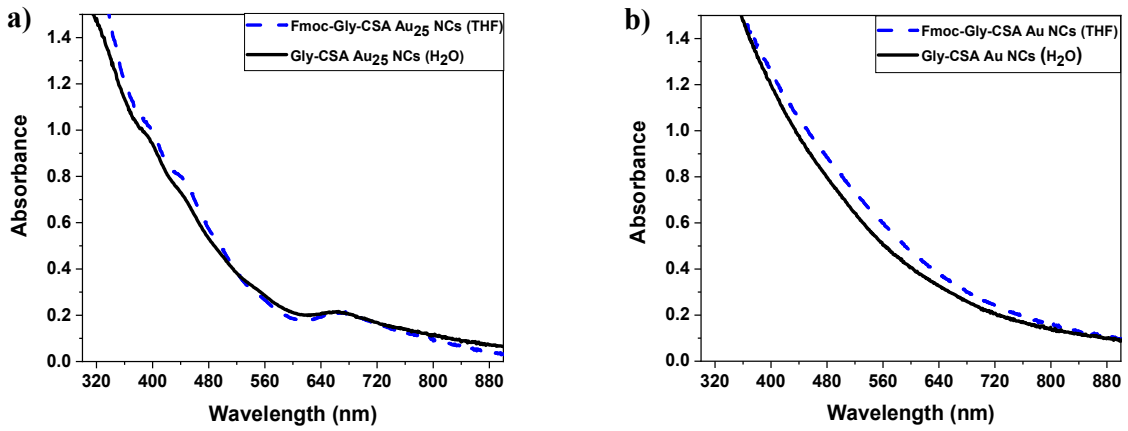

Figure 2.4. UV-Vis spectra of Fmoc-Gly-CSA and Gly-CSA-protected Au NCs synthesized using (a) 0.30 M $NaBH_4$ and (b) 0.23 M $NaBH_4$. Spectra for Fmoc-Gly CSA systems were collected in THF, while spectra for Gly-CSA systems were collected in H_2O.

^{1}H NMR measurements of the Fmoc-Gly-CSA ligand and Fmoc-Gly-CSA-protected Au NCs are shown in Figure **2.5**. Broad peaks are seen in the range between 6.8-8.5 ppm which are assigned to aromatic hydrogens of the fluorenyl ring of the Fmoc group. Broad overlapping peaks in the range between 3.5-4.3 ppm are assigned to the methylene group on the glycine, the methylene group on the cystamine, and the methylene and methine hydrogens of the Fmoc group, respectively. The ^{1}H NMR peaks of ligands attached to Au NCs (Figure **2.5b and c**) are all broadened compared to free ligands (shown in Figure **2.5a**). This is likely because of spin-spin relaxation (T_2) broadening due to the larger NC size.[34] In addition, deviations in Au-SR binding sites and as a result, distribution of chemical shifts could also contribute to broadening. Furthermore, the proton from the methylene group of cystamine which is attached to sulfur group is highly broadened such that it cannot be seen. The higher broadening of groups near the core relative to end groups has been reported by others and is a result of faster spin-spin relaxation (T_2)

due to higher packing density closer to the core and as a result, restricted movements of those groups.[35,27]

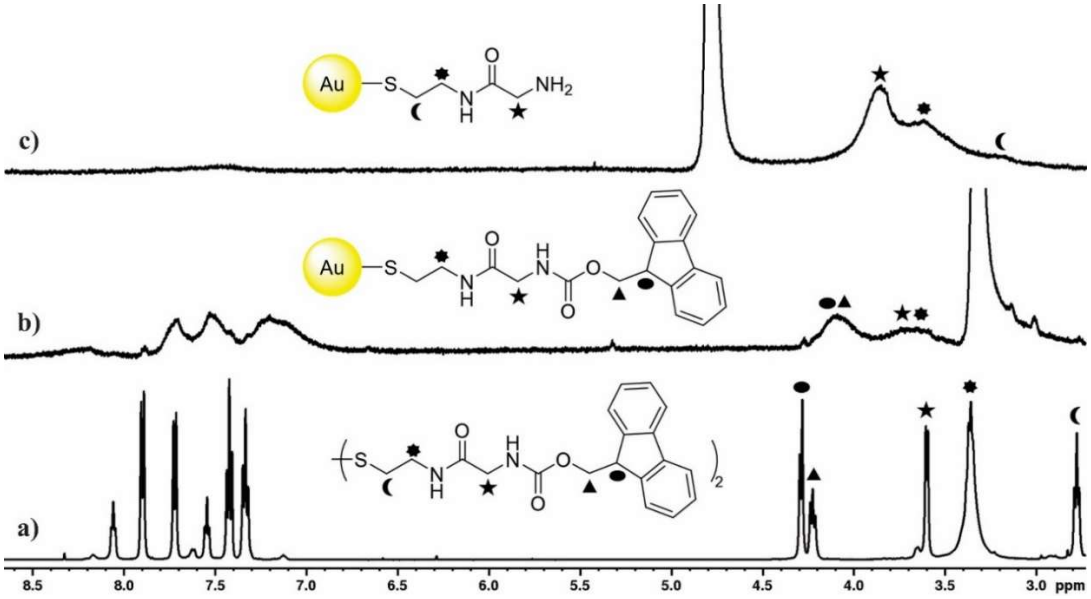

Figure 2.5. ^{1}H NMR spectra of (a) free Fmoc-Gly-CSA, (b) Fmoc-Gly-CSA-protected Au NCs in d_6-DMSO and (c) Gly-CSA-protected Au NCs in D_2O. NCs were synthesized using 0.30 M $NaBH_4$.

Figure **2.5c** shows the ^{1}H NMR of particles after deprotection. ^{1}H NMR of the Gly-CSA-protected Au NCs in D_2O shows no peaks for the fluorenyl ring of the Fmoc group, indicating that deprotection with piperidine was successful. Two broad peaks at about 3.6 and 3.8 ppm are assigned to methylene protons of cystamine and glycine, respectively. A significantly broad signal at 3.3 ppm is assigned to the methylene protons of cystamine that are attached to sulfur groups. The hydrogens of the amine group are absent in D_2O due to hydrogen-deuterium exchange, but they appear at around 8.0 ppm as a broad peak in d_6-DMSO (shown later in Figure **2.8a**).

The stability of Fmoc-Gly-CSA- and Gly-CSA-protected Au NCs were studied in solution. The stability towards precipitation of Fmoc-Gly-CSA-protected Au NCs in THF is size-dependent and the higher the reducing agent concentration, the smaller the NC size and as a result, the lower

the solubility/stability of Fmoc-protected Au NCs in THF. For these particles, π-π stacking of the aromatic groups in Fmoc may promote particle self-assembly and subsequent precipitation. For example, Fmoc-Gly-CSA-protected Au_{25} NCs were not easily redispersed in THF after purification. This is likely due to the higher density of the ligand around the small Au core of Au_{25} NCs, and as a result, higher π-π interactions. In contrast, Fmoc-Gly-CSA-protected Au NCs prepared at lower concentrations of $NaBH_4$ (0.15 M and 0.23 M) are stable against aggregation during and after the purification process. Furthermore, it is observed that these Au NCs (synthesized using 0.15 M and 0.23 M $NaBH_4$) are stable in THF for several weeks and the core size of the NCs prepared at 0.23 M $NaBH_4$ remained unchanged in THF for three weeks at room temperature. After deprotection, the Gly-CSA-protected Au NCs exhibit high stability in solution due to lack of π-π interactions. These particles were stable in water for at least three months after air was removed under vacuum (Figure **2.6a**) and only showed moderate aggregation when stored under N_2 without first pumping out dissolved O_2 from the water (Figure **2.6b**). However, particle growth and precipitation were observed for Gly-CSA-protected Au NCs dispersed in water and stored for one month in air. (Figure **2.6c**) The growth and precipitation of the NCs while stored in the air suggests that slow thiol oxidation occurs in the presence of O_2, which has been reported for other systems.[36]

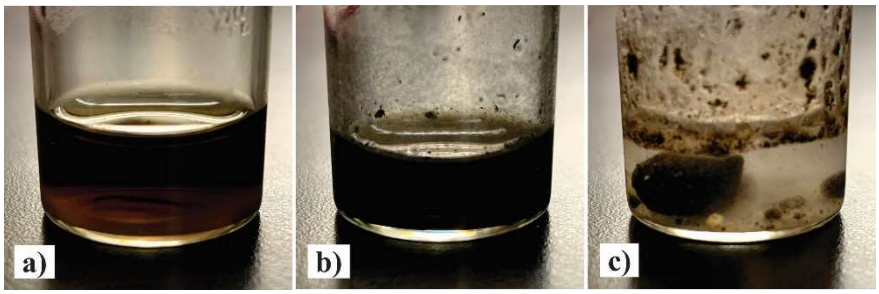

Figure 2.6. Stability of Gly-CSA-protected Au_{25} NCs in water (a) after removal of air under vacuum, (b) under N_2, and (c) under air stored for one month.

After synthesis of the Gly-CSA-protected Au NCs, functionalization of the primary terminal amine groups was investigated. The reactivity of Au MPCs derivatized with Gly-CSA was previously studied by our group.[27,28] Previously we studied the amide coupling reaction between terminal amine groups on MPCs and various activated esters and found that further functionalization can be performed, albeit sometimes with some (undesirable) growth in the Au core size. In this work, the reaction of Gly-CSA-protected Au NCs and methyl acrylate was investigated, and reactive ester functional groups were formed on the surface of Au NCs which can be a potential site for further functionalization and bio-conjugation. The synthetic strategy used is shown in Scheme **2.2**; two methyl acrylate groups were coupled to each primary amine by a Michael addition reaction. Au NCs first synthesized at 0.23 M and 0.30 M $NaBH_4$ were each used to study the reactivity of amine groups on Gly-CSA-protected Au NCs. Figure **2.7** shows the UV-Vis spectra and TEM images of the final clusters after reaction with methyl acrylate. As shown in Figure **2.7a** and **2.7b**, the UV-Vis spectra of particles after reaction are similar to the initial Gly-CSA-protected Au NCs. In addition, the final particles are fairly monodisperse based on TEM images, with average particle sizes of 1.8 ± 0.3 nm for the 0.23 M $NaBH_4$ sample and 1.2 ± 0.3 nm for the 0.30 M $NaBH_4$ sample, which are similar to the core sizes of the NCs before reaction.

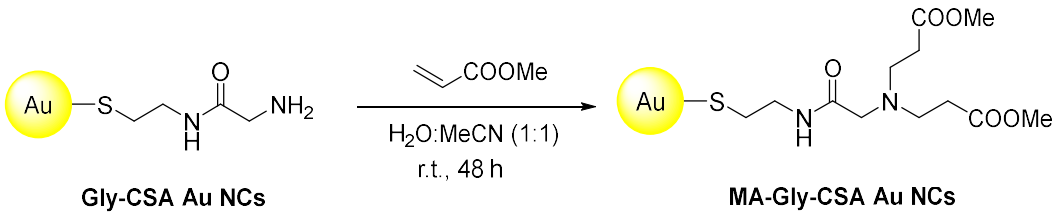

Gly-CSA Au NCs MA-Gly-CSA Au NCs

Scheme 2.2. Michael addition reaction of Gly-CSA-protected Au NCs with methyl acrylate (again, only one thiolate shown for clarity).

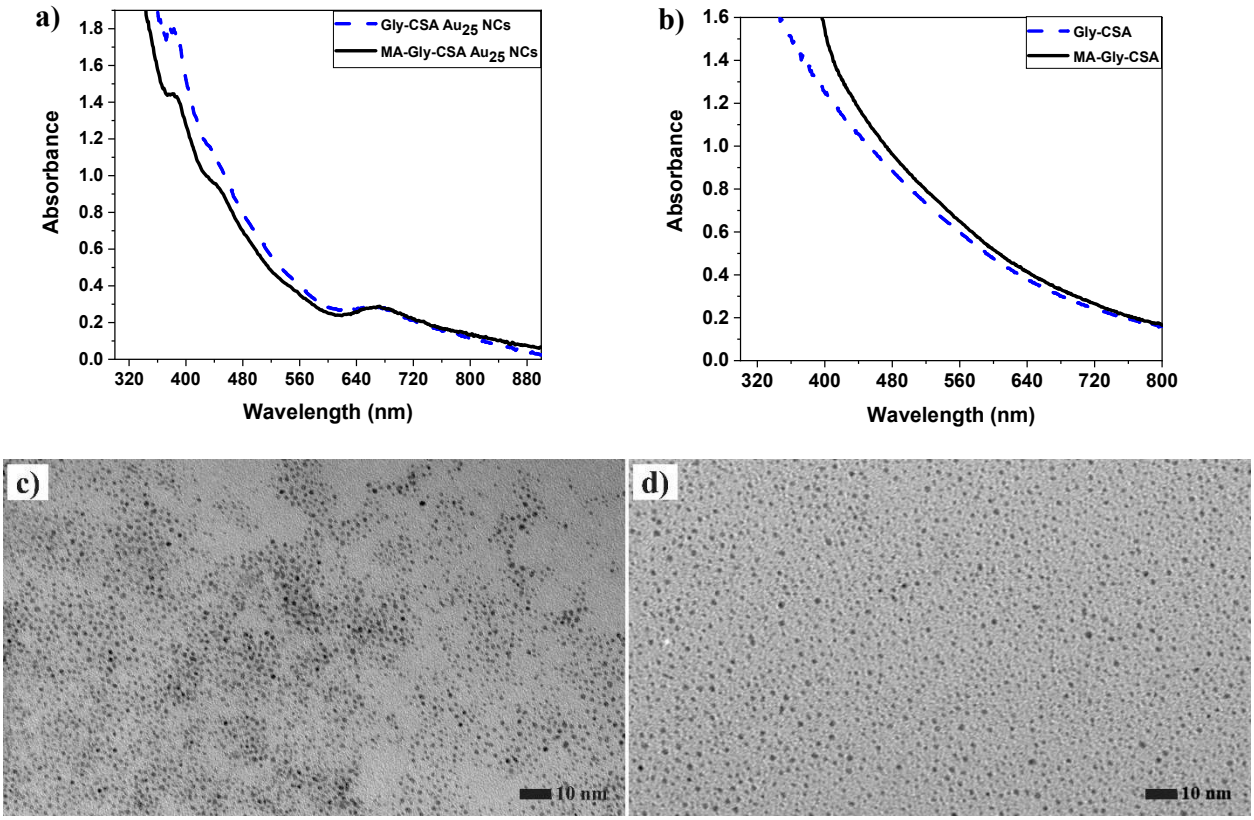

Figure 2.7. UV-Vis spectra and TEM images of Gly-CSA and MA-Gly-CSA-protected Au NCs synthesized using (a), (c) 0.30 M and (b), (d) 0.23 M of $NaBH_4$. UV-Vis spectra were obtained in H_2O: acetonitrile (1:1).

Figures **2.8a** and **2.8b** present the ^1H NMR and FTIR spectra of MA-Gly-CSA-protected Au NCs, respectively. The FTIR and ^1H NMR spectrum of Gly-CSA-protected Au NCs are presented for comparison. A new IR absorption peak at 1726 cm^{-1} for MA-Gly-CSA-protected Au NCs is evidence for the presence of C=O bonds of the ester group of methyl acrylate. Furthermore, the disappearance of the N-H peak in the FTIR (3349 nm and 3259 nm) and ^1H NMR (8.0 ppm, in d_6-DMSO) spectra after reaction with methyl acrylate proves that nearly all the amine groups are functionalized. In the ^1H NMR, the peak at 3.6 ppm is assigned to both the methyl group of the ester and the methylene group of cystamine. Two broad peaks at 2.7 and 3.0 ppm are assigned to methylene groups of methyl acrylate (-N-CH_2) and glycine, respectively. The overlapping peak

with the solvent peak at 2.5 ppm is assigned to methylene groups of methyl acrylate (-CH_2-COOMe). In order to better quantify the extent of the reaction, the ligands were removed from the NCs via cyanide etching of the Au core and also characterized by ^{1}H NMR, as shown in Figure **2.9**.[37] These etched ligand studies allow for more quantitative NMR interpretation, and show that the di-substituted product is the major product of the Michael addition reaction and a very negligible amount of mono-substituted product was observed (Figure **2.9**). All NMR assignments were verified by 2D-COSY NMR (Figure **2.10**).

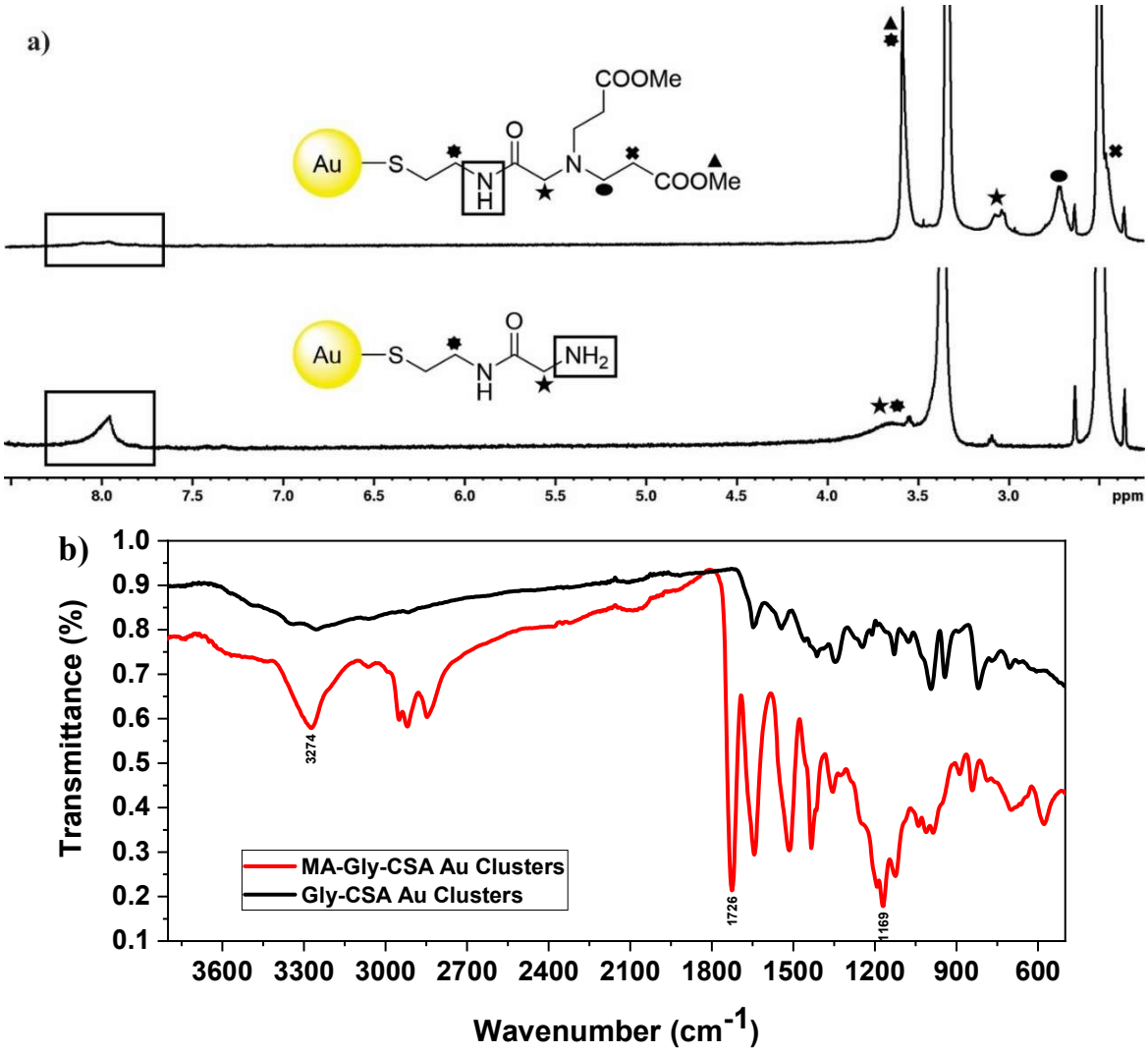

Figure 2.8. (a) ^{1}H NMR and (b) FTIR spectra of MA-Gly-CSA- and Gly-CSA-protected Au NCs in d_6-DMSO.

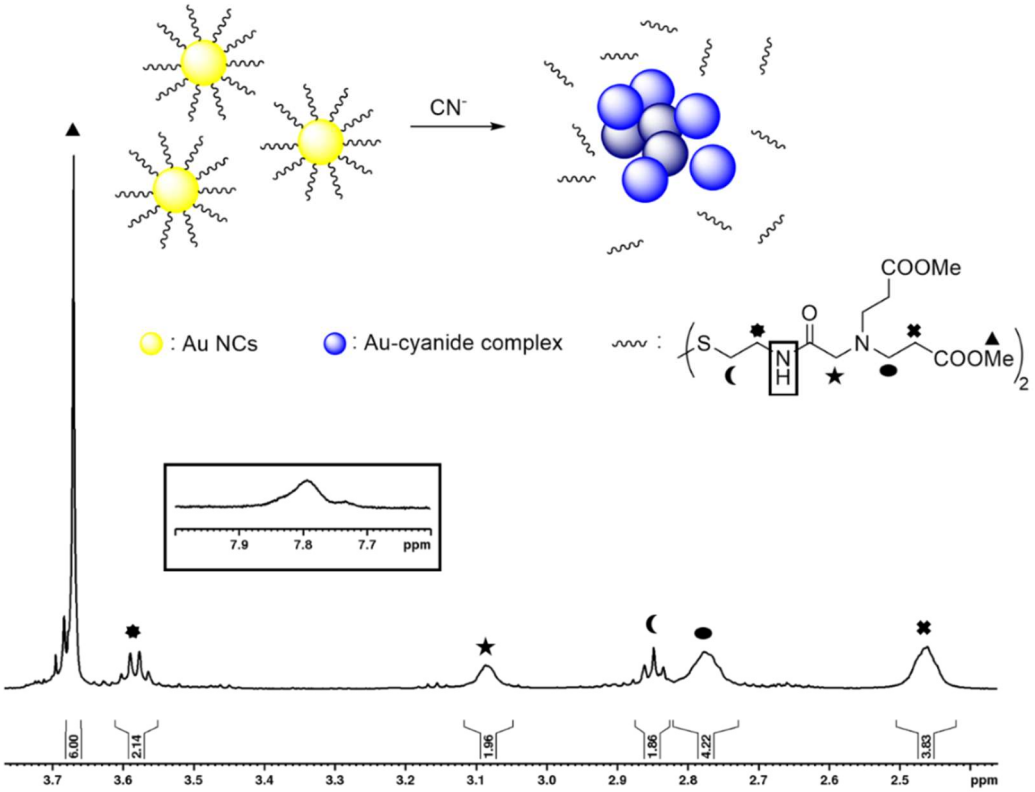

Figure 2.9. ^{1}H NMR of the resulting ligands removed from MA-CSA-Gly-protected Au NCs after cyanide etching in $CDCl_3$.

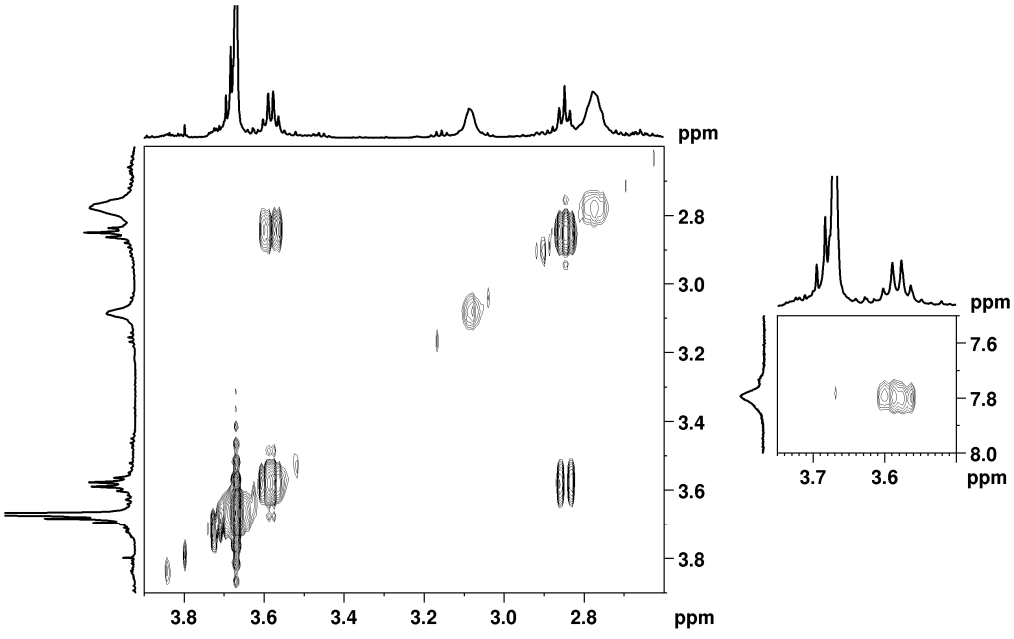

Figure 2.10. 2D-COSY NMR spectra of the resulting ligands removed from MA-CSA-Gly-protected Au NCs after cyanide etching in $CDCl_3$.

2.5 Conclusion

This work presents a single-phase synthetic method to produce atom-precise and stable glycine-cystamine (Gly-CSA)-protected Au NCs with reactive terminal primary amine groups. We have shown that using higher concentrations of the reducing agent ($NaBH_4$) in the original synthesis of Fmoc-Gly-CSA-protected Au NCs leads to smaller NCs and narrow size distributions. At a concentration of 0.30 M $NaBH_4$, Fmoc-Gly-CSA-protected $Au_{25}(SR)_{18}$ NCs have been synthesized which have characteristic UV-Vis absorption peaks at 690, 440, and 390 nm and core sizes of 1.1 ± 0.2 nm. Fmoc deprotection gives stable Au NCs with primary amine functional groups on the surface with no significant change of NC size or UV-Vis spectral signature. The incorporation of a reactive primary amine group results in Au NCs capable of being modified through organic reactions. In this work, methyl acrylate was added via a Michael addition reaction to the amine-terminated groups of Au NCs. No NC size change was observed after the reaction which makes these NCs a suitable candidate for applications that require multi-step functionalization. Furthermore, these active functional groups can be a potential site for the bio-functionalization of Au NCs.

2.6 References

(1) Templeton, A. C.; Hostetler, M. J.; Kraft, C. T.; Murray, R. W. Reactivity of Monolayer-Protected Gold Cluster Molecules: Steric Effects. *J. Am. Chem. Soc.* **1998**, *120*, 1906–1911.

(2) Yang, Y.; Wang, S.; Chen, S.; Shen, Y.; Zhu, M. Switching the Subcellular Organelle Targeting of Atomically Precise Gold Nanoclusters by Modifying the Capping Ligand. *Chem. Commun.* **2018**, *54*, 9222–9225.

(3) Kurashige, W.; Niihori, Y.; Sharma, S.; Negishi, Y. Recent Progress in the Functionalization Methods of Thiolate-Protected Gold Clusters. *J. Phys. Chem. Lett.* **2014**, *5*, 4134–4142.

(4) Woehrle, G. H.; Brown, L. O.; Hutchison, J. E. Thiol-Functionalized, 1.5-nm Gold Nanoparticles through Ligand Exchange Reactions: Scope and Mechanism of Ligand Exchange. *J. Am. Chem. Soc.* **2005**, *127*, 2172–2183.

(5) Park, C. S.; Zenasni, O.; Marquez, M. D.; Moore, H. J.; Lee, T. R. Hydrophilic Surfaces via the Self-Assembly of Nitrile-Terminated Alkanethiols on Gold. *AIMS Mater. Sci.* **2018**, *5*, 171–189.

(6) Qian, H.; Zhu, M.; Andersen, U. N.; Jin, R. Facile, Large-Scale Synthesis of Dodecanethiol-Stabilized Au_{38} Clusters. *J. Phys. Chem. A* **2009**, *113*, 4281–4284.

(7) Shivhare, A.; Ambrose, S. J.; Zhang, H.; Purves, R. W.; Scott, R. W. J. Stable and Recyclable Au_{25} Clusters for the Reduction of 4-Nitrophenol. *Chem. Commun.* **2013**, *49*, 276–278.

(8) Kazan, R.; Müller, U.; Bürgi, T. Doping of Thiolate Protected Gold Clusters through Reaction with Metal Surfaces. *Nanoscale* **2019**, *11*, 2938–2945.

(9) Giljohann, D.; Seferos, D.; Daniel, W.; Massich, M.; Patel, P.; Mirkin, C. National Institute of Health Public Access. *Angew. Chem., Int. Ed.* **2014**, *49*, 3280–3294.

(10) Nasaruddin, R. R.; Chen, T.; Yan, N.; Xie, J. Roles of Thiolate Ligands in the Synthesis, Properties and Catalytic Application of Gold Nanoclusters. *Coord. Chem. Rev.* **2018**, *368*,

60–79.

(11) Kaur, N.; Aditya, R. N.; Singh, A.; Kuo, T. R. Biomedical Applications for Gold Nanoclusters: Recent Developments and Future Perspectives. *Nanoscale Res. Lett.* **2018**, *13*, 1–12.

(12) Chen, L. Y.; Wang, C. W.; Yuan, Z.; Chang, H. T. Fluorescent Gold Nanoclusters: Recent Advances in Sensing and Imaging. *Anal. Chem.* **2015**, *87*, 216–229.

(13) Li, J.; Nasaruddin, R. R.; Feng, Y.; Yang, J.; Yan, N.; Xie, J. Tuning the Accessibility and Activity of Au25(SR)18 Nanocluster Catalysts through Ligand Engineering. *Chem. - Eur. J.* **2016**, *22*, 14816–14820.

(14) Lu, F.; Yang, H.; Tang, Y.; Yu, C. J.; Wang, G.; Yuan, Z.; Quan, H. 11-Mercaptoundecanoic Acid Capped Gold Nanoclusters with Unusual Aggregation-Enhanced Emission for Selective Fluorometric Hydrogen Sulfide Determination. *Microchim. Acta* **2020**, *187*, 1–9.

(15) Templeton, A. C.; Hostetler, M. J.; Warmoth, E. K.; Chen, S.; Hartshorn, C. M.; Krishnamurthy, V. M.; Forbes, M. D. E.; Murray, R. W. Gateway Reactions to Diverse, Polyfunctional Monolayer-Protected Gold Clusters. *J. Am. Chem. Soc.* **1998**, *120*, 4845–4849.

(16) Wu, Z.; Suhan, J.; Jin, R. One-Pot Synthesis of Atomically Monodisperse, Thiol-Functionalized Au_{25} Nanoclusters. *J. Mater. Chem.* **2009**, *19*, 622–626.

(17) Mathew, A.; Natarajan, G.; Lehtovaara, L.; Häkkinen, H.; Kumar, R. M.; Subramanian, V.; Jaleel, A.; Pradeep, T. Supramolecular Functionalization and Concomitant Enhancement in Properties of Au_{25} Clusters. *ACS Nano* **2014**, *8*, 139–152.

(18) Gunawardene, P. N.; Corrigan, J. F.; Workentin, M. S. Golden Opportunity: A Clickable Azide-Functionalized [Au25(SR)18]- Nanocluster Platform for Interfacial Surface Modifications. *J. Am. Chem. Soc.* **2019**, *141*, 11781–11785.

(19) Yu, Y.; Luo, Z.; Yu, Y.; Lee, J. Y.; Xie, J. Observation of Cluster Size Growth in CO-Directed Synthesis of $Au_{25}(SR)_{18}$ Nanoclusters. *ACS Nano* **2012**, *6*, 7920–7927.

(20) Meng, L.; Yin, J. H.; Yuan, Y.; Xu, N. 11-Mercaptoundecanoic Acid Capped Gold

Nanoclusters as a Fluorescent Probe for Specific Detection of Folic Acid: Via a Ratiometric Fluorescence Strategy. *RSC Adv.* **2018**, *8*, 9327–9333.

(21) Yu, H.; Chen, X.; Yu, L.; Sun, M.; Alamry, K. A.; Asiri, A. M.; Zhang, K.; Zapien, J. A.; Wang, S. Fluorescent MUA-Stabilized Au Nanoclusters for Sensitive and Selective Detection of Penicillamine. *Anal. Bioanal. Chem.* **2018**, *410*, 2629–2636.

(22) Choi, M. M. F.; Douglas, A. D.; Murray, R. W. Ion-Pair Chromatographic Separation of Water-Soluble Gold Monolayer-Protected Clusters. *Anal. Chem.* **2006**, *78*, 2779–2785.

(23) Hicks, J. F.; Seok-Shon, Y.; Murray, R. W. Layer-by-Layer Growth of Polymer/Nanoparticle Films Containing Monolayer-Protected Gold Clusters. *Langmuir* **2002**, *18*, 2288–2294.

(24) Lavenn, C.; Albrieux, F.; Bergeret, G.; Chiriac, R.; Delichère, P.; Tuel, A.; Demessence, A. Functionalized Gold Magic Clusters: $Au_{25}(SPhNH_2)_{17}$. *Nanoscale* **2012**, *4*, 7334–7337.

(25) Yuan, X.; Yu, Y.; Yao, Q.; Zhang, Q.; Xie, J. Fast Synthesis of Thiolated Au_{25} Nanoclusters via Protection-Deprotection Method. *J. Phys. Chem. Lett.* **2012**, *3*, 2310–2314.

(26) Yuan, X.; Zhang, B.; Luo, Z.; Yao, Q.; Leong, D. T.; Yan, N.; Xie, J. Balancing the Rate of Cluster Growth and Etching for Gram-Scale Synthesis of Thiolate-Protected Au_{25} Nanoclusters with Atomic Precision. *Angew. Chem., Int. Ed.* **2014**, *53*, 4623–4627.

(27) Lu, Y.; Dasog, M.; Leontowich, A. F. G.; Scott, R. W. J.; Paige, M. F. Fluorescently Labeled Gold Nanoparticles with Minimal Fluorescence Quenching. *J. Phys. Chem. C* **2010**, *114*, 17446–17454.

(28) Dasog, M.; Kavianpour, A.; Paige, M. F.; Kraatz, H. B.; Scott, R. W. J. Chemical Functionalization and Modification of Surface-Bound Cystamine-Giycine Monolayers on Gold Nanoparticles. *Can. J. Chem.* **2008**, *86*, 368–375.

(29) Zhu, M.; Aikens, C. M.; Hollander, F. J.; Schatz, G. C.; Jin, R. Correlating the Crystal Structure of A Thiol-Protected Au_{25} Cluster and Optical Properties. *J. Am. Chem. Soc.* **2008**, *130*, 5883–5885.

(30) Leontowich, A. F. G.; Calver, C. F.; Dasog, M.; Scott, R. W. J. Surface Properties of Water-

Soluble Glycine-Cysteamine-Protected Gold Clusters. *Langmuir* **2010**, *26*, 1285–1290.

(31) Schneider, C. A.; Rasband, W. S.; Eliceiri, K. W. NIH Image to ImageJ: 25 Years of Image Analysis. *Nat. Methods* **2012**, *9*, 671–675.

(32) Shivhare, A.; Wang, L.; Scott, R. W. J. Isolation of Carboxylic Acid-Protected Au_{25} Clusters Using a Borohydride Purification Strategy. *Langmuir* **2015**, *31*, 1835–1841.

(33) Wu, Z.; Gayathri, C.; Gil, R. R.; Jin, R. Probing the Structure and Charge State of Glutathione-Capped $Au_{25}(SG)_{18}$ Clusters by NMR and Mass Spectrometry. *J. Am. Chem. Soc.* **2009**, *131*, 6535–6542.

(34) Templeton, A. C.; Wuelfing, W. P.; Murray, R. W. Monolayer-Protected Cluster Molecules. *Acc. Chem. Res.* **2000**, *33*, 27–36.

(35) Wu, Z.; Chen, J.; Jin, R. One-Pot Synthesis of $Au_{25}(SG)_{18}$ 2- and 4-nm Gold Nanoparticles and Comparison of Their Size-Dependent Properties. *Adv. Funct. Mater.* **2011**, *21*, 177–183.

(36) Dasog, M.; Scott, R. W. J. Understanding the Oxidative Stability of Gold Monolayer-Protected Clusters in the Presence of Halide Ions under Ambient Conditions. *Langmuir* **2007**, *23*, 3381–3387.

(37) Liu, X.; Yu, M.; Kim, H.; Mameli, M.; Stellacci, F. Determination of Monolayer-Protected Gold Nanoparticle Ligand-Shell Morphology Using NMR. *Nat. Commun.* **2012**, *3*, 1–9.

Chapter 3

3 Development of Au Cluster-Cored Dendrimers by Direct and Divergent Routes

3.1 Abstract

The use of dendrimers and dendrons as stabilizing agents for metal NPs and clusters has been drawing great interest. Herein, we describe the synthesis of Au cluster-cored dendrimers by either direct synthesis or multi-step functionalization. Direct synthesis of Au cluster-cored dendrimers has been performed by the Brust-Shiffrin method using cystamine core poly(amidoamine) (PAMAM) dendrons (G0.5-COOMe, G1.0-NH_2, and G1.5-COOMe; see Scheme 3.1) as capping agents. Alternatively, a divergent approach to make similar clusters involving glycine-cystamine clusters was also attempted; this synthesis involves sequential Michael addition reactions of methyl acrylate followed by a subsequent amide coupling reaction with ethylenediamine on amine-terminated Au nanoclusters (NCs), to form dendritic architectures (G0.5-COOMe-Au, G1.0-NH_2-Au, and G1.5-COOMe-Au; see Scheme 3.1) around the Au core. The chemical structure of the ligands was confirmed by ^{1}H NMR after each functionalization reaction and cluster size was characterized by Transmission Electron Microscopy (TEM). In this study, Au cluster-cored dendrimers with amine- or ester-terminated groups on the surface with different core sizes have been produced. The resulting amine- and ester-terminated Au cluster-cored dendrimers synthesized by the divergent method are stable and resist aggregation in solution and in the presence of an excess of reducing agent. In contrast, amine-terminated Au cluster-cored

dendrimers synthesized by direct synthesis undergo aggregation in solution over time due to the high reactivity of the surface, which makes them unstable and limits their applications, while ester-terminated Au cluster-cored dendrimers formed by direct synthesis have much larger core sizes than found in the divergent approach. Finally, the effect of synthetic strategies to produce cluster-cored dendrimers as well as dendron generations on the accessibility of Au surface and catalytic activities of these clusters for 4-nitrophenol hydrogenation have been investigated. It is observed that the Au surface of cluster-cored dendrimers formed by direct synthesis has a lower density of ligands and as a result, is unpassivated which results in higher catalytic activities. Furthermore, Au cluster-cored dendrimers with less sterically bulky dendrons showed higher catalytic activities.

Cystamine core poly(amidoamine) (PAMAM) dendrons:

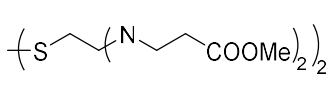

G0.5-COOMe

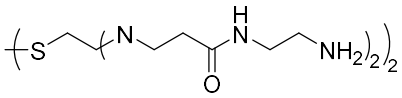

G1.0-NH$_2$

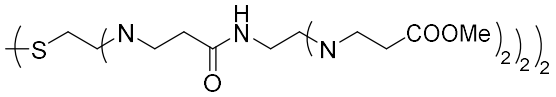

G1.5-COOMe

Gn-Au cluster-cored dendrimers:

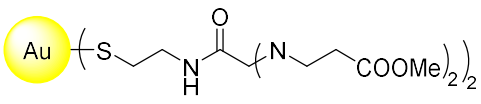

G0.5-COOMe-Au

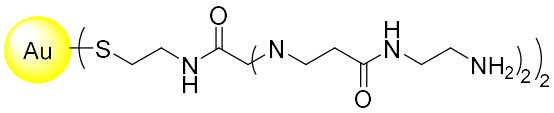

G1.0-NH$_2$-Au

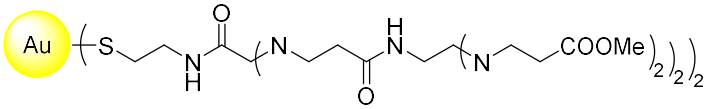

G1.5-COOMe-Au

Scheme 3.1. (a) poly(amidoamine) (PAMAM) dendrons with cystamine core and (b) Gn-Au cluster-cored dendrimers using Gly-CSA NCs as starting materials.

3.2 Introduction

Dendrimers are highly branched, star-shaped synthetic macromolecules with well-defined compositions and structures.[1,2] They have attracted growing interest among researchers because of their unique properties, such as size, reactivity and diversity of end groups, easy preparation, and biocompatibility which make them suitable for many important application areas, such as biolabeling, drug delivery, catalysis, and sensing.[3–6] Nanoparticle-cored dendrimers (NCDs) are a class of materials that possess a metal nanoparticle core stabilized by branched organic dendrons. These materials are stabilized through specific bonding interactions, such as covalent bonds, and have high stability compared to dendrimer-encapsulated NPs in which there are nonspecific bonding interactions between the NPs and the dendrimers.[7] Furthermore, stabilization of nanometer-sized particles with dendrons provides a thin organic layer on the nanoparticle surface with precisely defined structure and composition, with tunable surface chemistry which make them promising materials for applications such as sensing,[8,9] catalysis,[8,10,11] and biomedical applications.[12,13] For these reasons, the preparation of NCDs has drawn particular attention. During the past few years, significant progress has been made in the design and synthesis of NCDs with various metal cores, such as Au,[11,14,15] Pt,[16] and Pd.[10]

Synthetic methodologies for Au NCDs are classified into three categories.[12,7] The first strategy is direct synthesis in which thiol-containing dendrons and/or dendrimers are used as stabilizers during the synthesis of the Au NPs. However, the formation of Au NCDs by direct synthesis has some disadvantages as 1) a large excess of dendrons are needed in this strategy,[17] 2) for dendrons/dendrimers containing reactive functional groups such as amine or carboxylic acid groups, there is a strong affinity for both sulfur groups and the secondary functional groups towards

the Au surface which can lead to aggregation, and 3) it provides poor control over the size of the nanoparticle core, as the size of the core often directly depends on the steric bulk of the dendrons on the surface.[11] The second method to make NCDs involves place-exchange reactions of thiolate protecting groups on NPs by thiol-terminated dendrons. This method keeps the core size unchanged during the ligand-exchange reaction.[12,18] However, this method gives poor control over the exact degree of ligand exchange and can lead to low loadings of dendrons on the surface of Au NPs.[17] In addition, another limitation of the ligand-exchange method is that dendrons containing thiol or disulfide groups are hard to synthesize.[12] The third strategy involves the reaction of the surface functional groups of monolayer protected Au clusters (MPCs) with dendrons to make Au NCDs of different generations using either single reactions (convergent) or multistep reactions (divergent) approaches. There are several reports of convergent synthesis of NCDs which are based on reacting dendrons with functionalized NPs by a single coupling reaction.[17,19–21] For example, Shon *et al.* synthesized Au NCDs by a single ester coupling reaction between COOH-functionalized Au MPCs with OH-functionalized dendrons.[17] They reported that this method generates an unchanged average core size for NCDs with various dendron wedge densities and dendron generations. The convergent approach by a single coupling reaction is suitable to add high generation dendrons to the surface of NPs. However, it can lead to higher levels of defects arising from the steric hindrance of incoming dendrons and incomplete reactions on the surface.[11] The divergent approach is based on the post-functionalization of ligands on the surface of Au NPs by multistep reactions which leads to the growth of dendrons on the surface of NPs. While several reports have been published about the convergent synthesis of Au NCDs, very few examples of Au NCDs synthesized by the divergent strategy have been reported.[19] In 2007, Shon and coworkers reported the synthesis of Au NCDs by divergent approaches using COOH-functionalized Au NPs

with Michael addition reactions and amide coupling reactions.[19] They observed the formation of NPs aggregates which minimized the extent to further functionalization, and thus higher generation dendrons were not readily accessible.

Herein, I report the synthesis of Au cluster-cored dendrimers by a post-functionalization (divergent) strategy to generate ester and amine-terminated Au cluster-cored dendrimers with controlled core sizes and different dendron generations. In this strategy, multistep reactions (Michael addition reactions followed by amide coupling reactions) are employed to build dendritic structures on amine-functionalized Au nanoclusters (NCs). In this study, Gly-CSA-protected Au NCs were chosen as the initial NCs, and the surface was modified to produce Au cluster-cored dendrimers by multi-step functionalization. This is the first example of modifying Au cluster surfaces through organic reactions using amine-terminated Au NCs to make Au cluster-cored dendrimers by such a multi-step functionalization strategy. The advantages/disadvantages of this method compared to direct synthesis were studied, and it was found that the divergent method gives cluster-cored dendrimers with little to no change in core size, whereas poor control over core sizes is achieved by direct synthesis. Finally, the catalytic properties of the Au NCDs were investigated for the reduction of 4-nitrophenol, and the resulting activities of the NCDs were correlated to their structures.

3.3 Experimental Section

3.3.1 Materials

All solvents and chemicals were purchased commercially and used as received without any further purification. Cystamine dihydrochloride (98%), sodium cyanide (97%), sodium borohydride ($NaBH_4$), tetrahydrofuran (THF), dichloromethane (CH_2Cl_2), methanol (MeOH),

diethyl ether (Et_2O), *n*-butanol (C_4H_9OH), *n*-hexane (C_4H_{14}), ethyl acetate (CH_3COOEt), and acetonitrile (CH_3CN) were purchased from Fisher Scientific. Hydrogen tetrachloroaurate(III) trihydrate ($HAuCl_4 \cdot 3H_2O$, 99.9% on metal basis), tetraoctylammonium bromide (TOAB, 98%), ethylenediamine (99%), and methyl acrylate (99%) were purchased from Sigma Aldrich. Deionized water (resistivity 18.2 MΩ.cm) was used for all experiments. Deuterated chloroform ($CDCl_3$, 99.8 atom % D), deuterium oxide (D_2O, 99.9 atom % D), and deuterated dimethylsulfoxide (d_6-DMSO, 99.9 atom % D) were purchased from Cambridge Isotope Laboratories.

3.3.2 Synthesis of Cystamine Core PAMAM-COOMe (G0.5-COOMe)

Methyl acrylate (8.45 mL, 93.25 mmol) was added to a solution of cystamine dihydrochloride (5.00 g, 22.20 mmol) in 20 mL water all at once and the reaction was allowed to stir at room temperature for 48 h. Then, the reaction mixture was extracted by dichloromethane (2 × 20 mL) and dried by Na_2SO_4. After filtering, the solvent and excess methyl acrylate were removed by rotary evaporation under reduced pressure. The product as a light-yellow oil which weighed 9.86 g (89 % yield) after vacuum drying. ^{1}H NMR ($CDCl_3$, 500 MHz, ppm) δ 2.15 (t, 8H, J = 7.0 Hz, CH_2COOMe), 2.46 (bs, 12H, CH_2-N-$(CH_2)_2$), 2.50 (t, 4H, CH_2-S), 3.35 (s, 12H, CH_3). ^{13}C NMR ($CDCl_3$, 125 MHz, ppm): δ 32.5 (CH_2-CO), 36.3 (CH_2-S cystamine), 49.2 ($(CH_2)_2N$), 51.4 (CH_3), 53.2 (CH_2-N of cystamine), 172.7 (C=O).

3.3.3 Synthesis of Cystamine Core PAMAM-NH_2 (G1.0-NH_2)

A solution of ethylenediamine (35.13 mL, 201.35 mmol) in methanol (50 mL) was cooled to near 0 ℃. Then, a solution of G0.5-COOMe (2.00 g, 4.03 mmol) in methanol (20 mL) was added slowly over a 30 min time period to this cold solution. The reaction mixture was stirred

under nitrogen for 5 days. Then, the methanol was removed by rotary evaporation under vacuum. The excess of ethylenediamine was removed by azeotroping using *n*-butanol (200 mL). The product as a light-yellow viscous oil which weighed 2.03 g (83 % yield) after vacuum drying. ^{1}H NMR (D_2O, 500 MHz, ppm) δ 2.43 (t, 8H, J = 6.7 Hz, CH_2-CO), 2.7 (t, 8H, J = 6.3 Hz, CH_2NH_2), 2.83-2.88 (m, 16 H, CH_2-S and CH_2-N-$(CH_2)_2$), 3.30 (t, 8H, J = 6.3 Hz, NH-CH_2). ^{13}C NMR (D_2O, 125 MHz, ppm): δ 33.4 (CH_2-CO), 34.5 (CH_2-NH_2 of EDA), 35.7 (CH_2-S cystamine), 40.8 (CH_2NH of EDA), 49.5 (($CH_2)_2$N), 52.5 (CH_2-N of cystamine), 173.6 (C=O).

3.3.4 Synthesis of Cystamine Core PAMAM-COOMe (G1.5-COOMe)

Methyl acrylate (2.23 mL, 24.63 mmol) was added to a solution of G1.0-NH_2 (1.50 g, 2.46 mmol) in 20 mL methanol and the reaction was allowed to stir at room temperature for 48 h. The reaction mixture was extracted by dichloromethane (2 × 20 mL) and dried using Na_2SO_4. After filtering, the organic solution and excess methyl acrylate were removed from the mixture by using a rotary evaporator under reduced pressure. The product was purified by column chromatography with a silica gel using *n*-hexane: ethyl acetate: methanol (4:4:1) as the eluent. The product as a yellow oil weighed 2.59 g (81 % yield) after purification. ^{1}H NMR ($CDCl_3$, 500 MHz, ppm) δ 2.27 (t, 8H, J = 6.8 Hz, CH_2CO), 2.33 (t, 16H, J = 6.7 Hz, CH_2-COOMe), 2.44 (t, 8H, J = 6.0 Hz, CH_2-N (ethylenediamine)), 2.65 (t, 16H, J = 6.7 Hz, N-$(CH_2)_2$ (methyl acrylate)), 2.69-2.73 (m, 16 H, CH_2-S and CH_2-N-$(CH_2)_2$), 3.16-3.19 (q, 8H, J = 11.5 Hz and 5.7 Hz, NH-CH_2), 3.57 (s, 24H, CH_3). ^{13}C NMR ($CDCl_3$, 125 MHz, ppm): δ 32.2 (CH_2-CO), 33.3 (CH_2-CO of G0.5-COOMe), 35.7 (CH_2-S cystamine), 37.1 (CH_2-NH_2 of EDA), 49.1 (($CH_2)_2$N), 49.4 (($CH_2)_2$N), 51.0 (CH_3), 52.4 (CH_2-N of cystamine), 173.1 (C=O of G0.5-COOMe), 173.3 (C=O).

3.3.5 Direct Synthesis of Au Cluster-Cored Dendrimers Using Cystamine Core PAMAM Dendrimers as Caping Agents (G0.5-COOMe, G1.0-NH_2, and G1.5-COOMe)

$HAuCl_4 \cdot 3H_2O$ (0.147 mmol, 50 mg) was added to 10 mL THF followed by the addition of TOAB (0.177 mmol, 0.10 g). The colour changed from yellow to red. After 10 min, cystamine core PAMAM dendrons (0.292 mmol) (either G0.5-COOMe (0.145 g), G1.0-NH_2 (0.170 g), or G1.5-COOMe (0.270 g)) were added to the solution. After stirring for 5 min, freshly prepared $NaBH_4$ in 2.0 mL water was added to the solution all at once; the concentrations of $NaBH_4$ used was variable depending on the dendritic stabilizer used ($NaBH_4$ concentrations used in brackets): G0.5-COOMe (0.19 M and 0.23 M); G1.0-NH_2 (0.25 M); and G1.5-COOMe (0.23 M, 0.27 M)). After 24 h, 10 mL of Et_2O was added to the solution and the resulted precipitate was centrifuged and washed several times by Et_2O.

3.3.6 Divergent Synthesis of MA (Methyl Acrylate)-Gly-CSA-Au (G0.5-COOMe-Au) Cluster-Cored Dendrimers

Gly-CSA-protected Au NCs with two different core sizes have been used in the synthesis of cluster-cored dendrimers using the divergent method: 1.2 ± 0.3 nm and 1.8 ± 0.3 nm. Gly-CSA-protected Au NCs were synthesized using synthetic methodologies outlined in Chapter 2. Gly-CSA-protected Au NCs (5.0 mg) were dissolved in a 6 mL mixture of water:acetonitrile (1:1) followed by the addition of methyl acrylate (33.0 mmol, 3.0 mL). The reaction mixture was kept under N_2 for 24 h. Then 10 mL CH_2Cl_2 was added to the solution and the organic phase was separated and dried over sodium sulfate. CH_2Cl_2 and excess methyl acrylate was removed under

vacuum. The average yield of the resulting material was 4.6 mg. This material is referred to as G0.5-COOMe-Au NCs hereafter (0.5 generation dendrons).

3.3.7 Divergent Synthesis of EDA(Ethylenediamine)-MA-Gly-CSA-Au (G1.0-NH_2-Au) Cluster-Cored Dendrimers

G0.5-COOMe-Au NCs (5.0 mg) were dissolved in 5 mL methanol. Then 3.0 mL of ethylenediamine (45.0 mmol) was added to the mixture and the mixture was stirred under N_2 for 48 h. The clusters were precipitated out of the solution by the addition of 10 mL Et_2O. The brown precipitate was washed several times with Et_2O. The average yield of the resulting EDA-MA-Gly-CSA Au NCs was 4.2 mg.

3.3.8 Divergent Synthesis of MA-EDA-MA-Gly-CSA-Au (G1.5-COOMe-Au) Cluster-Cored Dendrimers

The procedure is similar to the synthesis of G0.5-COOMe-Au. In this synthesis, 5.0 mg of G1.0-NH_2-Au NCs and 5.0 mL of methyl acrylate (47.5 mmol) were used. The average yield of the resulting G1.5-COOMe-Au NCs was 4.5 mg.

3.3.9 Cyanide Etching of Au Cluster-Cored Dendrimers

A solution of Au cluster-cored dendrimers, G0.5-COOMe-Au or G1.5-COOMe-Au in chloroform or G1.0-NH_2-Au in water (5.0 mg/mL), was mixed with an aqueous solution of sodium cyanide (1.0 M) in a 1:1 volume ratio. The mixture was stirred at room temperature under air until the solution turned colourless. The free organic ligand was extracted by $CDCl_3$ (2 mL), dried over sodium sulfate and then characterized by ^1H NMR.

3.3.10 Catalytic Reduction of 4-Nitrophenol (4-NP)

The catalytic reaction was performed in a quartz cuvette and followed by UV-Vis spectroscopy. In a typical catalytic reaction, 2.0 mL of a solution of 4-NP (600. mM) in H_2O/THF (5:1) and Au cluster-cored dendrimer catalysts (0.050 mg/mL) were mixed and transferred into the cuvette and placed in the UV-Vis instrument. Then, freshly prepared $NaBH_4$ (0.50 M, 1.0 mL) was added to the mixture to initiate the reaction and UV-Vis measurements were taken every 2 seconds. The apparent reaction rate constant (k_{app}) was obtained by analyzing the corresponding UV-Vis absorption data and fitting the decay of the nitrophenolate absorbance via pseudo-first-order kinetics.

3.3.11 Characterization

UV-Vis analyses were done using a Varian Cary 50 UV-Visible spectrophotometer with an optical path length of 1 cm. Au NCs were analyzed by transmission electron microscopy (TEM) using a Hitachi HT 7700 TEM operating at 100 kV. TEM samples were prepared by drop-casting NC solutions onto a carbon-coated 400 mesh Cu TEM grid (Electron Microscopy Sciences, Hatfield, PA) and dried under ambient conditions before TEM analysis. Average NC diameters were determined by manually measuring approximately 100 NCs from images obtained for each sample using the ImageJ program.[23] All NMR spectra were recorded on a Bruker AMX-500 spectrometer operating at 500 and 125 MHz for ^{1}H and ^{13}C, respectively. Chemical shifts were referenced to the residual proton and carbon signals of deuterated solvents.

3.4 Results and Discussion

As mentioned earlier, there are several strategies to prepare Au nanoparticle-cored dendrimers (NCDs). The simplest and most common method is direct synthesis, which involves the one-step synthesis of the NCDs via reduction of the metal salt in the presence of dendrons bearing suitable moieties at their focal point. One strategy used in this chapter is based on the synthesis of atom-precise Au NCs followed by building the dendritic architecture on the NC surface (multistep reactions, divergent approach). Reactive atom-precise amine-terminated Au NCs with different core sizes (by controlling the concentration of the reducing agent) were first prepared by the Brust-Schiffrin method using a Fmoc-Gly-CSA capping agent, followed by deprotection of the Fmoc groups, as previously reported in Chapter **2**. The advantages/disadvantages of the divergent approach were thoroughly investigated compared to direct synthesis. Cystamine core PAMAM dendrimers of different generations **1** (G0.5-COOMe), **2** (G1.0-NH_2), and **3** (G1.5-COOMe) used for direct synthesis were prepared by Michael addition reaction of methyl acrylate with cystamine dihydrochloride (initiator core) and amidation of the resulting esters with ethylenediamine (Scheme **3.2**). Figures **3.1a** and **3.1b** present the ^{1}H NMR and ^{13}C NMR of the cystamine core PAMAM dendrimers, respectively. Au cluster-cored dendrimers (G0.5-COOMe-Au, G1.0-NH_2-Au, and G1.5-COOMe-Au) were then synthesized by direct synthesis using varying concentrations of reducing agent ($NaBH_4$).

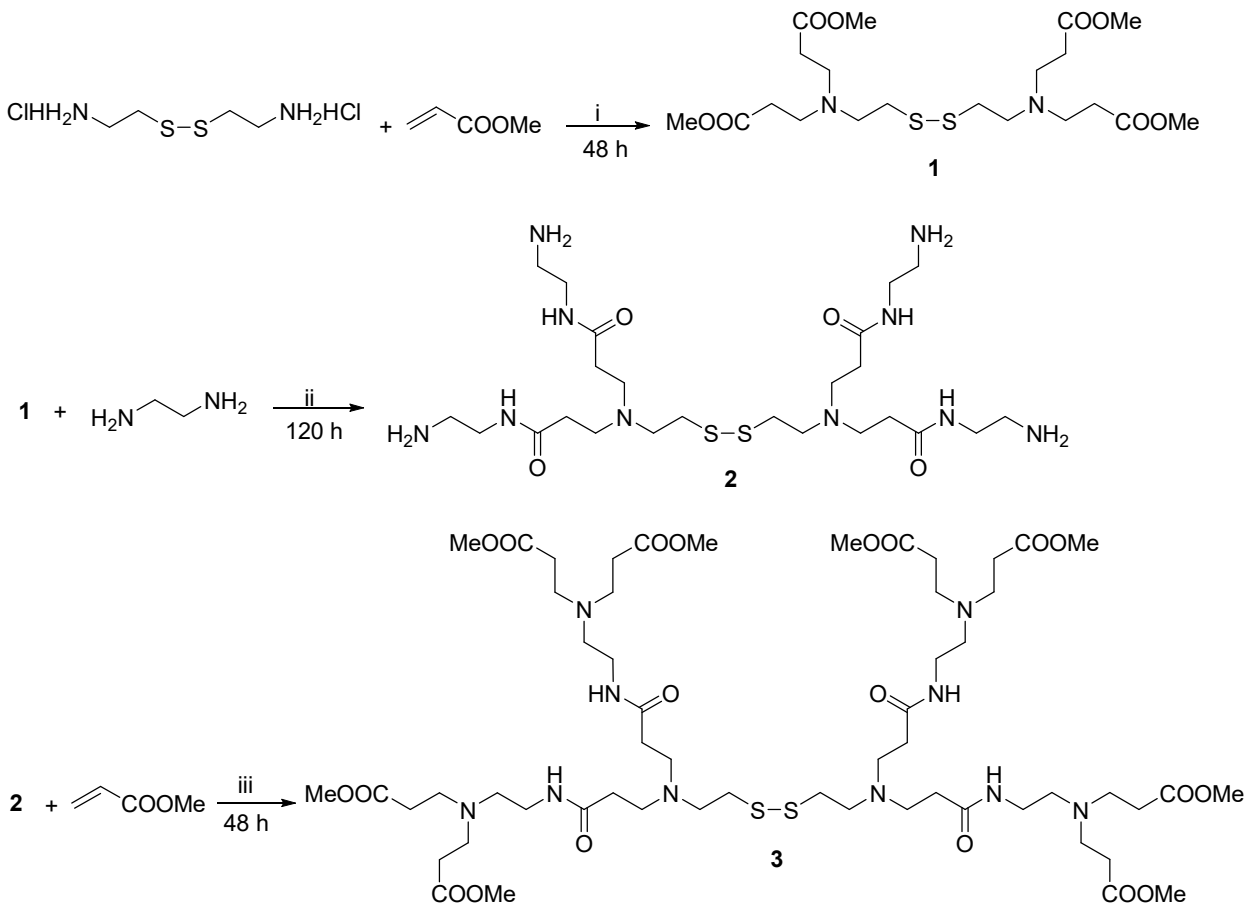

Scheme 3.2. Synthesis of cystamine core poly(amidoamine) (PAMAM) dendrons **1** (G0.5-COOMe), **2** (G1.0-NH_2), and **3** (G1.5-COOMe). Reagents and conditions: (i) H_2O, r.t.; (ii) MeOH, r.t.; (iii) MeOH, Et_3N, r.t.

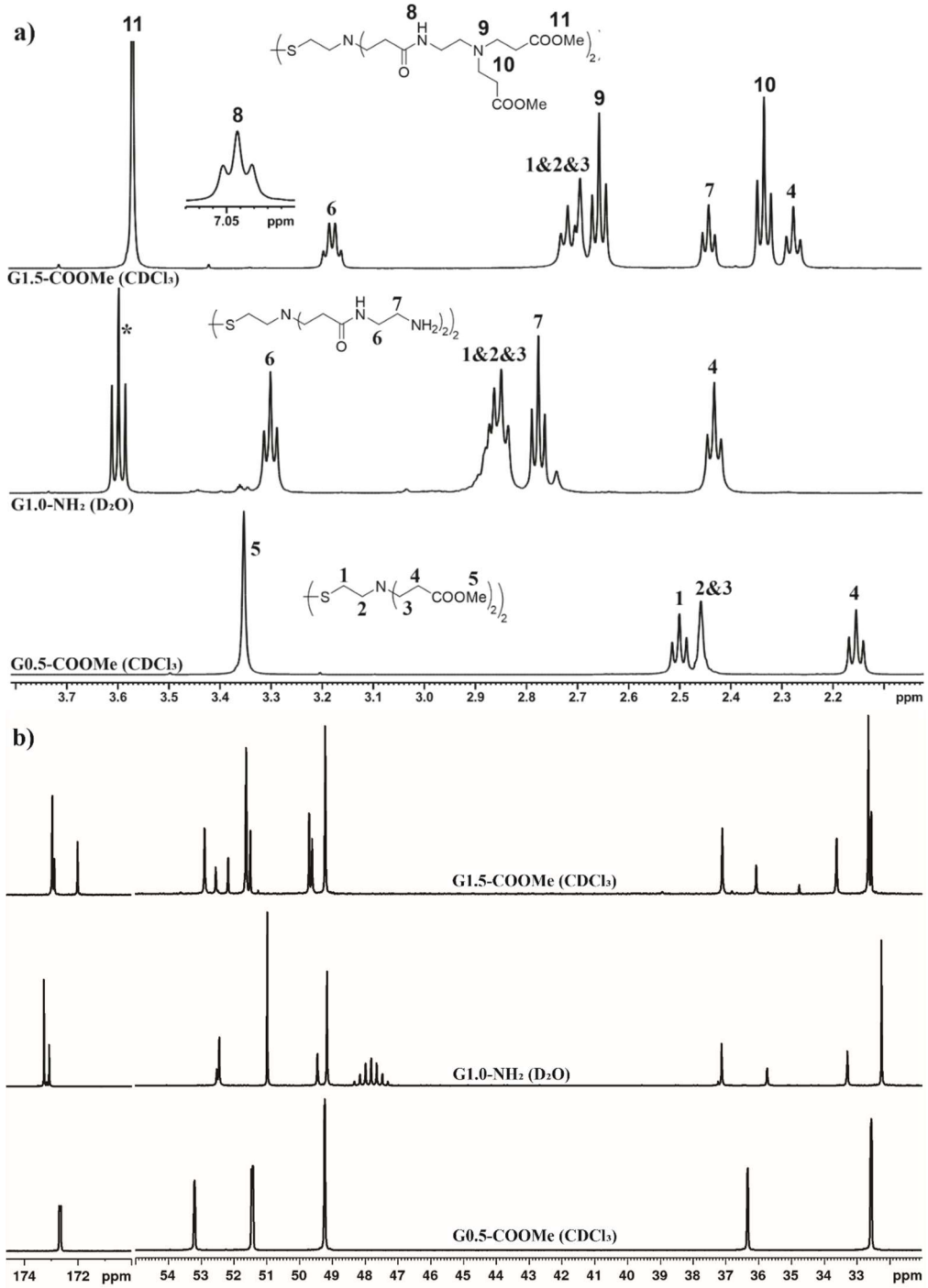

Figure 3.1. ^{1}H NMR (a) and ^{13}C NMR (b) spectra of free ligands G0.5-COMe ($CDCl_3$), G1.0-NH_2 (D_2O), and G1.5-COOMe ($CDCl_3$).

Direct synthesis of ester-terminated Au cluster-cored dendrimers was accomplished following the Brust-Schiffrin synthesis method using G0.5-COOMe and G1.5-COOMe dendrons

(Scheme **3.3**). According to UV-Vis measurements (Figure **3.2**), increasing the concentration of the $NaBH_4$ reducing agent in the reaction mixture from 0.19 M to 0.23 M for G0.5-COOMe (Figure **3.2a**) and from 0.23 M to 0.27 M for G1.5-COOMe (Figure **3.2b**) results in the formation of Au cluster-cored dendrimers with decreasing core diameters. As seen in Figure **3.2a**, a weak surface plasmon band at *ca.* 520-530 nm in the UV-Vis was observed using 0.23 M $NaBH_4$, whereas when using 0.19 M $NaBH_4$ the plasmon band increased in intensity and a small red-shift was also observed, which indicates an increasing core size. Attempts at making smaller NCs in this system with a further increase in the concentration of the reducing agent (above 0.23 M) led to rapid precipitation and the solution turned clear immediately (*i.e.,* no clusters remained in solution). Figure **3.2b** shows that increases in $NaBH_4$ concentration from 0.23 M to 0.27 M led to smaller core sizes in the 1.5-COOMe system. Based on UV-Vis spectra of G0.5-COOMe-Au and G1.5-COOMe-Au NCs synthesized at 0.23 M of $NaBH_4$ (Figure **3.2c**), there is a notable change in optical properties resulting from an increase in the size of the particle with an increase in the dendron generation. As seen in Figure **3.2c**, G1.5-COOMe-Au NCs exhibit a surface plasmon band at 520-530 nm in the UV-Vis spectrum, whereas G0.5-COOMe-Au NCs display a very weak surface plasmon band, which indicates a smaller core size. As a result, under the same reaction conditions, the size of the cores is larger with higher generation (G1.5-COOMe) ligands and in order to get particles with the same size of lower generation (G0.5-COOMe) NCs, higher concentrations of reducing agent are needed. TEM images (Figure **3.3**) were consistent with UV-Vis measurements; the smallest average core sizes seen for G0.5-COOMe-Au and G1.5-COOMe-Au NCs formed by direct synthesis were 2.8 ± 0.6 nm (at 0.23 M $NaBH_4$) and 3.0 ± 0.5 nm (at 0.27 M $NaBH_4$), respectively.

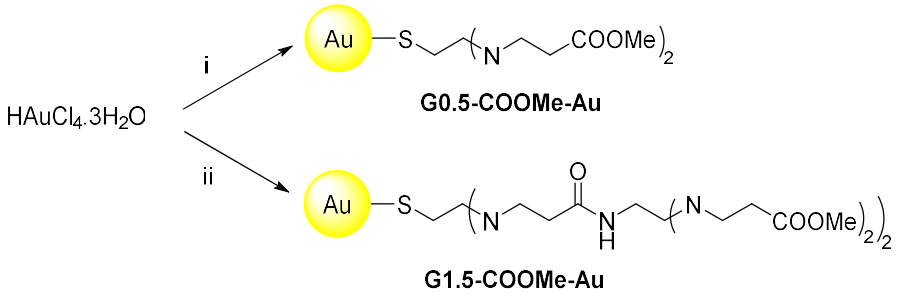

Scheme 3.3. Synthesis of G0.5-COOMe-Au and G1.5-COOMe-Au cluster-cored dendrimers by direct synthesis (Note: only one thiolate is shown around clusters for clarity). Reagents and conditions: step (1) add tetraoctylamonium bromide (TOAB), THF; step (2) add G0.5-COOMe (i) or G1.5-COOMe (ii); step (3) add $NaBH_4$ in 2.0 mL H_2O, 3h, r.t.

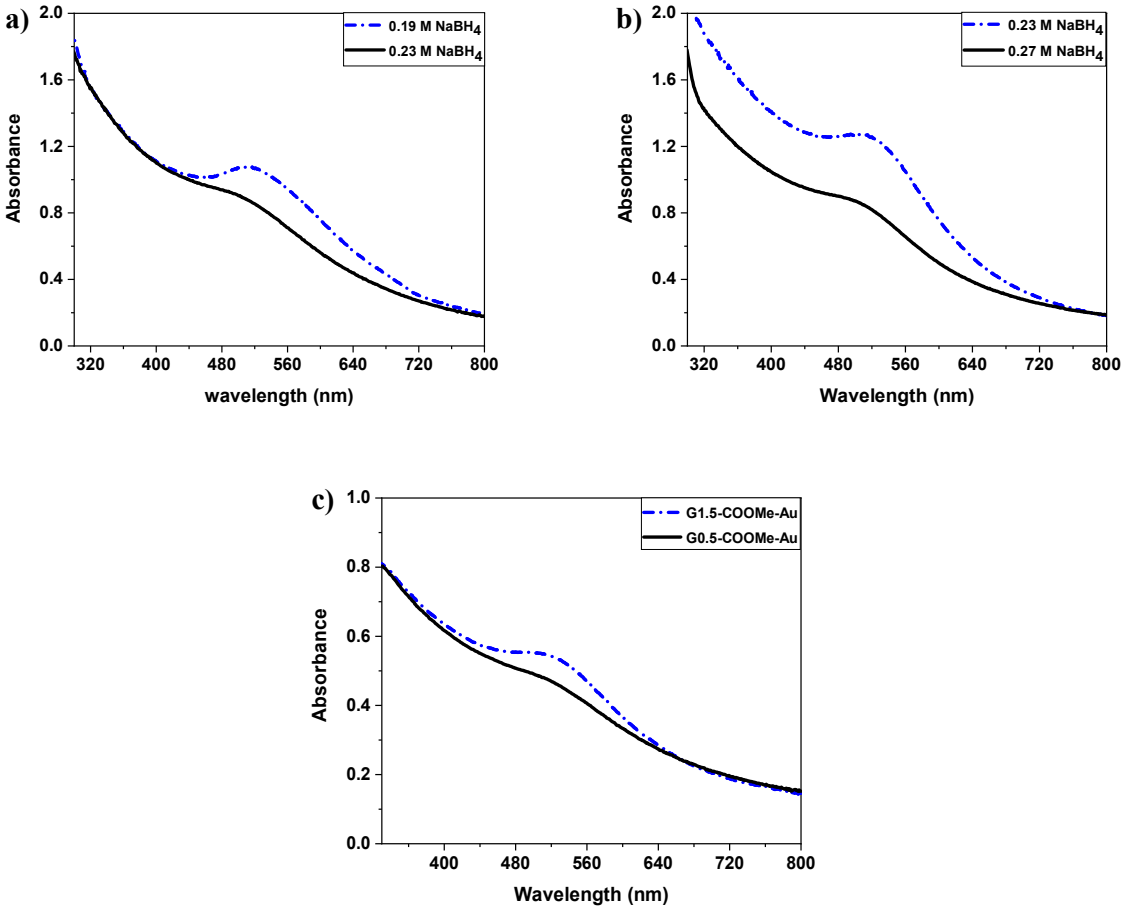

Figure 3.2. UV-Vis spectra of (a) G0.5-COOMe-Au and (b) G1.5-COOMe-Au NCs (in THF) synthesized using various concentrations of $NaBH_4$; (c) UV-Vis of G0.5-COOMe-Au NCs and G1.5-COOMe-Au NCs (50 mg/mL in THF) synthesized using 0.23 M $NaBH_4$.

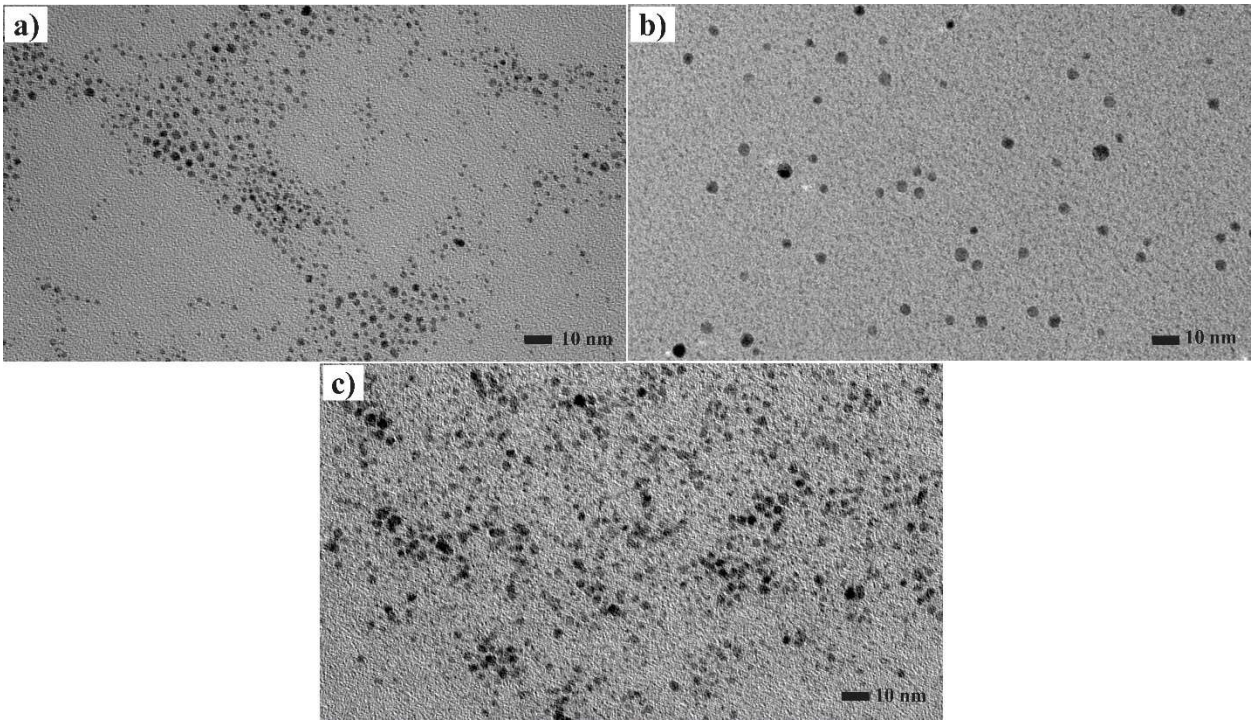

Figure 3.3. TEM images of directly-synthesized (a) G0.5-COOMe-Au NCs (2.8 ± 0.6 nm) and (b) G1.5-COOMe-Au NCs (4.2 ± 0.6 nm) synthesized using 0.23 M $NaBH_4$ and (c) G1.5-COOMe-Au NCs (3.0 ± 0.5 nm) synthesized using 0.27 M $NaBH_4$.

The direct synthesis of G1.0-NH_2-Au NCs was also attempted by the Brust-Shiffrin synthesis using G1.0-NH_2 as a capping agent using a method similar to the G0.5-COOMe-Au and G1.5-COOMe-Au syntheses (Scheme **3.4**). However, this approach ended up with large, unstable particles, which is likely due to the affinity of amine functional groups towards Au and the resulting agglomeration of particles. For example, when a THF solution containing 50 mg $HAuCl_4 \cdot 3H_2O$ and 2.2 equivalents of G1.0-NH_2 was reduced with $NaBH_4$ (0.25 M), the UV-Vis absorption spectrum in Figure **3.4a** initially showed a weak Au plasmon peak at 520 nm which grew in intensity over time. The presence of the Au plasmon peak at 520 nm, and particularly its growth as a function of time, indicates that the Au clusters are not completely stabilized by the dendrons. Rather, the Au clusters aggregate and merge to form larger particles. In contrast, when the same experiment is carried out using G.5-COOMe and G1.5-COOMe dendrons, reduction

results in a stable solution of Au cluster-cored dendrimers. Figure **3.4b** shows a TEM image of G1.0-NH_2-Au NCs after 24 h. The TEM result clearly shows fused domains and the formation of large aggregates. Thus overall, for the direct synthesis of Au cluster-cored dendrimers the final cluster size is a function of the concentration of reducing agent, generation of the dendrons, and surface chemistry of the dendrons. Furthermore, size control of the cluster-cored dendrimers by direct synthesis is difficult to achieve, and atom-precise clusters could not be synthesized.

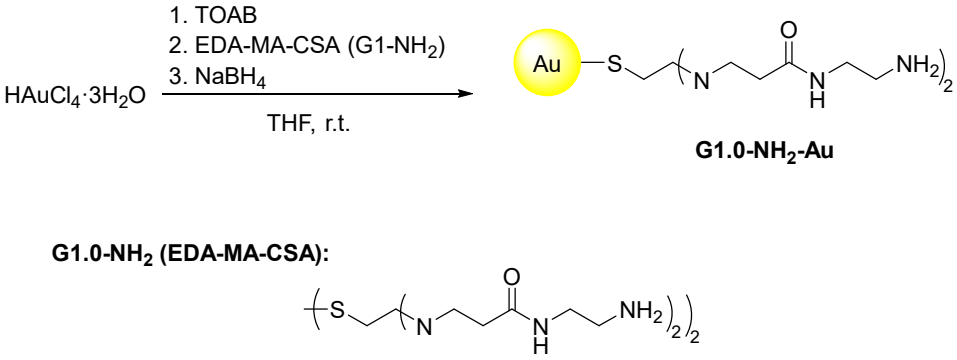

Scheme 3.4. Synthesis of G1.0-NH_2-Au NCs by direct synthesis (Note: only one thiolate is shown for clarity).

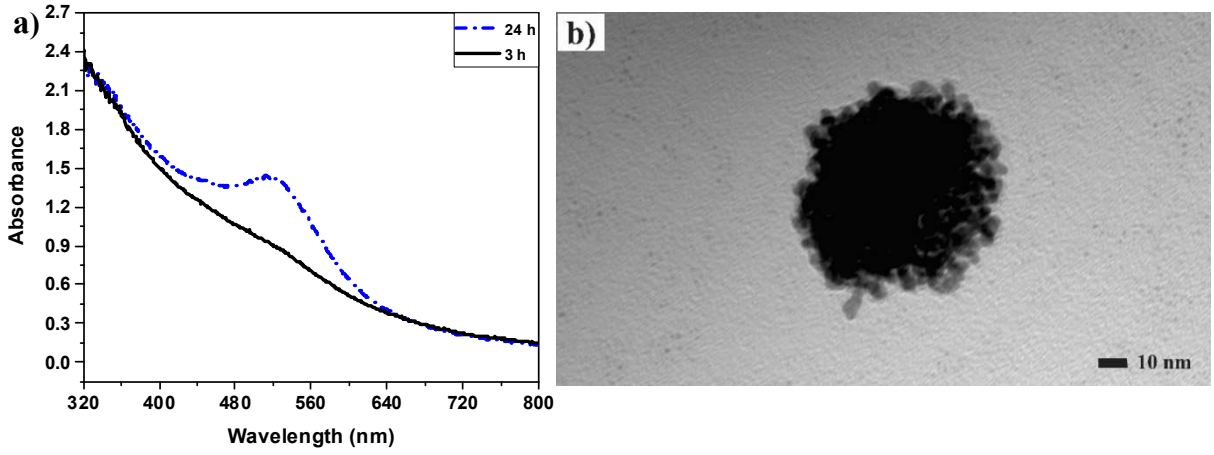

Figure 3.4. (a) UV-Vis spectrum and (b) TEM image of G1.0-NH_2-Au NCs synthesized using 0.25 M $NaBH_4$. UV-Vis spectra were obtained in THF.

For the alternative divergent synthesis of Au cluster-cored dendrimers, the first reaction was the reaction of methyl acrylate with primary amine groups of Gly-CSA-protected Au NCs by a Michael addition reaction in a 2:1 ratio, which was previously reported in Chapter **2** (Scheme **3.5**, **i**). This reaction produced MA-Gly-CSA-protected Au NCs (G0.5-COOMe-Au) with little to no change in the average core size according to UV-Vis (Figure **3.5a** and **3.5b**) and TEM images (Figure **3.6a** and Figure **3.6b**). G1.5-COOMe-Au NCs were synthesized in a stepwise manner by the reaction of G0.5-COOMe-Au with ethylenediamine to form G1.0-NH_2-Au NCs, followed by a subsequent second Michael addition reaction with methyl acrylate (Scheme **3.5**, **ii** and **iii**). Gly-CSA-protected Au NCs with average core sizes of 1.2 ± 0.3 nm and 1.8 ± 0.3 nm were each used for the divergent synthesis of Au cluster-cored dendrimers. As seen in Figure **3.4a**, divergent synthesis of Gn-Au (n = 0.5, 1, 1.5) cluster-cored dendrimers using Au NCs with an average core size of 1.2 ± 0.3 nm all exhibit three UV-Vis absorption peaks at around 690, 440, and 390 nm which are spectroscopic fingerprints of $Au_{25}(SR)_{18}$ NCs and are strongly suggestive of the formation of Au_{25} cluster-cored dendrimers.[24] Figure **3.5b** shows results for Gn-Au cluster-cored dendrimers with slightly larger core sizes (1.8 ± 0.3 nm); all functionalized clusters have similar increasing absorption at low wavelengths which is due to light scattering of the clusters, and no plasmon bands are seen for any of the derivatized clusters. The resulting Au cluster-cored dendrimers were stable and no precipitation or insoluble particles were seen during the synthesis and purification. They maintained a high solubility in water (for G1.0-NH_2-Au NCs) and various organic solvents, such as THF, methanol, and methylene chloride (for G0.5-COOMe-Au and G1.5-COOMe-Au NCs) for over two months in the absence of O_2 (O_2 pumped out by vacuum). Consequently, the resulting Au cluster-cored dendrimers prepared by the divergent strategy display similar sizes and optical properties as the original NCs after surface functionalization

(Figure **3.5a** and **3.5b**). With this method, one can synthesize Au cluster-cored dendrimers possessing various functionalities with precise core diameters including atom-precise $Au_{25}(SR)_{18}$ cluster-cored dendrimers.

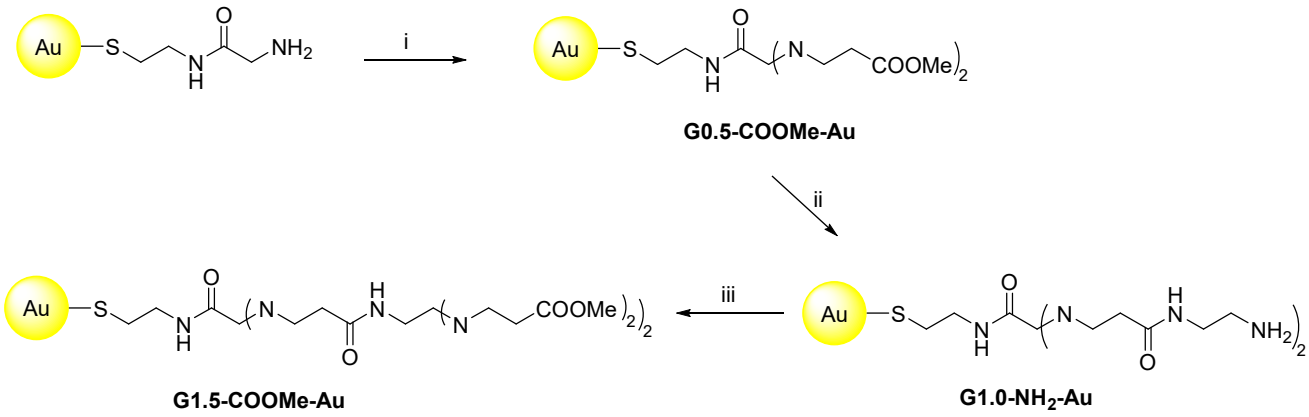

Scheme 3.5. Synthesis of Gn-Au cluster-cored dendrimers by divergent strategy (multistep reactions); (Note: only one thiolate on each cluster is shown for clarity). Reagents and conditions: (i) & (iii) methyl acrylate, H_2O:MeCN (1:1), r.t; (ii) ethylenediamine, MeOH, r.t.

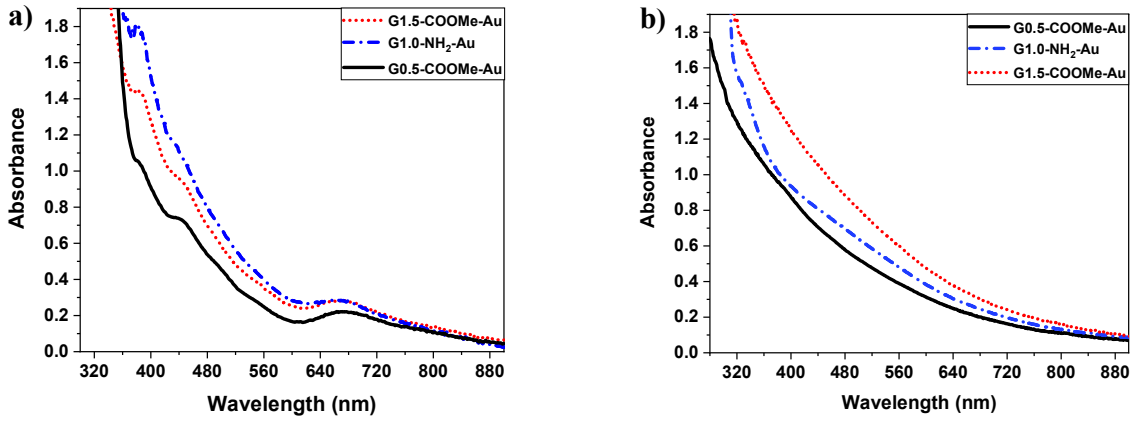

Figure 3.5. UV-Vis spectra of Gn-Au cluster-cored dendrimers synthesized by a divergent method using Au NCs with average core sizes of (a) 1.2 ± 0.3 nm and (b) 1.8 ± 0.3 nm; UV-Vis spectra were obtained in THF for G0.5-COOMe-Au NCs and G1.5-COOMe-Au NCs and in H_2O for G1.0-NH_2-Au NCs.

Figure **3.6a-f** show the TEM images of G0.5-COOMe-Au (**3.6a,b**), G1.0-NH_2-Au (**3.6c,d**), and G1.5-COOMe-Au (**3.6e,f**) cluster-cored dendrimers produced by Gly-CSA-protected Au NCs

with two average core sizes of 1.2 ± 0.3 nm (**3.6a,c,e**) and 1.8 ± 0.3 nm (**3.6b,d,f**). For G1.0-NH_2-Au NCs, the particles were found to be less dispersed compared to G0.5-COOMe-Au and G1.5-COOMe-Au NCs (Figure **3.6d**). This is partly attributed to a tendency of amine groups on the NC surface to hydrogen bond to each other upon drying. However, unlike the directly-synthesized system, no significant multi-cluster aggregation occurred after functionalization. When using Gly-CSA-protected Au NCs with an average core size of 1.2 ± 0.3 nm as the starting material, the final sizes of the G0.5-COOMe-Au, G1.0-NH_2-Au, and G1.5-COOMe-Au NCs were 1.2 ± 0.3 nm, 1.5 ± 0.4 nm, and 1.3 ± 0.3 nm. Similarly, when using Gly-CSA-protected Au NCs with an average core size of 1.8 ± 0.3 nm as the starting material, the final sizes of the G0.5-COOMe-Au, G1.0-NH_2-Au, and G1.5-COOMe-Au NCs were 1.8 ± 0.3 nm, 2.0 ± 0.4 nm, and 1.9 ± 0.3 nm, respectively. It indicates that divergent strategy gives more control over the Au core size and small core sizes with high monodispersity could be formed by divergent approach.

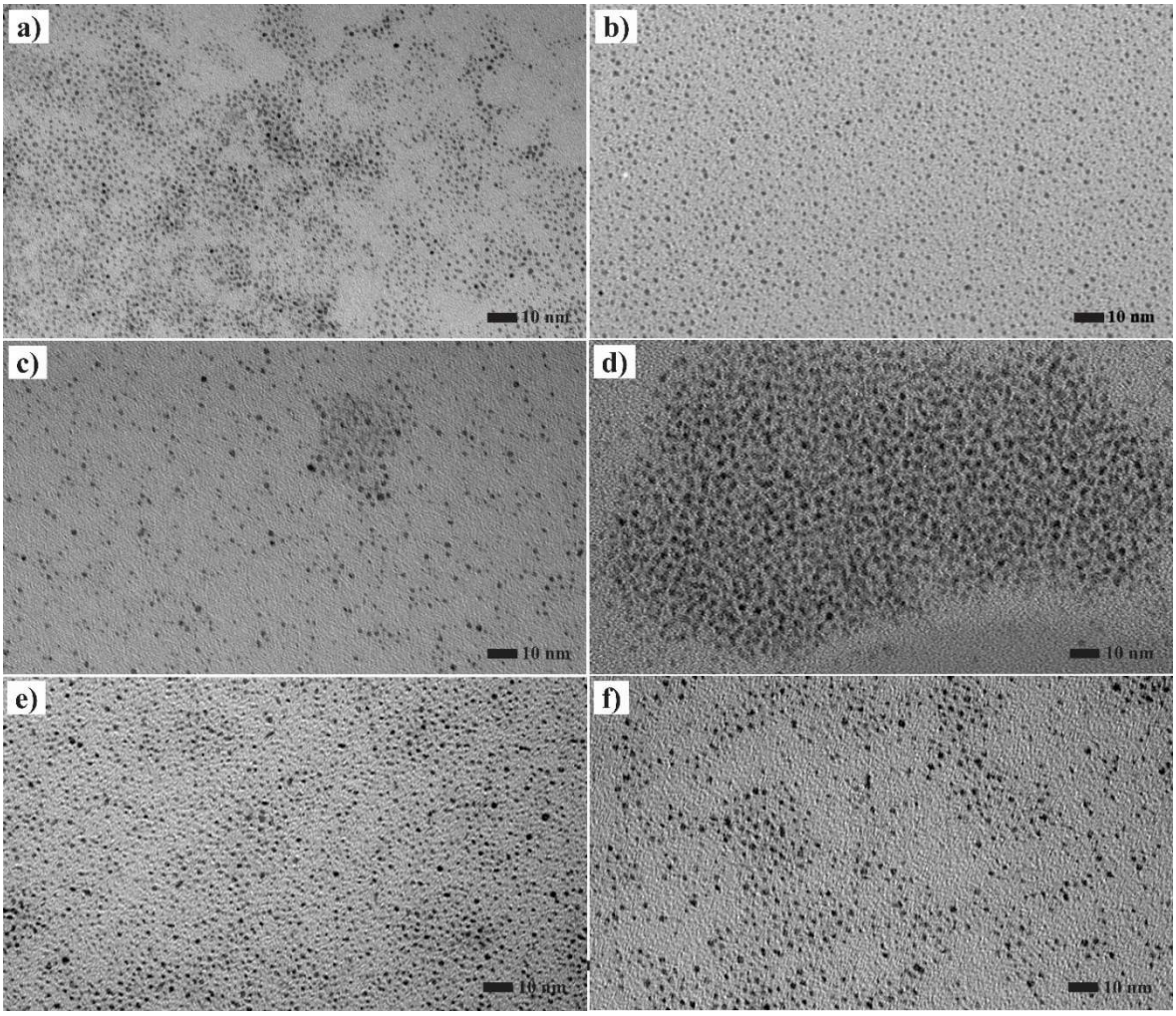

Figure 3.6. TEM images of (a,b) G0.5-COOMe-Au, (c,d) G1.0-NH_2-Au, and (e,f) G1.5-COOMe-Au NCs synthesized by a divergent method using Gly-CSA-Au NCs with average core sizes of (a,c,e) 1.2 ± 0.3 nm and (b,d,f) 1.8 ± 0.3 nm.

Figure **3.7** shows the ^{1}H NMR spectra of Au cluster-cored dendrimers synthesized by divergent method. The ^{1}H NMR peaks of ligands attached to Au cluster-cored dendrimers are all broadened compared to free ligands (shown in Figure **3.1a**), which is likely because of spin-spin relaxation (T_2) broadening due to the larger cluster size.[34] Peaks at 3.6 ppm for G0.5-COOH-Au NCs and G1.5-COOH-Au NCs are assigned to methyl groups of the ester and indicate the success of the reaction of methyl acrylate with surface amine groups of Gly-CSA-protected Au NCs and

G1.0-NH_2-Au NCs, respectively. The ^{1}H NMR signals of G1.0-NH_2-Au NCs appear at positions that are almost identical to those of free G1.0-NH_2 (Figure **3.1a**). Two broad peaks at around 2.7-2.8 and 3.2-3.3 ppm are assigned to the methylene hydrogens of ethylenediamine, which proves that the covalent attachment of ethylenediamine was successful. Furthermore, the methyl proton signal of ester groups at 3.6 ppm has vanished, which also indicates that the functionalization was successful.

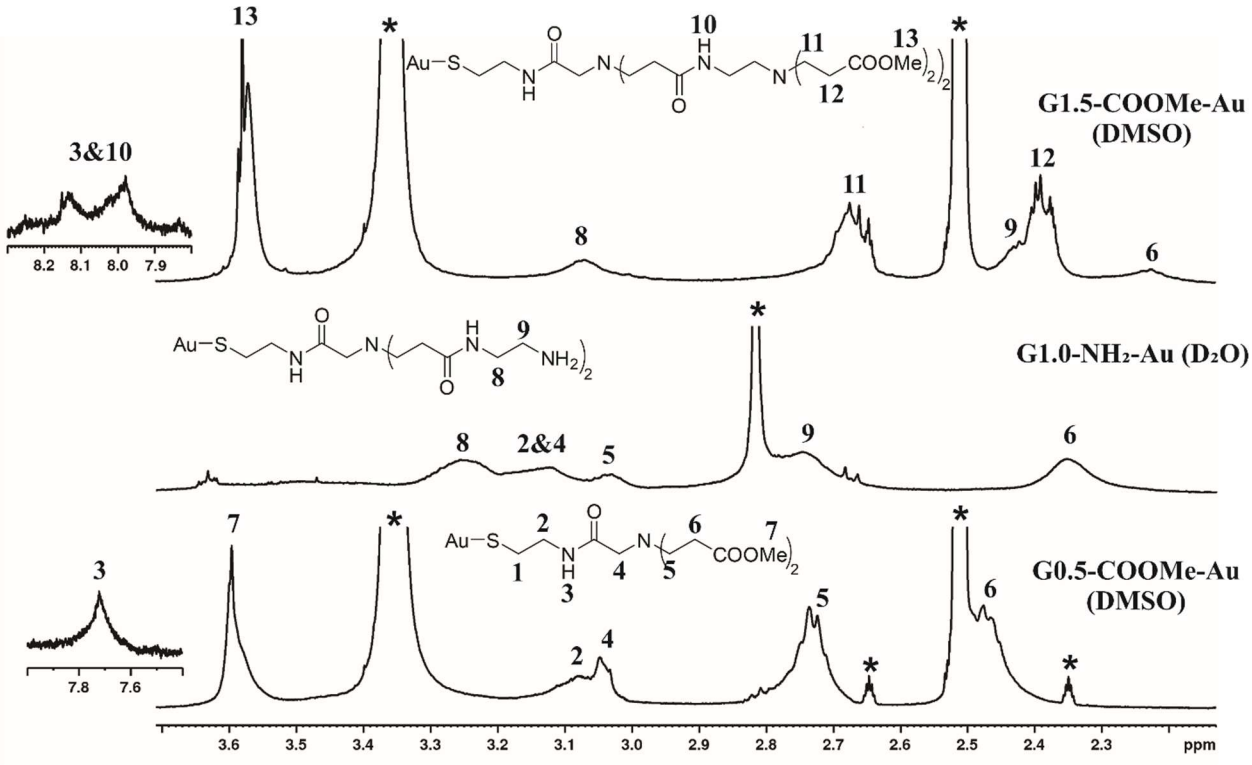

Figure 3.7. ^{1}H NMR spectra of Gn-Au cluster-cored dendrimers (G0.5-COOMe-Au (d_6-DMSO), G1.0-NH_2-Au (D_2O) and G1.5-COOMe-Au (d_6-DMSO)) synthesized by the divergent strategy; (Note: only one ligand in the structures and branching not shown for simplicity, * shows the peaks due to solvent impurities).

In order to quantify the extent of derivatization of the NCDs, the ligands of the Au cluster-cored dendrimers formed by the divergent strategy were removed from the surface via cyanide etching of the Au core and characterized by ^{1}H NMR, as shown in Figure **3.8**. These etched ligand

studies allow for more quantitative NMR interpretation. The number of methylene hydrogens of CH_2-S- groups (peak **1** in Figure **3.8**) is slightly less than two hydrogens in both ligands (1.86 H for G0.5-COOH-Au and 1.34 H for G1.5-COOH-Au), which is likely due to the fact that both disulfide and thiol groups form in the solution after etching (since the chemical shifts of these two groups are slightly different; the second peak is buried under the peak at 2.75 and 2.65 ppm for the G0.5-COOMe system and G1.5-COOMe system, respectively). Also, based on the integrated intensity of the methyl groups of esters, it is observed that in G0.5-COOH-Au the di-substituted product is the major product of Michael addition reaction and a very negligible amount of other products have been observed. Note for the G1.5-COOH-Au system, there is a second small peak in the methyl region for the ester which is likely due to the monosubstituted product. An estimated 80% of methyl acrylate substrates have fully participated in reactions and produced G1.5-COOMe while about 20% mono-substituted product have been produced. Etching products of G1.0-NH_2 could not be characterized by ^{1}H NMR, likely because the obtained water-soluble amine-terminated ligand interacted with the Au salt in water after etching.

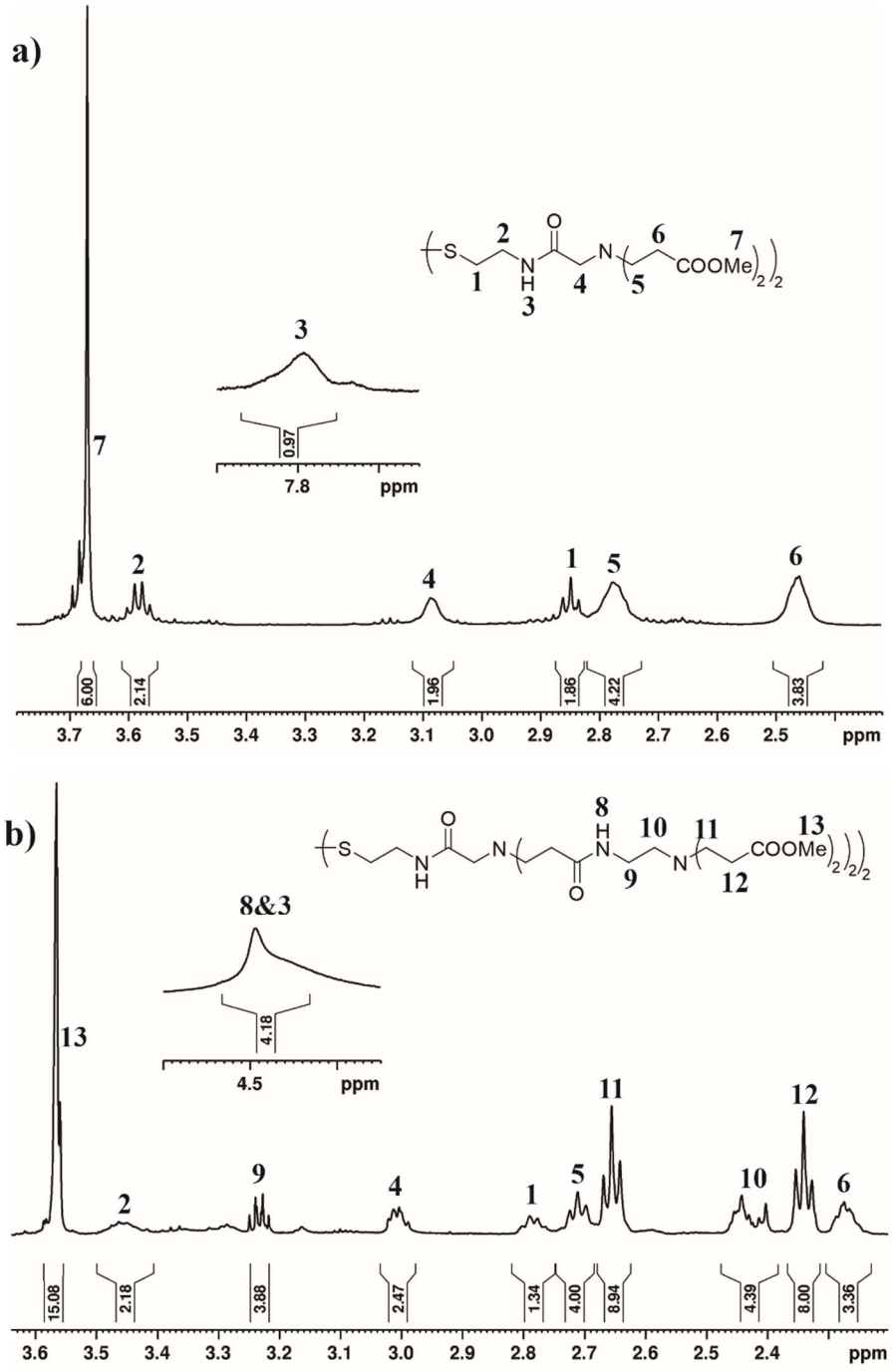

Figure 3.8. ^{1}H NMR of the resulting ligands removed from (a) G0.5-COOMe-Au and (b) G1.5-COOMe-Au in $CDCl_3$ after cyanide etching.

The catalytic activity of Au cluster-cored dendrimers prepared by different methodologies with different dendritic generations was investigated using the reduction of 4-nitrophenol with

$NaBH_4$. 4-NP reduction was chosen as our group,[25] and others,[26,27] have previously shown that this reaction gives a good indication of the available surface area of metallic particles. In this study, the role of both the synthetic methodology used and the steric bulk of the dendrons on the catalytic activity of Au cluster-cored dendrimers was examined. Figure **3.9a** shows the time evolution UV-Vis absorption spectra for the hydrogenation of 4-NP with $NaBH_4$ catalyzed by G0.5-COOMe-Au (synthesized by the direct synthesis strategy). A decrease of the absorption peak at 400 nm is seen as well as a small increase at ca. 300 nm after the addition of $NaBH_4$, which suggest the conversion of 4-NP (which exists as the nitrophenolate in basic conditions) to 4-aminophenol. Figure **3.9b** shows that the catalytic reaction is a pseudo-first-order reaction as a linear relationship is seen between $-\ln(C_t/C_o)$ at λ = 400 nm and reaction time. G0.5-COOMe-Au NCs synthesized by the divergent strategy and direct synthesis methods with an almost similar core size (3 nm) were synthesized and used to compare the effect of synthetic methodologies on catalytic activities. The results are shown in Figure **3.10a**. The Au cluster-cored dendrimers synthesized by the direct synthesis method showed higher catalytic activity compared to the similar cluster-cored dendrimers produced by the divergent method. The higher activity for the directly-synthesized clusters might be due to the fact that the Au surface of cluster-cored dendrimers formed by direct synthesis has a lower density of organic layers and as a result, is less passivated. Thus, the Au core is more accessible which results in higher catalytic activities. The result is consistent with previous work by the Fox group in which they showed that the Au NCs with high generations of dendrons have large void spaces near the core and subsequently exhibit excellent catalytic activity.[11]

The effect of dendron generations of different lengths (and thus steric bulk of the dendron) on the catalytic performance of Au cluster-cored dendrimers was also investigated. G0.5-COOMe-Au and G1.5-COOMe-Au NCs synthesized by both the divergent and direct synthesis approaches

were used for this investigation. Figure **3.10b** shows that the accessibility of the G0.5-COOMe NCs synthesized by the divergent method is higher as the apparent rate constant (k_{app}) is higher at 0.040 s^{-1} than that seen for G1.5-COOMe-Au (0.031 s^{-1}). This result is consistent with the fact that the accessibility of Au core should be higher when using shorter and sterically-less bulky ligands. Again, cluster-cored dendrimers made using the direct synthesis route showed higher activities. However, G1.5-COOMe-Au NCs synthesized by direct synthesis showed a higher reaction rate compared to G0.5-COOMe-Au NCs (Figure **3.10c**). The reason could be by increasing the generation of dendrons, the density of organic layers on the core decreased due to steric hindrance. As a result, the Au surface of the higher generation of the directly-synthesized Au cluster-cored dendrimers is less passivated and shows higher catalytic activity.

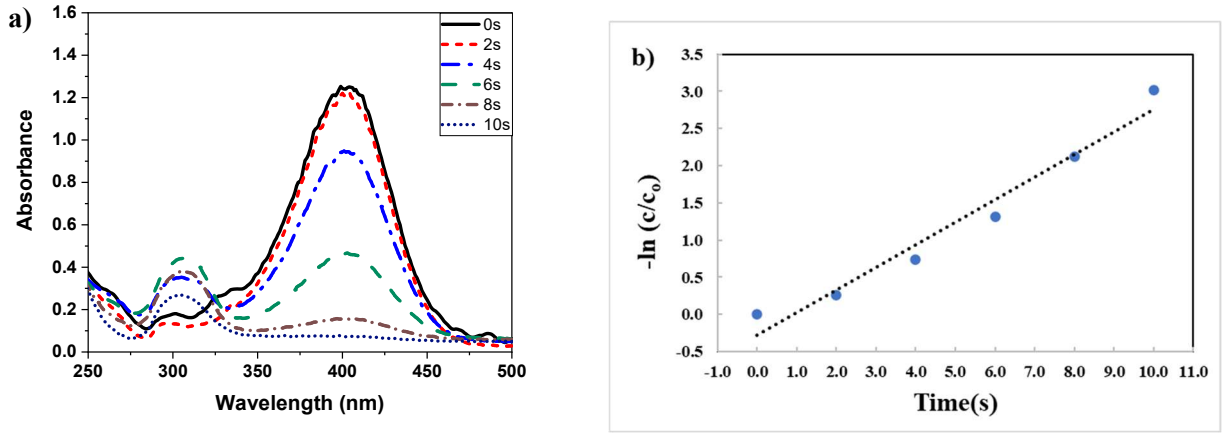

Figure 3.9. (a) UV-Vis absorption spectra of the reduction of 4-NP catalyzed by G0.5-COOMe-Au NCs synthesized by the direct strategy method. (b) Plot of $-\ln(c/c_0)$ vs. reaction time.

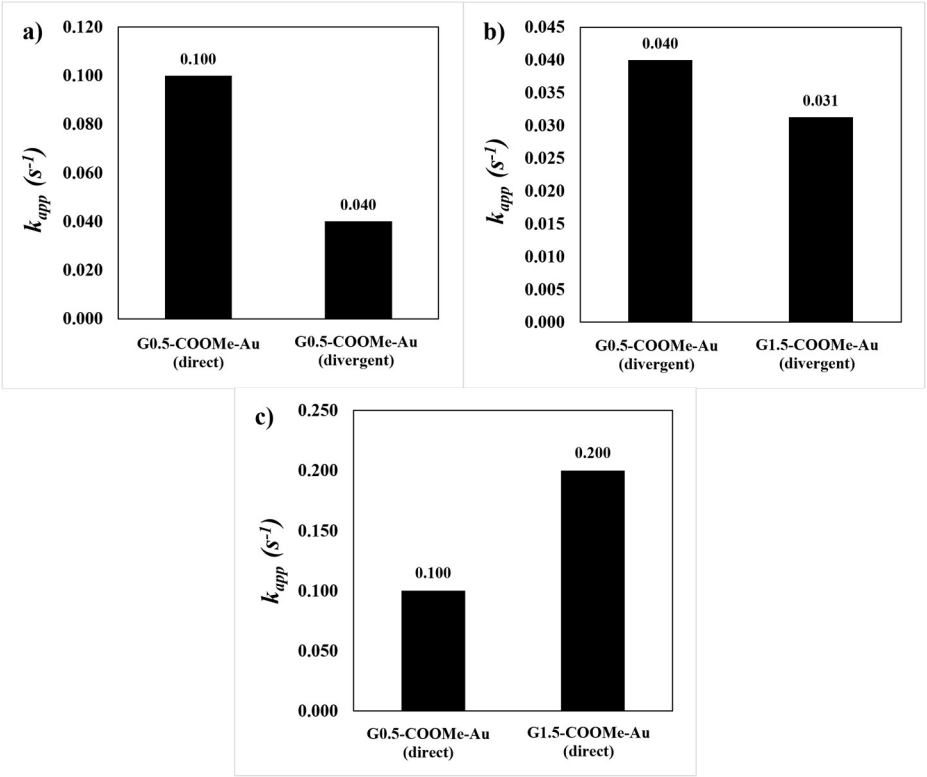

Figure 3.10. The apparent reaction rate constant (k_{app}) of Au cluster-cored dendrimers synthesized with (a) different methodologies (G0.5-COOMe-Au NCs synthesized by direct synthesis and divergent method) and different dendron generations, (b) G0.5-COOMe-Au and G1.5-COOMe-Au NCs formed by the divergent method, and (c) G0.5-COOMe-Au and G1.5-COOMe-Au NCs formed by direct synthesis method.

3.5 Conclusions

In this study, the synthesis of Au cluster-cored dendrimers has been studied by direct synthesis and post-functionalization (divergent) strategies to generate ester and amine-terminated cluster-cored dendrimers. The resulting ester-terminated Au cluster-cored dendrimers by direct synthesis are stable and the core size directly depends on the concentration of the reducing agent as well as the generation of the dendrons. The direct synthesis of amine-terminated cluster-cored dendrimers formed large and unstable particles due to particle aggregation during and after synthesis which shows that surface chemistry is also quite important. In contrast, excellent size control of the cluster-cored dendrimers is achieved using the divergent method (post-functionalization) and atom-precise clusters have been synthesized. With this method, Au cluster-cored dendrimers could be synthesized with various functionalities and precise core diameters including atom-precise $Au_{25}(SR)_{18}$ cluster-cored dendrimers. Finally, the catalytic activity of these Au cluster-cored dendrimers was undertaken for the 4-nitrophenol reduction reaction. Au cluster-cored dendrimers synthesized by direct synthesis show higher catalytic efficiency for the reduction of 4-NP. This might be due to a lower density of organic layers and as a result greater accessibility of the core which results in higher catalytic activities. Lower activities were seen for clusters made using the divergent method and increasing the steric bulk of the dendritic ligands led to lower activity in that system, likely due to reduced access of the substrate to the Au cluster core.

3.6 References

(1) Tomalia, D. A. Birth of a New Macromolecular Architecture: Dendrimers as Quantized Building Blocks for Nanoscale Synthetic Polymer Chemistry. *Prog. Polym. Sci.* **2005**, *30*, 294–324.

(2) Abbasi, E.; Aval, S. F.; Akbarzadeh, A.; Milani, M.; Nasrabadi, H. T.; Joo, S. W.; Hanifehpour, Y.; Nejati-Koshki, K.; Pashaei-Asl, R. Dendrimers: Synthesis, Applications, and Properties. *Nanoscale Res. Lett.* **2014**, *9*, 1–10.

(3) Cloninger, M. J. Biological Applications of Dendrimers. *Curr. Opin. Chem. Biol.* **2002**, *6*, 742–748.

(4) Lee, C. C.; MacKay, J. A.; Fréchet, J. M. J.; Szoka, F. C. Designing Dendrimers for Biological Applications. *Nat. Biotechnol.* **2005**, *23*, 1517–1526.

(5) Jang, W.-D.; Kamruzzaman Selim, K. M.; Lee, C.-H.; Kang, I.-K. Bioinspired Application of Dendrimers: From Bio-Mimicry to Biomedical Applications. *Prog. Polym. Sci.* **2009**, *34*, 1–23.

(6) Mhlwatika, Z.; Aderibigbe, B. A. Application of Dendrimers for the Treatment of Infectious Diseases. *Molecules* **2018**, *23*, 2205–2237.

(7) Kumar, V. K. R.; Gopidas, K. R. Synthesis and Characterization of Gold-Nanoparticle-Cored Dendrimers Stabilized by Metal-Carbon Bonds. *Chem. Asian J.* **2010**, *5*, 887–896.

(8) Cheng, X.; Rong, L. H.; Cao, P. F.; Advincula, R. Core-Shell Gold Nanoparticle-Star Copolymer Composites with Gradient Transfer and Transport Properties: Toward Electro-Optical Sensors and Catalysis. *ACS Appl. Nano Mater.* **2021**, *4*, 1394–1400.

(9) Daniel, M. C.; Aranzaes, J. R.; Nlate, S.; Astruc, D. Gold-Nanoparticle-Cored Polyferrocenyl Dendrimers: Modes of Synthesis and Functions as Exoreceptors of Biologically Important Anions and Re-Usable Redox Sensors. *J. Inorg. Organomet. Polym.* **2005**, *15*, 107–119.

(10) Gopidas, K. R.; Whitesell, J. K.; Fox, M. A.; Carolina, N. Catalytic Applications of a Palladium-Nanoparticle-Cored Dendrimer. *Nano Lett.* **2003**, *3*, 1757-1760.

(11) Gopidas, K. R.; Whitesell, J. K.; Fox, M. A. Nanoparticle-Cored Dendrimers: Synthesis and Characterization. *J. Am. Chem. Soc.* **2003**, *125*, 6491–6502.

(12) Brunetti, V.; Bouchet, L. M.; Strumia, M. C. Nanoparticle-Cored Dendrimers: Functional Hybrid Nanocomposites as a New Platform for Drug Delivery Systems. *Nanoscale* **2015**, *7*, 3808–3816.

(13) Li, X.; Kono, K. Functional Dendrimer–Gold Nanoparticle Hybrids for Biomedical Applications. *Polym. Int.* **2018**, *67*, 840–852.

(14) Gopidas, K. R.; Whitesell, J. K.; Fox, M. A. Metal-Core-Organic Shell Dendrimers as Unimolecular Micelles. *J. Am. Chem. Soc.* **2003**, *125* (46), 14168–14180.

(15) Kumar, V. K. R.; Gopidas, K. R. Synthesis and Characterization of Gold-Nanoparticle-Cored Dendrimers Stabilized by Metal-Carbon Bonds. *Chem. -Asian J.* **2010**, *5*, 887–896.

(16) Yang, P.; Zhang, W.; Du, Y.; Wang, X. Hydrogenation of Nitrobenzenes Catalyzed by Platinum Nanoparticle Core-Polyaryl Ether Trisacetic Acid Ammonium Chloride Dendrimer Shell Nanocomposite. *J. Mol. Catal. A* **2006**, *260*, 4–10.

(17) Shon, Y. S.; Choi, D.; Dare, J.; Dinh, T. Synthesis of Nanoparticle-Cored Dendrimers by Convergent Dendritic Functionalization of Monolayer-Protected Nanoparticles. *Langmuir* **2008**, *24*, 6924–6931.

(18) Elbert, K. C.; Lee, J. D.; Wu, Y.; Murray, C. B. Improved Chemical and Colloidal Stability of Gold Nanoparticles through Dendron Capping. *Langmuir* **2018**, *34*, 13333–13338.

(19) Cutler, E. C.; Lundin, E.; Garabato, B. D.; Choi, D.; Shon, Y. S. Dendritic Functionalization of Monolayer-Protected Gold Nanoparticles. *Mater. Res. Bull.* **2007**, *42*, 1178–1185.

(20) Zhao, F.; Li, W. Dendrimer/Inorganic Nanomaterial Composites: Tailoring Preparation, Properties, Functions, and Applications of Inorganic Nanomaterials with Dendritic

Architectures. *Sci. China Chem.* **2011**, *54*, 286–301.

(21) Li, Z.; Hu, J.; Yang, L.; Zhang, X.; Liu, X.; Wang, Z.; Li, Y. Integrated POSS-Dendrimer Nanohybrid Materials: Current Status and Future Perspective. *Nanoscale* **2020**, *12*, 11395–11415.

(22) Schneider, C. A.; Rasband, W. S.; Eliceiri, K. W. NIH Image to ImageJ: 25 Years of Image Analysis. *Nat. Methods* **2012**, *9*, 671–675.

(23) Zhu, M.; Aikens, C. M.; Hollander, F. J.; Schatz, G. C.; Jin, R. Correlating the Crystal Structure of A Thiol-Protected Au_{25} Cluster and Optical Properties. *J. Am. Chem. Soc.* **2008**, *130*, 5883–5885.

(24) Templeton, A. C.; Wuelfing, W. P.; Murray, R. W. Monolayer-Protected Cluster Molecules. *Acc. Chem. Res.* **2000**, *33*, 27–36.

(25) Shivhare, A.; Ambrose, S. J.; Zhang, H.; Purves, R. W.; Scott, R. W. J. Stable and Recyclable Au25 Clusters for the Reduction of 4-Nitrophenol. *Chem. Commun.* **2013**, *49*, 276–278.

(26) Li, J.; Nasaruddin, R. R.; Feng, Y.; Yang, J.; Yan, N.; Xie, J. Tuning the Accessibility and Activity of $Au_{25}(SR)_{18}$ Nanocluster Catalysts through Ligand Engineering. *Chem. -Eur. J.* **2016**, *22*, 14816–14820.

(27) Nasaruddin, R. R.; Chen, T.; Li, J.; Goswami, N.; Zhang, J.; Yan, N.; Xie, J. Ligands Modulate Reaction Pathway in the Hydrogenation of 4-Nitrophenol Catalyzed by Gold Nanoclusters. *ChemCatChem* **2018**, *10*, 395–402.

Chapter 4

4 Conclusions and Future Work

4.1 Conclusions

The first part of my project focused on the synthesis and characterization of amine-terminated Au NCs. A strategy to produce stable atom-precise amine-terminated Au_{25} NCs was realized by careful control of the reducing agent concentration in the synthesis of the NCs. In the second part, two synthetic strategies to generate cluster-cored dendrimers and how the synthesis method affects the core size and surface chemistry and as a result the catalytic properties of NCs have been studied.

In Chapter 2, a new single-phase synthetic method has been introduced to produce atom-precise amine-terminated Au nanoclusters by Fmoc-protected glycine-cystamine ligands. The presence of the Fmoc protecting group prevents unwanted interactions between Au surfaces and amines during the Au NC synthesis. Following Fmoc deprotection, stable Au NCs with primary amine functional groups on the surface were generated with little to no change in NC size. The synthesized Au NCs are monodisperse, water-soluble, and stable in solution for several months. The core size directly depends on the concentration of the reducing agent. According to UV-Vis measurements, increasing the concentration of the reducing agent in the reaction mixture and subsequent Fmoc deprotection results in the formation of Gly-CSA-protected Au NCs with decreasing core diameter. Three absorption peaks were observed at around 690, 440, and 390 nm

when using a concentration of 0.30 M of the reducing agent, which are spectroscopic fingerprints of Au_{25} NCs and are strongly suggestive of the formation of Gly-CSA-protected $Au_{25}(SR)_{18}$ NCs. The stability of Fmoc-Gly-CSA- and Gly-CSA-protected Au NCs were studied in solution. It is observed that the stability towards precipitation of Fmoc-Gly-CSA-protected Au NCs in THF is size-dependent. The NCs with smaller core sizes have lower solubility/stability in the solution. For these particles, π-π stacking of the aromatic groups in Fmoc may promote particle self-assembly and subsequent precipitation. The Gly-CSA-protected Au NCs exhibit high stability in solution due to lack of π-π interactions. To investigate the reactivity of primary amine end groups, methyl acrylate was added via a Michael addition reaction to the amine-terminated groups of Au NCs. No NC size change was observed after the reaction which makes these NCs a suitable candidate for applications that require multi-step functionalization.

In Chapter 3, two methodologies have been studied to synthesize Au cluster-cored dendrimers: direct synthesis and post-functionalization (divergent method). Gly-CSA-protected Au NCs from Chapter 2 were chosen as the initial NCs to produce Au cluster-cored dendrimers by multi-step functionalization. In the direct synthesis of cluster-cored dendrimers, the core size directly depends on the concentration of the reducing agent. Furthermore, an increase in the core size of the particles was observed with an increase in the dendron generation which indicates that the core size also depends on the dendron generation. The direct synthesis of amine-terminated cluster-cored dendrimers formed large and unstable particles due to particle aggregation during and after synthesis which shows that surface chemistry also controls the core size. In contrast, excellent size control of the cluster-cored dendrimers is achieved using the divergent method (post-functionalization). Atom-precise $Au_{25}(SR)_{18}$ cluster-cored dendrimers were synthesized by this method. The resulting amine- and ester-terminated Au cluster-cored dendrimers synthesized by

the divergent method are stable and no aggregation was observed in solution during or after synthesis. Finally, the catalytic activity of the cluster-cored dendrimers was investigated for the reduction of 4-nitrophenol with $NaBH_4$ and the effect of synthetic strategies as well as dendron generations on the accessibility of the Au surface were studied. It is speculated that the Au surface of cluster-cored dendrimers formed by direct synthesis has a larger size and thus the lower density of ligands and as a result, have unpassivated surfaces which results in higher catalytic activities. Furthermore, a study on the effect of dendron generations on the catalytic activity suggests that NCs with less sterically bulky dendrons show higher catalytic activities. The catalytic results highlight the importance of the synthetic methodology and the dendron generation for cluster-cored dendrimer catalysts.

4.2 Future Work

4.2.1 The Synthesis of Carboxylic Acid-Terminated Au Cluster-Cored Dendrimers

As mentioned earlier, direct synthesis of carboxylic acid and amine-terminated thiol-stabilized Au NCs is a large challenge due to the strong affinity of both amine and thiol groups towards Au. Also, place exchange reactions which are a tool to produce various NPs and NCs with a diverse range of core sizes and functional groups in the ligand shell often lead to incomplete exchange or even no exchange for some ligands. Furthermore, in this method, the size of the core may also be changed. To access carboxylic acid-terminated cluster-cored dendrimers, the basic hydrolysis of ester groups of ester-terminated Au cluster-cored dendrimers to the corresponding sodium carboxylate salt (Scheme **4.1**) could be attempted. This should lead to the fabrication of carboxylic acid-terminated Au cluster-cored dendrimers without significant change in size. The

resulting sodium carboxylate terminated clusters would likely exhibit micellar properties and possibly show interesting catalytic sieving of charged substrates.[1]

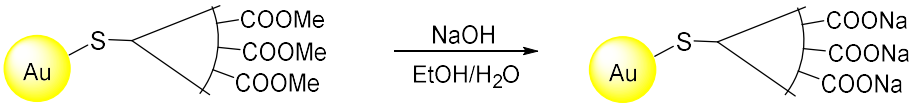

Scheme 4.1. Basic hydrolysis of ester-terminated Au cluster-cored dendrimers.

4.2.2 Convergent Synthesis of Au Cluster-Cored Dendrimers

Recently convergent approaches have been used as an effective and facile method to synthesize cluster-cored NPs and NCs. This method is based on a strategy in which the synthesis of thiolate-protected Au NPs and NCs is followed by a single reaction of the surface functional groups of the particles with prefabricated dendrons. Since the reaction happens on the surface of the particles, this method can lead to Au cluster-cored NPs and NCs with no change in the core size. Future work could focus on a new strategy (convergent approach) to construct Au cluster-cored dendrimers by a single coupling reaction of ester-terminated Au NCs with dendrons such as Newkome-type dendrons (Scheme **4.2**). In this method, a limited number of reactions are performed on the same cluster, and as a result, it could be possible to obtain particles with fewer or no structural defects on the surface. Furthermore, a major advantage of this strategy is to overcome the limitation of using thiol-containing dendrons.[2] The consequence of this strategy is to have more control over the process and higher purity of prepared particles. Furthermore, a variety of Au cluster-cored dendrimers can be synthesized with the same core and different dendrons as well as the same dendron and different core sizes. Alternative characterization techniques such as mass spectrometry, thermogravimetric analysis (TGA), and zeta potential analysis could also be performed in order to better understand the composition of the synthesized Au NCs.

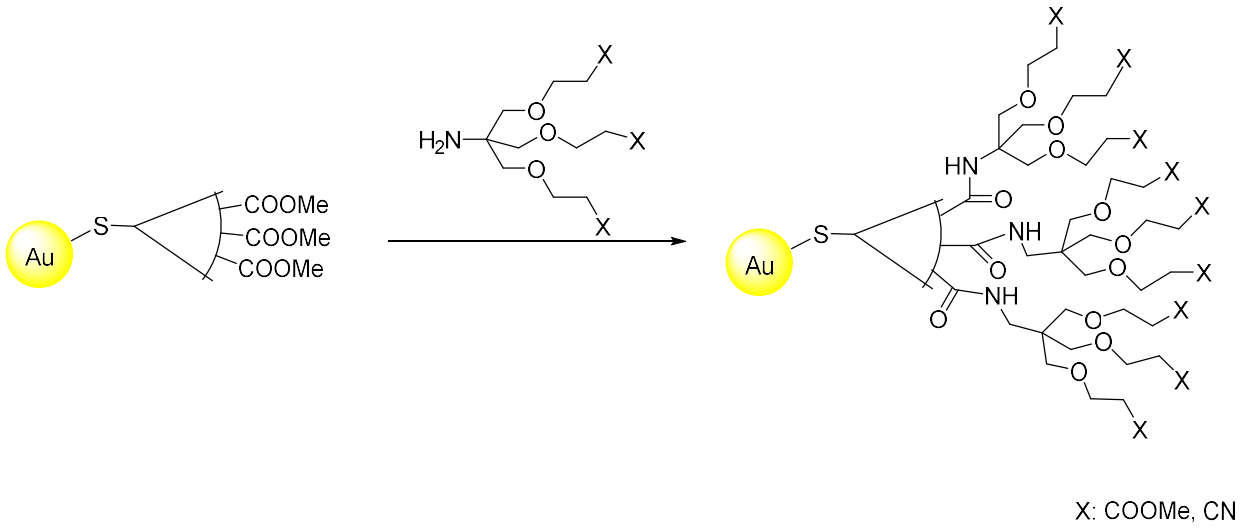

Scheme 4.2. Convergent synthesis of Au cluster-cored dendrimers using Newkome-type dendrons.

4.3 References

(1) Gopidas, K. R.; Whitesell, J. K.; Fox, M. A. Metal-Core-Organic Shell Dendrimers as Unimolecular Micelles. *J. Am. Chem. Soc.* **2003**, *125*, 14168–14180.

(2) Love, C. S.; Ashworth, I.; Brennan, C.; Chechik, V.; Smith, D. K. Dendron-Protected Au Nanoparticles-Effect of Dendritic Structure on Chemical Stability. *J. Colloid Interface Sci.* **2006**, *302*, 178–186.